

**Distance-Estimated Landmark Vector Model
for Vision-Based Homing Navigation**

Seung-Eun Yu

The Graduate School
School of Electrical and Electronic Engineering
Yonsei University

Distance-Estimated Landmark Vector Model for Vision-Based Homing Navigation

A Masters Thesis

Submitted to the Department of
Electrical and Electronic Engineering
and the Graduate School of Yonsei University
in partial fulfillment of the
requirements for the degree of
Master of engineering

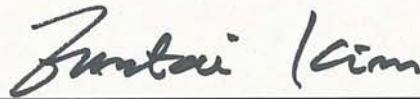
Seung-Eun Yu

June 2011

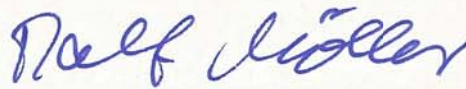
This certifies that the master's thesis
of Seung-Eun Yu is approved.



Thesis Supervisor: DaeEun Kim



Euntai Kim



Ralf Möller

The Graduate School
Yonsei University
June 2011

Abstract

Returning home from an outward journey is a skill important for the survival of many insects and other animals. Animals have developed navigation skills using various senses, including visual, auditory, olfactory, magnetic, and internal motion sensors as odometry. Their homing performance is shown to be robust. Inspired by their efficient navigation capabilities, researchers have begun designing bio-inspired navigation algorithms for robotic experiments. Here we pay attention to the landmark navigation of insects due to their excellent navigation performance.

Vision-based homing navigation has been studied through a number of bio-inspired algorithms. Since vision contains richer information than any other senses, many advanced techniques can be adopted by the vision-based navigation. A remembered view of home location from a variety of positions was used for the development of the navigation algorithm. In this thesis, among several different types of the methods and objectives of the homing navigation, we focus on searching the direction of movement as a way to reach the goal location from an arbitrary position, named as homing navigation.

A visual homing method exploits the intensity of images and relies on landmarks. Various ideas have been suggested regarding the feature selection criterion and the correspondence-matching algorithm for the landmark-based navigation. As a step toward developing the visual homing method, we designed three objectives in this thesis: (1) to suggest a new homing navigation algorithm, (2) to evaluate the performance of the suggested navigation method in various perspectives along with the comparison with other existing vision-based navigation methods, and (3) to apply the method to robotic experiments and to analyze the results.

First we suggest a new algorithm for the homing navigation, so-called the distance-estimated landmark vector (DELV) method. The method uses the landmark information in snapshot images as vectors, which is used to determine a homing vector. Second its performance is measured in various forms, such as vector maps, angular error, and the success rate in homing with catchment area. Comparing its results to those of other existing navigation methods, we demonstrate the effectiveness of our method. Other navigation methods were compared to the DELV method with and without a reference compass. Lastly the robotic experiments were conducted under two different environments: one with artificial landmarks and the other with natural landmarks such as desk,

flower pot, chair and others.

In conclusion we propose a new algorithm for landmark-based homing navigation and investigate its performance in various point of views. The analysis results on the characteristics of the method suggest a future direction for further enhancements in the navigation algorithm.

Acknowledgements

This thesis work would not have been possible without the support of many people. It is a pleasure to thank to all of those who supported me in all the respects during the completion of my thesis project. I am heartily thankful to my supervisor, Prof. DaeEun Kim, whose encouragement, guidance, and support from the initial to the final level enabled me to develop an understanding of the subject. I like to show my gratitude to Prof. Euntai Kim and Prof. Möller for critical reading and comments on my thesis. All the group members at the Biological Cybernetics Lab. have helped and inspired me. In particular, I like to thank Miyoung Sim for her friendship and help in the lab. I am grateful to Jaehong Lee and Sangwook Park for their support and help through our interactions. Finally, I thank my parents and my brother for supporting me throughout all my studies. This thesis would not have been possible without their love and care.

Declaration

I declare that this thesis was composed by myself, that the work contained herein is my own except where explicitly stated otherwise in the text, and that this work has not been submitted for any other degree or professional qualification except as specified.

(Seung-Eun Yu)

Table of Contents

1	Introduction	1
1.1	Why bio-inspired model for robotic navigation?	1
1.2	Vision-based robot navigation	3
1.3	Motivation and objectives	4
1.4	Organization of dissertation	4
2	Background	7
2.1	Navigation in animals	7
2.2	Local visual homing	12
2.2.1	Holistic methods	13
2.2.2	Landmark-based methods	15
2.3	Summary of Chapter 2	20
3	Distance-estimated landmark vector (DELV) method	21
3.1	Basic concepts	21
3.2	Methods	22
3.2.1	Distance estimation	23
3.2.2	Distance quantization	25
3.2.3	Reference map and localization	27
3.2.4	Arrangement matching with landmark vectors	28
3.3	Mathematical description	30
3.3.1	Landmark matching in the arrangement order	31
3.3.2	The DELV method and the average landmark vector (ALV) model	34
3.4	Summary of Chapter 3	37
4	Navigation performance	39

4.1	Performance evaluation	40
4.2	Simulation experiments	42
4.3	Simulation experiments: with quantized distance	51
4.4	Robotic experiments	55
4.4.1	Results with artificial landmarks	55
4.4.2	Results with natural landmarks	59
4.5	Summary of Chapter 4	62
5	DELV with reference compass	65
5.1	Performance evaluation	66
5.2	Simulation experiments	69
5.3	Robustness analysis	71
5.3.1	Occlusion problem	73
5.3.2	Navigation method with visual reference compass	77
5.4	Summary of Chapter 5	80
6	Conclusion	83
6.1	Estimation and quantization of the landmark distance	84
6.2	Comparison with other methods	85
6.3	Future work	86
6.3.1	Landmark extraction	86
6.3.2	Localization	86
6.3.3	Occlusion problem	87
6.3.4	Interaction with odometry information	88
6.3.5	Combination with place cell	89
6.3.6	Biological modeling	90
	Bibliography	91

List of Figures

2.1	Foraging trip of an individual ant, <i>Cataglyphis fortis</i> . Outbound trips are depicted by solid lines and inbound trajectories by stippled lines. N represents the nest, and F is the food location. The length of the outbound path is 354.5m and the maximal distance from the nest is 113.2m. Time marks depicted as small filled circles are given every 60sec. (Reprinted from Müller and Wehner (1994))	9
2.2	Homing path of two desert ants <i>Cataglyphis fortis</i> . N is the nesting site, and F is the feeding site. The ants had arrived at F (dotted trajectory) and were subsequently, after returning to N, displaced back to F to return home with vector information removed (solid trajectory). Both paths show similar returning. (Reprinted from Wehner et al. (1996a)) .	10
2.3	Summary of the firing properties of a CA1 Hippocampal Place Cell. The figure at the top shows the ‘firing rate map’ with the time-averaged firing rate of the cell as a function of the rat’s head position. Two maps at the bottom show the spike activity on two separate paths through the field. The black line indicates the moving path of the rat, red dots are the location at which action potentials were fired, and the grey pixels indicate the location of the firing field, copied from the rate map. (Reprinted from Muller (1996))	11
2.4	Difference function of the r.m.s. pixel differences of the image. The location of the reference image has the steepest value of the difference function. (Reprinted from Zeil et al. (2003))	14

2.5	Warping method. The warping is applied to produce a warped(distorted) view from the original current view. The warped view is compared to the reference snapshot image to determine the image distance. Differently hatched squares in the figure indicate pixels with different intensities. The one-dimensional images are closed in horizontal direction as indicated for the snapshot image. (Reprinted from Möller (2009))	15
2.6	Example of landmark extraction based on the luminance. After applying a threshold to each pixel, a horizontal area is extracted. A pixel in the segmented horizon will be black if more than 50% of the pixels in the corresponding column are black. (Reprinted from Lambrinos et al. (2000))	17
2.7	Computing a homing direction with non-distinctive landmarks. Each landmark i produces a local correction vector V_i , the summation of which determines the homing direction H_s . Given only landmark bearing information, each correction vector attempts to improve the perceived bearing of its landmark to better match with that observed from home H . (Reprinted from Weber et al. (1999))	18
2.8	Average landmark vector (ALV) model using edges as landmark features. Vectors attached to the outer ring are landmark vectors contributing to the dashed ALV computed for the snapshot position. The thin solid vector is the current ALV, and the thick solid vector is the computed home vector. (Reprinted from Lambrinos et al. (2000))	20
3.1	Landmark vector representation with distance estimation: (a) a landmark diagram, (b) unit-length landmark vectors, and (c) landmark vectors with distance (polar coordination) (Reprinted from Yu and Kim (2011d))	23
3.2	Image shift of landmarks. The agent moves from the position P to C (moving distance d), the head orientation angle changes by ψ , and the viewing angle of a landmark from θ to $\theta + \delta$ (Adapted from Yu and Kim (2010a))	24
3.3	Example of the landmark distance quantizations: (a) one-level quantization, that is, an equidistance assumption and (b) an example of three-level distance quantization (Adapted from Yu and Kim (2011d))	26

3.4	Rotational shift of landmark arrangements. Projecting perceived landmark vectors (x_1, x_2, x_3) (black arrows) into the reference map (large circles) depends on the landmark arrangements (x_i indicates the projection of the i -th landmark) (a) correctly matched arrangement, (b) $(L1, L2, L3)$ match (x_3, x_1, x_2) , respectively, and (c) $(L1, L2, L3)$ match (x_2, x_3, x_1) , respectively (Reprinted from Yu and Kim (2011d))	28
3.5	Landmark vectors in the reference map with the estimation of head orientations; (x_1, x_2, x_3) are the projected landmark vectors for (a) correct head angle (b) a deviation angle 45° of the head orientation (c) a deviation angle 90° of the head orientation. (Reprinted from Yu and Kim (2011d))	28
3.6	Visualization of the (a) DELV and (b) ALV model in same environment. In (b), landmark vectors are represented as dashed arrows, and solid arrows are the average landmark vectors. The large thick solid line arrow is the homing vector (Adapted from Yu and Kim (2011b)).	34
4.1	Description of the predictive image-matching method (Franz et al., 1998); (a) the possible directions of movement for the agent and (b) the prediction of the captured image for each corresponding direction of movement (Reprinted from Yu and Kim (2011c)).	41
4.2	Vector map with the DELV method applied in three different environments: (a) environment 1, (b) environment 2, and (c) environment 3. .	43
4.3	Spatial errors in homing vector; Marker of each point indicates the amount of angular error (\bullet : less than 45° , \star : between 45° and 90° , and \triangle : greater than 90°) with corresponding vector maps in Figure 4.2. .	43
4.4	Error graphs for the DELV results in three different environments 1, 2, and 3 shown in the vector maps in Figure 4.2.	44
4.5	Catchment area with vector map for each environment. (a) 98.52%, (b) 95.41%, and (c) 77.66% of the environment. The squared region indicates that the corresponding point is inside the catchment area. . .	45
4.6	Vector map with the landmark arrangement matching method with different moving distance d : (a) $d = 20$, (b) $d = 50$, (c) $d = 100$, and (d) $d = 150$	46

4.7	Performance of the DELV method with varying moving distances in angular error graphs. Corresponding vector map results are in Figure 4.6.	47
4.8	Vector maps and angular error performance; (a)-(e) vector maps with the suggested DELV method in environments of various landmark distribution and (f) error graphs for vector maps in (b), (c), and (e). . . .	48
4.9	Vector maps; (a) the DELV method and (b) the predictive image-matching method (Adapted from Yu and Kim (2011c))	49
4.10	Performance comparison of (a) error curves of angular difference for the DELV method and predictive image-matching method and (b) the success rate among 100 trials with respect to the distance from home without a reference compass (Adapted from Yu and Kim (2011c)) . . .	49
4.11	Trajectories of a mobile robot at the same starting points for applying each (a) DELV method ($d = 50$) and (b) predictive image-matching method. Black stars indicate starting points. (Adapted from Yu and Kim (2011c))	50
4.12	Vector map with the DELV method with different quantization levels of the landmark distance: (a) level 3, (b) level 4, and (c) level 5 (● : actual and ○ : perceived location of landmarks).	52
4.13	Error curves and success rate: (a) error curve results by applying DELV with quantized distances of level 1 to 5 of the corresponding vector map results in Figure 4.12 and (b) success rate for each method	52
4.14	Vector maps and angular error performance for quantized DELV: (a)-(e) vector maps with the suggested DELV method with quantization level 3 in environments of various landmark distribution and (f) error graphs for vector maps in (a), (d), and (e).	54
4.15	Mobile robot and its environment: (a) an experimental environment with four cylindrical landmarks and the (b) ROOMBA robot with an omnidirectional camera on top. (Reprinted from Yu and Kim (2010b))	55
4.16	Omnidirectional camera and the captured image: (a) camera on the robot and (b) the snapshot taken with the camera at home location (Reprinted from Yu and Kim (2011c))	56

4.17	Panoramic snapshot image and landmark detection: (a) panoramic image converted from the omnidirectional snapshot image as Figure 4.16 (b) and (b) the landmark represented as white area (Adapted from Yu and Kim (2010b))	56
4.18	Vector map obtained in the mobile robot experiments (a) with the DELV method (adapted from Yu and Kim (2010b)) and the (b) predictive image-matching method. The dots indicate the direction of decided homing vector.	57
4.19	Error graphs of the DELV and predictive image-matching methods based on the vector map in Figure 4.18 (Adapted from Yu and Kim (2010b)).	58
4.20	Vector map with the DELV method with different quantization levels of landmark distances; (a) level 1, (b) level 4, and (c) level 5.	58
4.21	Error curves results applying DELV with quantized distance of level 1, 2, and 5 of corresponding vector map results in Figure 4.20	59
4.22	Unstructured environment for robotic experiments with natural landmarks such as a table, a flower pot and a drawer (Reprinted from Yu and Kim (2011d)).	60
4.23	Panoramic snapshot images and segmentation of landmarks; (a) and (b) are panoramic snapshots taken and (c) and (d) show the region of interests by eliminating floor, ceiling and wall. The landmarks are marked as squared regions (Reprinted from Yu and Kim (2011d)).	60
4.24	Vector map and homing path for several points from the experimental environment shown in Figure 4.22. Landmarks are described as circles and rectangles in the map showing (a) homing path and (b) homing vector (Reprinted from Yu and Kim (2011d)).	61
5.1	Summary of the homing vector (<i>HV</i>) computation in both (a) DELV and (b) ACV method. Dotted arrows: landmark vectors at home location, solid arrows: landmark vectors at current location (Reprinted from Yu and Kim (2011b))	68
5.2	Vector map with DELV method applied in three different environments with reference compass (Reprinted from Yu and Kim (2011b)).	69

5.3	Spatial errors in homing vector. Marker of each point indicates the amount of angular error (.: less than 45° , *: between 45° and 90° , and \triangle : greater than 90°) with corresponding vector maps in Figure 5.2. (Reprinted from Yu and Kim (2011b)).	69
5.4	Error graphs for DELV results in three different environments 1, 2, and 3 shown in vector maps in Figure 4.2.	70
5.5	Catchment area with vector map for each environment: (a) 92.01%, (b) 97.04%, and (c) 84.91% of the environment. The squared region indicates that the corresponding point is inside the catchment area (Reprinted from Yu and Kim (2011b)).	70
5.6	Vector maps: (a) DELV method (b) ACV method, and (c) ALV model with a reference compass	71
5.7	Performance comparison of (a) error curves of angular difference for DELV, ACV, and ALV method all with reference compass and (b) success rate among 100 trials with respect to the distance from home with a reference compass	72
5.8	Trajectories of a mobile robot at the same starting points for (a) DELV method ($d = 50$), (b) ACV method, and (c) ALV model with starting point indicated as black stars	72
5.9	Graphs showing error points as the number of occluded landmarks increases from (a) zero, (b) one to (c) two (Reprinted from Yu and Kim (2011b)).	74
5.10	Catchment area with vector map for each environment: (a) 92.01%, (b) 82.04%, and (c) 59.11% of the environment. The number of landmarks is zero for (a) and one, two for (b) and (c), respectively (Reprinted from Yu and Kim (2011b)).	74
5.11	Vector maps and catchment area obtained with (a) DELV, (b) ACV and (c) ALV algorithms along with the heading direction estimation obtained with the visual compass method. Catchment areas for each case are 74.85%, 47.04%, and 40.68%, respectively (Reprinted from Yu and Kim (2011b)).	79
5.12	Error graphs obtained from the DELV, ACV, and ALV methods with the visual compass method. The corresponding vector maps are shown in Figure 5.11 (Reprinted from Yu and Kim (2011b)).	80

List of Tables

5.1	Error point rate(%) for each environments with different landmark distribution (Adapted from Yu and Kim (2011b))	75
5.2	Error point rate(%) for each environments with different landmark number (Adapted from Yu and Kim (2011a))	76
5.3	Catchment area rate(%) for each environments with different landmark distribution (Adapted from Yu and Kim (2011b))	77
5.4	Catchment area rate(%) for each environments with different landmark number (Adapted from Yu and Kim (2011a)).	78

Chapter 1

Introduction

Small insects and other animals have their own simple navigation algorithms. Although they operate with small number of neurons, they demonstrate great ability in accurately returning to their nests. Such a mechanism, which is feasible for the lower level organisms, has inspired many researchers conduct to overcome the problem of complexity of the conventional navigation algorithms in robotics. By modeling the biological methods of insects and other animals, the navigation systems can be more effective yet simpler. Further they do not require a larger amount of memory than the conventional algorithms. In this chapter, we introduce a bio-inspired robotic navigation system, especially with emphasis on the use of visual information, and present the motivation and objectives of the paper.

1.1 Why bio-inspired model for robotic navigation?

Many animals as birds, fish, and turtles migrate seasonally over thousands of kilometers distances, while insects as bees and ants return to important places after foraging or exploring the environment. Returning home after an outward journey is an important skill required for the survival of many insects and other animals. Animals have developed navigation skills using various senses, including visual (Wehner and R ber, 1979), auditory (Rossier et al., 2000), olfactory (Papi, 1990), magnetic (Luschi et al., 1996), and internal motion senses(Collett and Collett, 2000).

Navigation skills of animals show robust performance with regard to homing. Inspired by such efficient navigation capabilities, researchers have begun designing bio-

inspired algorithms for robotic systems. Ethologists studied the behavior of animals by examining how they explore the environment and return home immediately after finding and collecting food. The performance of animals in navigation and environment perception exceeds that of any other mathematical methods developed for mobile robots. Therefore, it is natural for researchers to attempt the imitation of the behavior of animals and to obtain the level of their natural performance.

Recently there have been a number of researches modeling robotic systems after animals. Mimicking the appearance of insects and other animals led to a novel movement or unique function in robots, and modeling the behavioral mechanism of the animals have guided researchers to the development of their work in various perspectives.

For example, recently a climbing robot mimicking the behavior of gecko was developed (Kim et al., 2008). The robot's gait and motion coordination was introduced from the characteristics observed from the gait of a gecko. The study on the adhesive foot of a gecko led to the development of a novel material with directional adhesion, which enables the climbing ability of a gecko-robot. The robotic model of cricket phototaxis (Webb, 1995) and robotic model and system of olfactory-guided exploration strategies of invertebrates (Grasso, 2001) were suggested by modeling the behavior of animals using unique senses. In addition, the navigation of Sahabot using the polarized light compass was inspired by studies of homing behavior in the desert ant (Lambrinos et al., 1997). Biomimetics is an important field of research for both engineering and biology. In a technological point of view, we can obtain a more efficient system inspired by animals while the implementation of the behavior of animals in computational methods allows biologist to verify and examine hypotheses in a more objective and numerical way.

One of the advantages of a bio-inspired system is its ability to respond to an external stimulation in a simple and immediate manner. Insects and other animals are not able to compute complex mechanisms to process perceived information and make judgements as computers. Animals are specialized to particular sensor mechanisms. Therefore, systems modeling the sensory and mechanical system of animals would lead to much simpler and adaptive system than the other mechanical devices. Hence, studying the behavioral mechanism of the animals and applying their algorithms computationally can be associated with implementation of a compact intelligent system in robotics. In this respect, the bio-inspired researches are worth studying, and therefore can be expected to show various performance.

1.2 Vision-based robot navigation

Since it takes richer information than any other senses and is able to adopt many advanced techniques, vision has been widely researched for navigation. Early works mainly focused on the mapping of environmental structure so that a mobile robot could detect objects and navigate through the environment autonomously. A geometrical interpretation of the environment allows the robot to estimate its own position and identify the structure of the environment. One of the early works of mapping in visual navigation was elaborated by Moravec (1977). In this work, a stereo vision is used with the binocular set of cameras to reconstruct the environment. Objects in an indoor environment are set with cones on the floor. After estimating the position and the size of the objects and mapping them on a 2-D map as an obstacle, the object-free area is assigned as an allowed region for the path from the current position to the goal position. Recently, a number of researches have investigated both mapping and localizing the moving agent simultaneously, which is often called SLAM (Simultaneous Localization and Mapping) (Davison, 2003).

However, due to its complexity and the requirement of large memory space, mapping an environment is considered to be not plausible for insects and other small animals. Thus, for modeling the navigation algorithms of insects and animals, it is more convincing to focus on simpler information processing. Instead of geometrical mapping, insects may use a topological representation of space or even have no stored information about the space but only focus on the current view and the memorized scene from a goal point. The navigation in this paper concerns a type of navigation which plans a path and trajectory in its own way to reach the goal point without a geometrical map of the environment.

Since various types of the navigation methods implemented by animals and insects exhibit the extremely large range of navigation in nature, Gallistel (1990) defined navigation as *the capacity to plan and execute a goal-directed path* while Franz and Mallot (2000) edited and defined as below.

“Navigation is the process of determining and maintaining a course or trajectory to a goal location.”

Following this definition, we may narrow the scope of navigation to determining the direction of movement as a way to reach the goal location from an arbitrary position.

View-based homing navigation has been studied through a number of bio-inspired algorithms. These methods were developed to navigate home using a remembered view of the home location from a variety of positions. We consider the landmark navigation of insects because of their excellent navigation performance.

1.3 Motivation and objectives

Motivated by the simple yet robust vision-based navigation of insects, we propose various ideas to model the landmark-based navigation algorithms. The main purpose of this research is to find a novel and efficient homing navigation method.

The detailed objectives are as follows:

Suggestion of vision-based homing navigation method. We introduce Distance- Estimated Landmark Vector (DELV) model as one of the landmark-based homing navigation algorithms. We also suggest a method based on quantized landmark distances.

Performance comparison with and without a reference compass. We compare our suggested method with several existing image-based navigation methods, which do not require any reference compass. We also compare the results of the DELV method with the reference compass information combined with the suggested landmark navigation algorithm and evaluate the performance in various perspectives.

Robotic experiments and further evaluation on the method. We present the results of robotic experiments for the suggested method. In addition, evaluate the robustness of the method and compare it with other methods.

1.4 Organization of dissertation

In this chapter, we introduced the motivation and concept of bio-inspired research and the objectives of the vision-based homing robot navigation methods, which we propose and investigate in this paper.

In Chapter 2, background on the existing visual navigation algorithms is given by reviewing earlier works. Vision-based navigation can have many different types. Among different types, we focus on homing navigation. The homing navigation can be classified as one of the guidance methods. The visual homing method, which relies on image information, can be divided into two groups: holistic method and landmark-based method. Several methods in each classification will be discussed later in the following chapters for the performance comparison.

In Chapter 3 we propose the landmark-based homing navigation algorithm. The method consists of three major steps: a distance estimation, the creation of a reference map and localization step, and the arrangement matching of landmark vectors. Starting from basic concepts of the proposed algorithm, we describe the detailed procedure of method along with the mathematical description. The performance of the proposed method is shown in the following Chapter 4. The simulation experiments in various conditions are provided with respect to the angular error for determined homing vectors, and the success rate in homing. Results of robotic experiments are shown for the two different types of environments with artificial and natural landmarks. Results are compared to those of the image-based navigation methods without a reference compass.

In Chapter 5, we apply the quantized distance information to the proposed DELV navigation model. The concept of the estimated distance quantization is explained and experimental results are presented. The results of the performance in both simulation and robotic experiments are shown.

Our DELV navigation method does not necessarily require the reference compass information, and shows a similar level of performance with a small amount of enhancement when the reference compass is applied. Thus, in Chapter 6, the DELV method with a reference compass is compared to another landmark-based navigation method which requires compass information. For the appropriate comparison in performance, detailed conditions were set equally for both methods. Along with the comparison of the angular error and the percentage of catchment area, the robustness of the method is examined with respect to the occlusion problem.

Finally, the performance results from different experiments and environments are discussed in Chapter 7. We explain the advantages of the DELV method and discuss the future directions as an extension of this research work.

Chapter 2

Background

Many insects and other animals determine a homing direction based on visual information. A ‘snapshot model’ was suggested to explain their navigation system. The snapshot model compares a current snapshot image with the snapshot taken at a goal location to obtain a direction toward the goal. A number of methods have been suggested to process the snapshot image. Holistic methods assess the similarity between the current and the goal images, and the agent navigates in the direction that decreases the discrepancy because the difference between the two images would be minimized at the goal point. On the other hand, landmark-based methods consider particular features in several images in order to match the common regions. In landmark-based methods, distinctive features are selected and identified. Then the regions are matched based on the correspondence of the features in order to derive a movement vector. To propose a new homing navigation algorithm, we examine the central ideas in the algorithms of both methods, and probe the advantage and weakness of each method.

2.1 Navigation in animals

The most popularly known navigation method for insects and other animals is path integration, which is also known as *dead reckoning*. The path integration is known to be used in many animals such as desert ants (Müller and Wehner, 1988), fiddler crabs (Zeil and Hemmi, 2006), honeybees (Collett and Collett, 2000) and gerbils (Etienne and Jeffery, 2004; Mittelstaedt and Mittelstaedt, 1980). This approach integrates the distance and direction of movement to enable animals to find their way home. Based

on movement speed and directional information, they continually calculate their position relative to the starting point. An internal reference compass and internal motion sensors are required to perform the path integration. After accumulating the angle and distance data until foraging or exploration ends, animals can have the direct path information consisting of the direction and the distance to the target position, which is usually home. This information will allow agents to head directly toward their goal position within some errors. The path integration technique is useful in an unfamiliar environment, especially when no visual landmarks exist as guidance cues.

An outstanding example of the path-integration-using insect is a desert ant *Cataglyphis fortis* (Müller and Wehner, 1994). Figure 2.1 shows the path of a desert ant of returning home after an outward journey for foraging food. Compared to the tortuous outbound path (solid line), the inbound path is closer to a straight line (stippled line). The path integration is important and useful to desert ants, since they live in a desert which is usually a featureless large area with no prominent landmarks. The foraging desert ants keep track of their own current position with respect to home by integrating the trajectory of the movement. Since the vector summation of ants are not as precise as we do by the computer, but rather done by simple approximation, the method produces small navigational errors. The desert ant can return home using path integration even after a journey of hundreds of meters (Wehner and Srinivasan, 1981).

Mittelstaedt and Mittelstaedt (1980) showed the homing ability of gerbils, *Meriones unguiculatus* by path integration. In the experiment, gerbils could retrieve their youngs from a circular arena by returning to the nest location starting from the border of the arena. When the platform was rotated, they returned to the position where they thought was home, which was actually a deviated point from the real home by the amount of which the platform was rotated. The performance indicated the idiothetic behavior of gerbils, yielding that the vertebrate as well as the invertebrate species perform path integration for navigation using internal cues.

The path integration has been studied widely and implemented in various forms including simple robotic navigation (Yamauchi et al., 1999) and a neural model (Haferlach et al., 2007).

However, since path integration depends on the integrated movement paths, errors may arise after a long-term exploration. As the navigational errors are also accumulated along with the useful information during the exploration, the resulting vector pointing

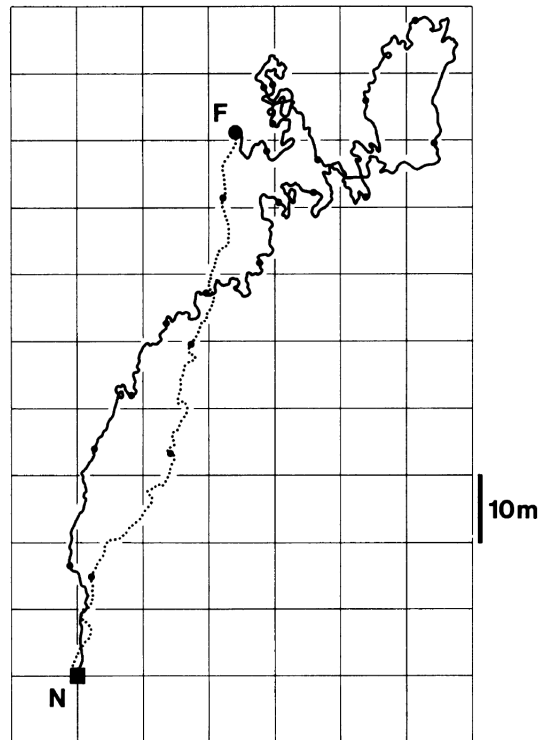


Figure 2.1: Foraging trip of an individual ant, *Cataglyphis fortis*. Outbound trips are depicted by solid lines and inbound trajectories by stippled lines. N represents the nest, and F is the food location. The length of the outbound path is 354.5m and the maximal distance from the nest is 113.2m. Time marks depicted as small filled circles are given every 60sec. (Reprinted from Müller and Wehner (1994))

the target position would possess a considerable amount of deviation. Errors in motion or reference direction accumulate, meaning that the longer the outward trip, the more difficult will be the return trip. However, if it were possible to exploit additional information to path integration, the number of accumulated errors would decrease. When no information is available about the integrated path, the animal can use visual senses such as the image of the horizontal skyline surrounding the nest (Basten and Mallot, 2010) or a distribution of landmarks (Wehner et al., 1996b).

Researchers have observed that desert ants are able to return home successfully after short wanderings when they are displaced to an unknown location, indicating that ants use visual information in addition to path integration (Wehner et al., 1996a). They compared the homing path of normal ants and that of the ants whose vector information is removed. As in Figure 2.2, the ants without vector information returned home in almost the same path as it did with the homing vector from path integration. Combining

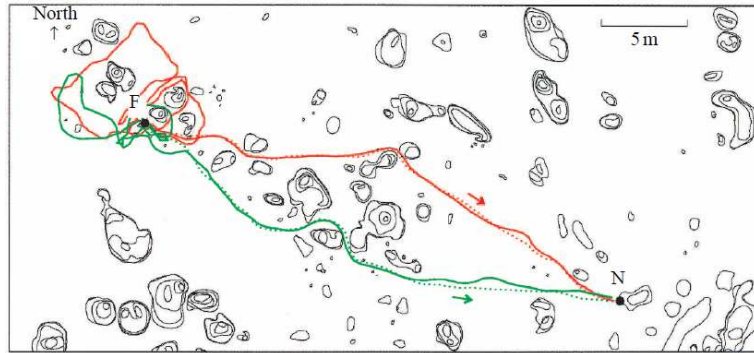


Figure 2.2: Homing path of two desert ants *Cataglyphis fortis*. N is the nesting site, and F is the feeding site. The ants had arrived at F (dotted trajectory) and were subsequently, after returning to N, displaced back to F to return home with vector information removed (solid trajectory). Both paths show similar returning. (Reprinted from Wehner et al. (1996a))

multiple sources of information leads to more successful homing. As well as desert ants, crabs (Hemmi and Zeil, 2003), and gerbils (Etienne et al., 1996) also combine internal motion cue and the vision-based information which continuously interact in a complementary way to return home more accurately. The visual information is an external cue while the self-motion is considered as an internal cue. The simplest way of binding these two different informations is to first use path integration to get near the nest, and then switch to the searching for the familiar visual cues near the nest. Both hamsters (Seguinot et al., 1993) and ants (Müller and Wehner, 1994) use this type of method to combine path integrator and visual guide.

Various methods were suggested to explain the algorithm of insects and other animals handling the visual information. Different visual image processing strategies lead to different types of movement and performance in navigation.

Rodents and gerbils exploit the place cells of hippocampus for processing visual information (Butz et al., 2010). The hippocampus is a neural network structure that supports the spatial representation in mammals (Trullier and Meyer, 2000; Touretzky and Redish, 1996). Place cells are associated with certain visual locations, and when the animal explores specific region in space, the place cells are activated based on the places visited, leading to the production of cognitive maps (Trullier and Meyer, 2000). The firing pattern is the place fields (Muller, 1996) (see Figure 2.3). The firing place cells correspond to the local environment in the neuronal representation. This topolog-

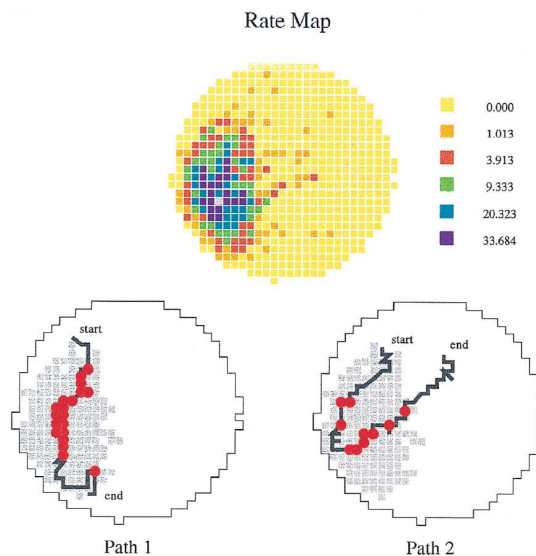


Figure 2.3: Summary of the firing properties of a CA1 Hippocampal Place Cell. The figure at the top shows the ‘firing rate map’ with the time-averaged firing rate of the cell as a function of the rat’s head position. Two maps at the bottom show the spike activity on two separate paths through the field. The black line indicates the moving path of the rat, red dots are the location at which action potentials were fired, and the grey pixels indicate the location of the firing field, copied from the rate map. (Reprinted from Muller (1996))

ical representation of the environment can be used to identify the present location and to navigate to the desired endpoint (O’Keefe and Burgess, 1996).

While mammals as rodents and gerbils use place cells for the vision-based navigation, insects use a much simpler representation of the environment. Many hymenopterans, socially organized insects, are known to perform visual landmark-based navigation to guide them in their return to their nest. Insects perform homing navigation using snapshot images taken at specific locations, which is somewhat different from rodents. Such method is called ‘snapshot model’ (Cartwright and Collett, 1983, 1987; Collett, 1996). The snapshot model basically compares the current snapshot image with the snapshot image taken at the goal location to obtain the direction toward the goal. Comparing snapshot images, among the several possible directions, the moving direction that decreases the discrepancy between two images the most is chosen as a homing direction. The snapshot model has shown its potential to be actually used in insects through experiments (Cartwright and Collett, 1983), and since it is a simple and effective method proved its performance in various suggested navigational algorithms.

Detailed characteristics of such algorithms will be given in the following.

2.2 Local visual homing

Many insects and other animals return home by exploiting visual information in different methods (Wehner et al., 1996a; Hemmi and Zeil, 2003; Etienne et al., 1996). Navigation can be in many different types such as *place recognition-triggered response*, *topological navigation*, *metric navigation*, and *guidance* (Trullier et al., 1997). Trullier et al. (1997) and Franz and Mallot (2000) elaborated the *guidance* navigation method in classifying navigation into several categories. Considering the configuration of the surrounding objects, the *guidance* method can process an egocentric object information and determine the goal direction (Franz et al., 1998; Graham and Collett, 2002). Therefore, acquiring spatial information of the environment, the agent obtains direction to the goal point, its current location compared to the goal, and the configuration of the objects surrounding.

For the navigation of animals, returning to the starting point of a journey is the most important and interesting task but yet the simplest form of navigation for animals including humans. This type of navigation is called homing, which could be classified as one of the guidance methods. Many social insects as ants, bees, and wasps do foraging trips and exploring the surrounding environment of their nest. These trips may range from hundreds to thousands of meters (Wehner and Srinivasan, 1981). Therefore, local homing along with the simple and computationally cheap navigation method is an important point of view in the simple navigation of insects, which also receives attention from the neuroethology.

Based on multiple snapshot images, the agent can obtain depth information of the view. Several approaches were suggested using multiple vision sensors to extract accurate depth information (Stürzl and Mallot, 2002) or special sensors as panoramic stereoscopic sensor (Huang and Klette, 2009). However, in modeling inspired by the navigation of insects, it is more appropriate to use a simple vision sensor. The information that can be easily obtained with the common snapshot image is the intensity.

The intensity of the snapshot image can be easily obtained from an ordinary image through vision sensor. The visual homing method by exploiting the intensity of image can be coarsely classified into two groups: *holistic method* and *landmark-based*

method. Holistic method treats the obtained image as a whole. It does not require any matching procedure neither any feature selection procedures and deals with the image intensity information as taken. On the other hand, in the landmark-based method, features in the environment are considered as *landmarks*, and the navigation method attempts to establish features between two images. This method varies with respect to the feature selection criterion and the correspondence matching algorithm.

2.2.1 Holistic methods

Holistic methods assess the similarity between the current and the goal images, and the agent navigates in the direction that decreases the discrepancy because the difference between the two images would be minimized at the goal point. Holistic methods perform local visual navigation without any correspondence matching procedures. By treating the image as a whole, the methods avoid the correspondence problems arising when features are not distinctive enough to distinguish one from another. While correspondence matching methods require both feature extraction and the matching procedures, the feature matching between images is not necessary in holistic methods. Different metrics are used to calculate the level of difference; the direction of movement can be determined based on the descent of the image distance using the root mean-square difference of pixel intensities (Zeil et al., 2003) or through the Euclidean distance in some parameter space, in which the parameters can be derived from the whole image. The *DID(descent in image distance) method* and the *warping* are two of the various algorithms in holistic methods.

Descent-in-image-distances(DID) method has been introduced by Zeil et al. (2003) and investigated by many researchers (Stürzl and Zeil, 2007; Möller et al., 2007). The image difference becomes much smaller when two points are closer as in Figure 2.4. Although the shape and smoothness of the curve varies with respect to the illumination and display, the characteristics of the minimum image difference at the goal point is maintained (Stürzl and Zeil, 2007). By applying simple gradient descent methods, the navigation algorithm successfully finds the direction to the goal location. Möller and Vardy (2006) showed the extension of the DID method by including the prediction concept. “Matched filter” indicates the fixed template flow fields for purely translational movement. That is, by projecting the intensity gradient onto the matched filter, the agent could predict the image it would obtain when the corresponding movement

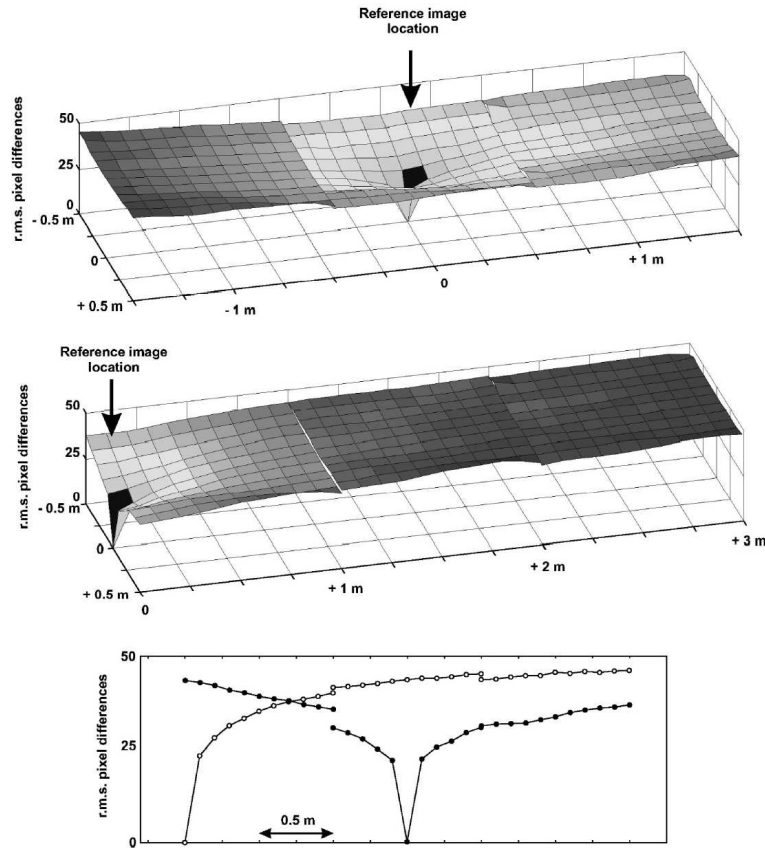


Figure 2.4: Difference function of the r.m.s. pixel differences of the image. The location of the reference image has the steepest value of the difference function. (Reprinted from Zeil et al. (2003))

is performed. Therefore, the method yields the homing direction by computing the descent in image distance of the matched-filter.

Another method of the holistic methods is the *warping*. Franz et al. (1998) suggested the method of appropriately distorting the current snapshot image to best match the target snapshot image as described in Figure 2.5. The agent predicts new image for every possible directions to move from the current location by warping the image in a predicted manner. This prediction is equivalent to the concept of projecting the one dimensional landmark information on the matched filters of flow fields. Then the method determines the homing direction, which matches the predicted image best with the reference image. However, The predictive warping method is largely affected by the characteristics of the environment. When there are too many objects in the environment, the performance is degraded. Möller (2009) elaborated the warping method computationally and showed the performance for several databases. In addition to original

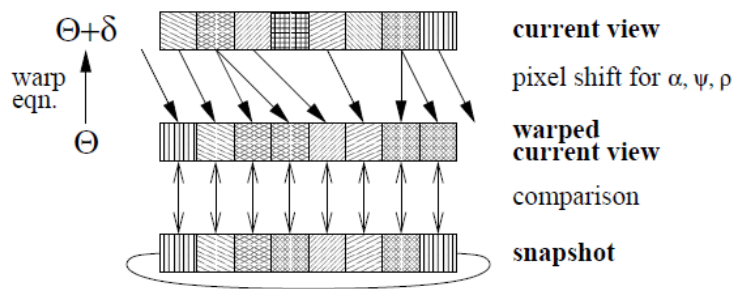


Figure 2.5: Warping method. The warping is applied to produce a warped (distorted) view from the original current view. The warped view is compared to the reference snapshot image to determine the image distance. Differently hatched squares in the figure indicate pixels with different intensities. The one-dimensional images are closed in horizontal direction as indicated for the snapshot image. (Reprinted from Möller (2009))

warping method, 2D-warping method was also suggested with improved performance (Möller et al., 2010). Similar to the descent-in-image-distance (DID) method, fitting the warped image with the appropriate curve to the minimum point of the computed distance in images yields the horizontal and vertical angle in mathematical way.

While the DID method searches the descent in image distance, the warping method searches for the minimum point of distance in the image and distort the image to fit the reference image. Since the warping does not require reference compass, it is a competitive navigation method with fine performance.

2.2.2 Landmark-based methods

Landmark-based methods consider features or landmarks in the environment and set up correspondence between features in two images: one from the goal and the other one from the current location. Since the landmark-based method determines a direction to move by establishing a connection between features, one of the factors that affects the performance of the method is the type of features in the image to be selected.

One of the most popular feature SIFT (Scale Invariant Feature Transform) has been used to determine landmarks of the environment and localize the mobile agent (Se et al., 2002; Lowe, 2004). Using SIFT can be efficient but yet requires large amount

of computation. For simpler methods of selecting features, one can use information such as color of the objects, dark and bright regions, and edges and corners. Color is an efficient criterion to distinguish landmarks (Szenher, 2008). Gourichon et al. (2002) created one-dimensional panoramic snapshots with colors defined as HSV (Hue, Saturation, and Value) parameters rather than RGB. The HSV representation is much less dependent of luminance level than the RGB color model so that it can robustly detect landmarks. Goedemé et al. (2005) also suggested a reduced form of SIFT features to work on color images by including the matching of color descriptor of the feature patch. Another type of simple feature extraction method is corner extraction (Vardy and Oppacher, 2003). One of the popularly used corner detection scheme is Harris detector where only the local convolutions and sums are required for the computation.

As it is shown above, selecting distinctive features leads to the necessary matching procedure of each feature. Therefore the feature extraction method attempts to provide identifiable information for each feature. Instead of selecting distinctive features the navigation method can select non-distinctive landmarks and include an additional matching procedure. As suggested from the experiments on insects, the use of dark and bright regions as the landmarks suggested through the experiments on insects provides non-distinctive landmarks of a given image. In the navigation of honeybees, the sector matching was done by pairing every light and dark sectors, the gap and landmark, in the snapshot with the closest sector in the image of the same intensity (Cartwright and Collett, 1987). Landmark extraction based on the luminance level of the image has shown to be useful in robotic experiments. Hong et al. (1991) exploited the luminance intensity information of each one-dimensional circular form of snapshot. Lambrinos et al. (2000) showed image processing for landmark navigation by segmenting a region into black and white areas obtained with omni-directional cameras in Figure 2.6.

Weber et al. (1999) demonstrated a computation of the homing direction based on several non-distinctive landmarks. The correspondence between landmarks does not guarantee 100% correct matching, but only works as an approximation. To avoid the complexity in computation, they decided to accept some deviation in homing direction instead of searching for the optimal solution. The suggested method first computes a correction vector based on the difference between the bearings to a specific landmark from the goal location and the current snapshot image. This correction vector is a direction which makes the discrepancy between two bearings smaller, that is, if the agent moves toward the correction vector, the bearing to the landmark from the current loca-

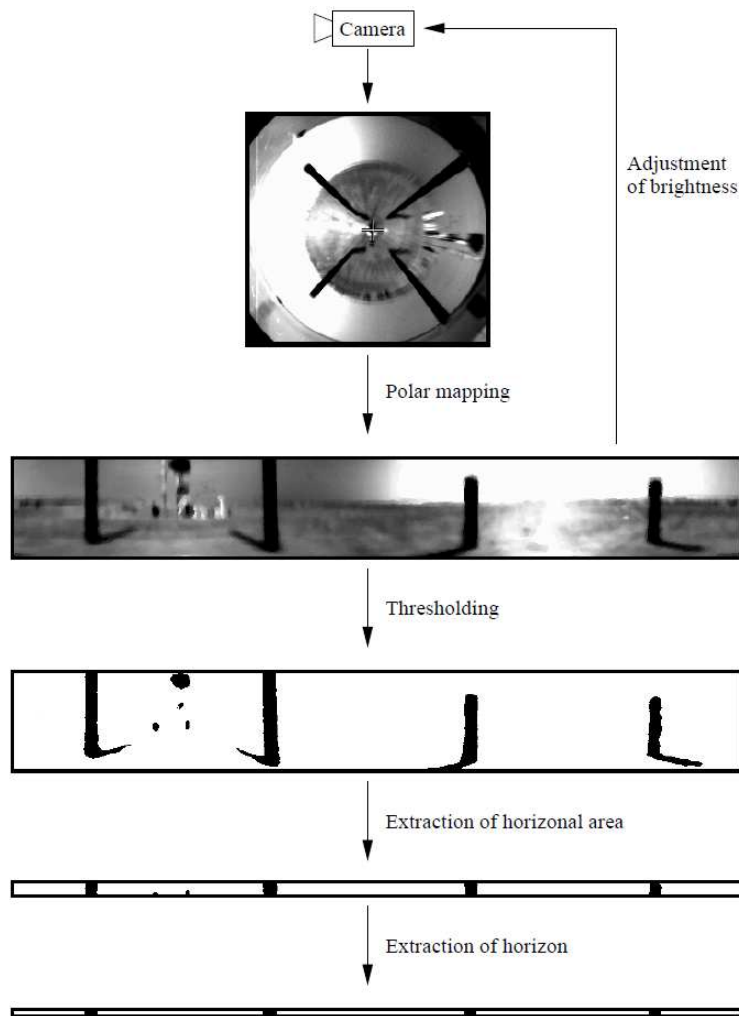


Figure 2.6: Example of landmark extraction based on the luminance. After applying a threshold to each pixel, a horizontal area is extracted. A pixel in the segmented horizon will be black if more than 50% of the pixels in the corresponding column are black. (Reprinted from Lambrinos et al. (2000))

tion becomes more similar to that of the goal location. The correction vector will be smaller if the angular difference between the bearings of the landmark from the goal and the current location is smaller (see Figure 2.8). Based on these characteristics, the homing direction can be computed by summing all the correction vectors for every landmarks available. Since the method does not search for every matching possibility but only consider few candidates, however, the arrangement can be mismatched and lead to a wrong vector for some cases. Although this homing direction may not correctly point the goal from the current location, the homing direction computed at the next step may improve the accuracy through iteration. Consequently, the homing

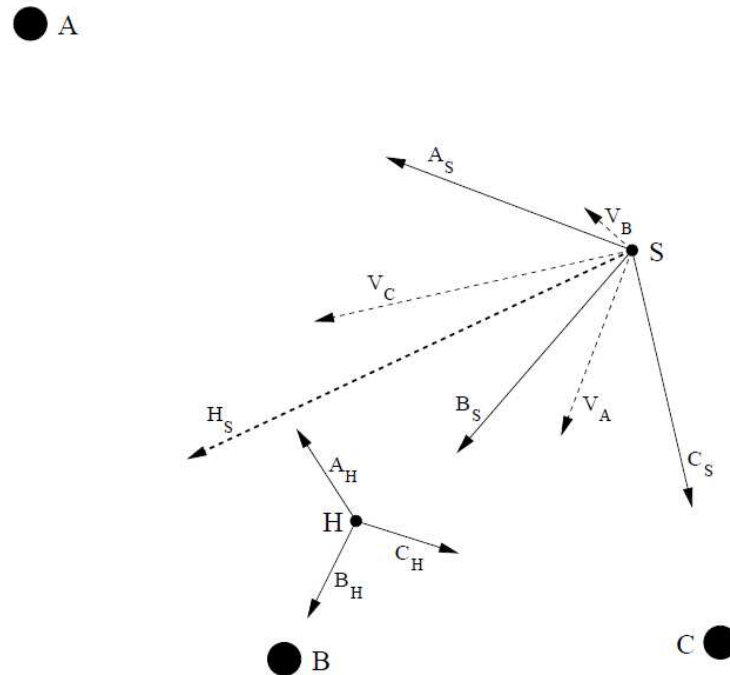


Figure 2.7: Computing a homing direction with non-distinctive landmarks. Each landmark i produces a local correction vector V_i , the summation of which determines the homing direction H_S . Given only landmark bearing information, each correction vector attempts to improve the perceived bearing of its landmark to better match with that observed from home H . (Reprinted from Weber et al. (1999))

performs successfully moving incrementally toward the goal location.

The correspondence of ambiguous features between images can be searched by computing the distances between them (Matsumoto et al., 2002). *Block matching* method introduced in the work of Vardy and Möller (2005) decides the match by searching the smallest difference between points under the assumption that two images to be compared were taken with the same orientation. The correspondence search by block matching is not made for every position in the image but only for some sampled positions, which are considered as landmark. Established matches for every sampled points lead to correspondence vectors. Each correspondence vector ideally indicates the direction of movement corresponding to the current snapshot image emerging from the reference snapshot. Inversely, by mapping every correspondence vectors on the image, it is possible to point the direction of movement to the goal point where the reference snapshot image was taken.

Unlike the navigation with perfect correspondence matching, using the non-distinctive

landmarks can result in serious deviation in homing vector. If landmarks are not distinctive, the matching between two images cannot be done precisely, but only in an approximate or probabilistic way. In the landmark-based navigation method, if the correspondence between features cannot be established, the decision of homing vector relies on a roughly estimated result. However, we can expect a gradual decrease of the uncertainty of the estimated result through the exploration, as in the probabilistic data association method used in SLAM.

There are also landmark-based methods without any correspondence matching. The average landmark vector (ALV) model, suggested by Lambrinos et al. (2000), requires an extraction of features but does not perform feature matching. In the ALV model, all the features are treated equally. The extracted features do not possess any characteristics to distinguish one from another. The ALV is calculated from the unit landmark vectors for each landmark and then it is compared with the ALV obtained at the home point. Each detected landmark vector has a unit length, and the average of landmark vectors at each point is considered to be sufficient to represent the whole snapshot image. This method uses a rather simple representation of the surrounding environment, since the only information that needs to be stored at each location is one average landmark vector. Instead of comparing two images, it is now enough to compare two average landmark vectors. Thus, instead of decreasing the discrepancy between two snapshots the agent can derive the homing vector by subtracting two ALVs. By storing the ALV at the goal point, the ALV obtained at current location is compared with the reference ALV from the goal location to determine the direction to home. The vector representation is shown in Figure 3.6. The ALV method ignores other detailed properties of the landmarks, such as the size or distance from the agent, and only considers the angular position as seen by the navigator. This navigation algorithm is simple and computationally cheap, and shows an excellent performance (Lambrinos et al., 2000). However, on the other hand, it requires a reference compass to determine the direction to move along. The ALV method can also be easily implemented in robotic experiments involving simple image processing and vector calculations. Since the ALV method requires a reference compass, its use in robotics requires a compass sensor, the precision of which plays an important role in the performance of the model (Möller, 2000). Studies on the behavior of animals have demonstrated the possibility that the ALV model is adopted by insects and other small animals (Möller, 2001). As mentioned earlier, due to the simple representation of landmarks in the environ-

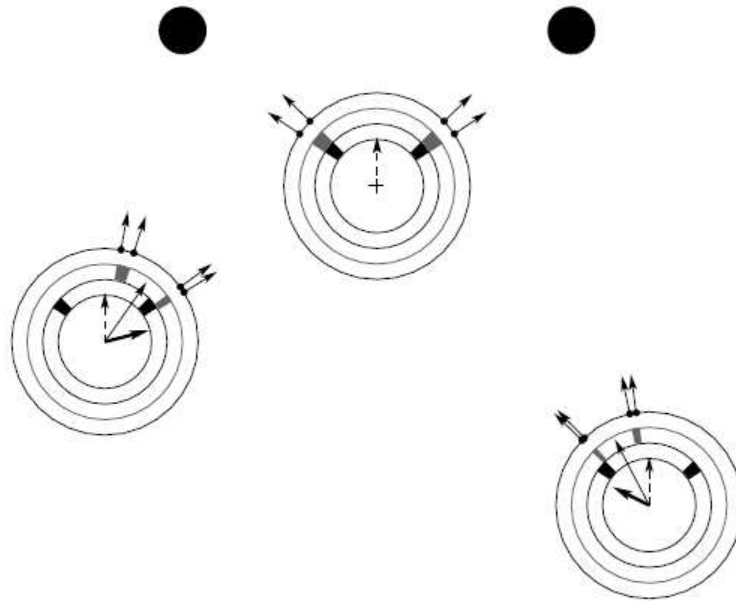


Figure 2.8: Average landmark vector (ALV) model using edges as landmark features. Vectors attached to the outer ring are landmark vectors contributing to the dashed ALV computed for the snapshot position. The thin solid vector is the current ALV, and the thick solid vector is the computed home vector. (Reprinted from Lambrinos et al. (2000))

ment, ALV can be implemented efficiently in the neural network architecture (Hafner, 2001; Hafner and Möller, 2001; Wei et al., 2005; Smith et al., 2007), and in robotic experiments (Goldhoorn et al., 2007).

2.3 Summary of Chapter 2

We examined various biologically inspired methods in local visual homing, which are simple and can be easily implemented. They do not need special sensor or platform but only require information processed from the image intensity of snapshot images. They are simple and still show good performance in local homing. A number of biological mechanisms have been shown to be appropriate for the implementation on the robot navigation (Hong et al., 1991; Lambrinos et al., 2000). For the more realistic implementation, it would be effective to combine two or more strategies to navigate through the environment. As many researchers have compared different navigation methods, the selection and application of an appropriate visual homing algorithm to the robot is important for the implementation of the robot navigation system.

Chapter 3

Distance-estimated landmark vector (DELV) method

In this chapter, we propose a new algorithm for homing navigation, distance-estimated landmark vector (DELV) method (Yu and Kim, 2010b). Our new landmark-based navigation algorithm uses distance estimation and landmark matching based on the arrangement order. The distance estimation is obtained from the egomotion of the agent. Since we exploit the distance information in addition to landmarks, we first apply the distance concept to the landmark vectors instead of setting the landmark vectors as unit length. The length of a landmark vector is set as an estimated distance or as a quantized distance. The next step is a demonstration of the landmark navigation method without a reference compass but with the distance estimation of landmarks. Replacing the compass information with the landmark arrangement order, our navigation method exhibits a successful homing performance. The DELV method was suggested in our previous works (Yu and Kim, 2010b, 2011c) and the effect and results of quantized distance applied to DELV were described as well (Yu and Kim, 2010a, 2011d).

3.1 Basic concepts

The distance-estimated landmark vector (DELV) method sets a set of landmark vectors in a way to determine the homing direction. The concept of the landmark vector in the DELV method is similar to that of the ALV model but as a significant difference.

The average landmark vector (ALV) model, suggested by Lambrinos et al. (2000),

calculates ALV based on the unit landmark vectors and then compare it with the ALV of the home location. Each detected landmark vector has a unit length, and the average landmark vector at each point is considered to be sufficient to represent the whole snapshot image. Subtracting the ALV of the home point from the ALV of the current location, the agent can determine the homing vector. To obtain the homing vector based on two average landmark vectors, however, it is necessary to have a reference compass information. The ALV model only focuses on the direction to the home point without any estimation on the current location of the agent.

Since the ALV method requires a reference compass, its use in robotics requires a compass sensor, the precision of which thus plays an important role in the performance of the model (Möller, 2000). Thus, it would be advantageous if the algorithm could operate only with visual information and with no need for a compass or other sensors.

As noted above, several navigation models require compass, however, the accuracy of the compass sensor can be affected by the motor movement of a mobile robot. Therefore, it is important to create a navigation method that does not require a reference compass. In this regard, several visual homing methods using the whole image rather than computed parameters have been suggested as navigation method without a reference compass.

3.2 Methods

Figure 3.1 shows a landmark vector representation with distance estimation in the omni-directional view. Figure 3.1 (a) is the omni-directional ring with perceived landmarks at the current location. Figure 3.1 (b) and (c) illustrate the landmark vectors. In the unit landmark vector model, all the landmark vectors have the same unit length (as in Figure 3.1 (b)) and each landmark is considered to be the same distance from the agent. In our distance estimation method, the landmark vectors can have different lengths depending on their distances to the agent.

Because of the added distance information to the landmark vectors, our proposed method can operate in the absence of reference compass information. The robotic agent can determine the proper direction based on the landmark distribution even without a compass. In this thesis, we discuss an efficient matching algorithm of landmark arrangements by using the distance estimation. Since matching each individual land-

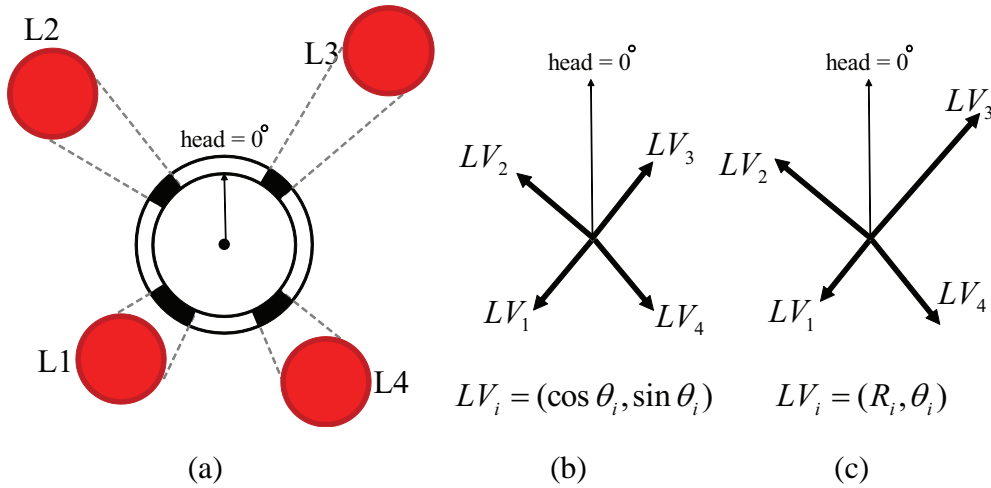


Figure 3.1: Landmark vector representation with distance estimation: (a) a landmark diagram, (b) unit-length landmark vectors, and (c) landmark vectors with distance (polar coordination) (Reprinted from Yu and Kim (2011d))

mark in different scenes requires a significant amount of information and a huge computational cost, we decided to exploit the linear order of landmark arrangements. With landmarks of no distinctive features, we perform a simple search for the appropriate order rotating the landmark arrangement to determine the homing direction. Repeating the same process, the agent is gradually guided toward the home point. We call this method as distance-estimated landmark vector (DELV) method, and will give a more detailed description of the procedure in the following.

3.2.1 Distance estimation

In the DELV method, we use an omni-directional snapshot image to acquire landmark information. An omni-directional camera provides the mobile robot with a 360° view, snapshot panoramic images of its surroundings. The omni-directional snapshot gives a panoramic image so that the agent can observe objects in every direction. Since a landmark does not disappear from the view with an omni-directional camera as long as the robot does not move significant distance, it is useful to record the landmark positions. Therefore, the viewed objects are not limited to its angular position of the agent whereas the traditional cameras have a limited view. This omni-directional feature allows more efficient (Sun et al., 2004) and unconstrained movement of the robot. In addition to this advantage, the omnidirectional camera provides a view similar to that

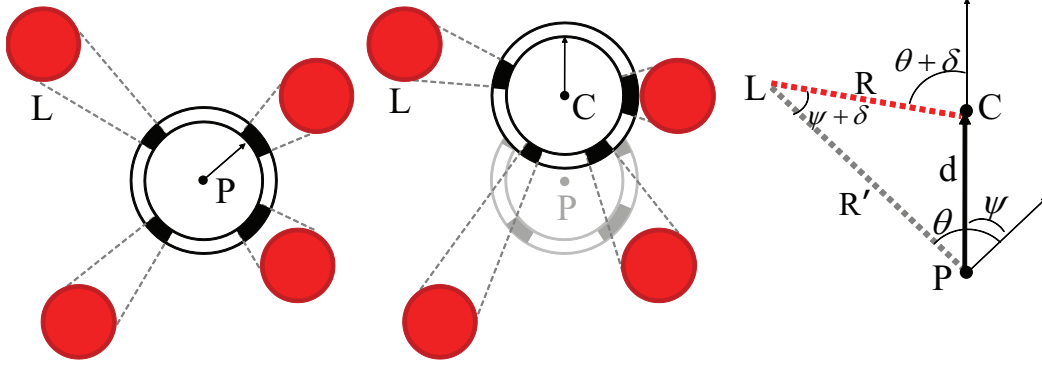


Figure 3.2: Image shift of landmarks. The agent moves from the position P to C (moving distance d), the head orientation angle changes by ψ , and the viewing angle of a landmark from θ to $\theta + \delta$ (Adapted from Yu and Kim (2010a))

of the insects' eyes. In fact this camera has been used popularly in many bio-inspired navigation method (Franz et al., 1998; Huber and Bühlhoff, 1998).

The distance to the landmark can be estimated from the angular shift of the landmark arising from the forward step move of the agent. The geometric relationship between distance and angular shift are described in Figure 3.2.

For the distance estimation, let us assume that the agent moves one step from point P to C as in Figure 3.2. The agent moves distance d for one time step. As the agent moves one step forward, the angular position of the landmark changes from θ to $\theta + \delta$. The angle θ and $\theta + \delta$ indicates the bearings of landmark at the point P and C , respectively, while ψ is the change of the heading direction in two points. For simplicity, the triangle $\triangle PLC$ in Figure 3.2 shows the relationship between each angle and the distance. The distance R from the location C to the landmark L is what we need to determine the current location at C . And the distance R' as the previous distance between L and P will be stored in the reference map. Applying the sine law to the triangle, Equation 3.1 is derived, leading to Equation 3.2.

$$\frac{\sin(\delta + \psi)}{d} = \frac{\sin(\theta - \psi)}{R} = \frac{\sin(\theta + \delta)}{R'} \quad (3.1)$$

$$R = \frac{d \sin(\theta - \psi)}{\sin(\delta + \psi)} \quad (3.2)$$

The estimation of the distance R based on two sequential images is related to a stereo-vision or optical flow analysis. If there exist moving objects in the environment, those

objects can be separated from the background. Inversely, if the platform moves instead of the objects in the environment, the objects will give a motion parallax showing their boundaries with respect to the backgrounds. The calibrated stereovision system would provide more accurate distances, but two images in sequence can provide sufficient information for the landmark distance estimation. To carry out this operation, the robot takes two snapshots, one before and one after each step. This procedure is called a unit movement of the mobile robot, which is involved with the estimation of landmark distances based on the agents egomotion. In order to estimate the distance R , there must be a correspondence of the landmarks between the previous and current images.

3.2.2 Distance quantization

The distance to a landmark is estimated with Equation 3.2. Since the equation includes θ , δ and d , the accuracies of these variables can affect the estimation. The angular position θ is affected by the noise in the captured image and thereby the angular deviation δ is, and the distance d is mainly influenced by odometry error. Furthermore, it is plausible to argue that insects or other animals may perceive the distances to landmarks in a simpler manner as several classes. In other words, instead of calculating their exact distances, they may place landmarks into broad distance classes, such as, near, in medium range, or distant. Therefore, we introduce the quantized distance information.

The distance-quantization categorizes the distances to landmarks into several distance levels. For instance, if the quantization level is 2, every landmark in the view will be sorted as either distant or near, while for level 3, they will be categorized as distant, mid-range, or near. Quantization level 1 corresponds to the equidistant assumption, as in the ALV method, that all landmarks lie at same distance. As the discretization level increases, the classifications become finer, and, at the limit of the highest level quantization, the true distance can be obtained.

Distance discretization leads to the simplification of the landmark vector representation. The discretization is relatively insensitive to noise as long as the landmark is assigned to the correct class of the distance level. Even though the changes in distance can affect the perceived arrangement of landmarks, this method is still useful for navigation if such changes do not alter the relative distances from the agent. Figure 3.3 shows an example of one and three-level quantization of landmark distances. The filled circles indicate the actual position of the landmarks with respect to the agent in

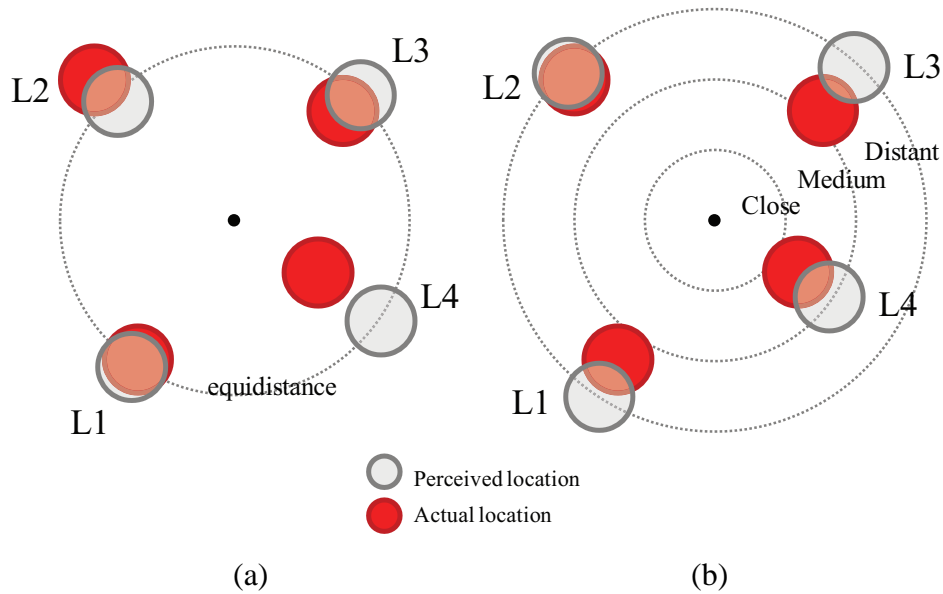


Figure 3.3: Example of the landmark distance quantizations: (a) one-level quantization, that is, an equidistance assumption and (b) an example of three-level distance quantization (Adapted from Yu and Kim (2011d))

the center (black dots). Transparent circles show the perceived position of landmarks adjusted by the estimated distance quantization. The one-level quantization in Figure 3.3 assumes every landmark to be at the same distance from the agent. It has the same concept of an equidistance assumption in the predictive image-matching method, the ALV model and the average correction vector (ACV) model suggested by Hong et al. (1992). Figure 3.3 (b) shows three levels of distance-quantization yielding to the perceived distance into three classes: the close one, the distant one, and the one in medium distance. Based on their relative distance from the agent, quantized distances are assigned to each landmark for each class landmarks belong to. Therefore, for example, in 3 level of discretization, each class, close, medium and distant has certain predetermined distances, and landmarks would be perceived to be only in those distances. Through the quantization process, the perceived distances of the landmarks do not represent the true distances any more. Still the overall configurations remain the same as the true ones. Let us label the bottom left landmark $L1$ and proceed to number the rest in a clockwise manner. The $L4$ is the “actual” closest landmark and it is still the closest one among the “perceived” locations. In this example, the rest of the landmarks are perceived to be at the same distance, however, the relative distances of landmarks from the agent are not altered. For example, it will not classify $L3$ as being more distant than $L2$. The effectiveness of this distance discretization procedure will be shown in

following experiments.

3.2.3 Reference map and localization

The ALV model stores the sum of landmark vectors at the home location. In the average correction vector (ACV) model, the individual landmark vectors with unit length at home is memorized. The stored landmark vectors are then compared with those obtained at the current location in order to determine the homing direction. Similarly, in the distance estimation method, each landmark vector at the nest is stored in a reference map. The reference map is defined as a set of landmark vectors perceived at the nest and does not possess any detailed information on the environment beyond the simple landmark vectors. The reference map includes the distance and angular direction from the starting point to each landmark. The reference map can be created with the distance estimation by Equation 3.1 applying the unit movement technique. Equation 3.2 computes the distance R' of a landmark in the reference map.

$$R' = \frac{d \sin(\theta + \delta)}{\sin(\theta - \psi)} \quad (3.3)$$

For every perceived i -th landmark ($i = 1, 2, \dots, N$) in the environment, the landmark vector $LV_i = (R_i, \theta_i)$ can be found, where N is the number of landmarks. The distance R_i is obtained from Equation 3.3 and θ_i is the angular position of the landmark viewed from the home location.

An agent at an arbitrary position with the stored reference map and perceived landmark vectors can derive the current location by projecting the landmark vectors to the reference map. That is, the estimated distances and the angular positions of the landmarks can serve as a basis information for the localization of the agent in the environment.

Once the reference map is built at the home location, the mobile robot does not need to collect any additional information on the environment or movement directions during the exploration phase until it decides to return home. The homing phase is composed of a series of unit movements. The mobile robot repeatedly takes snapshots and moves one step forward so that it can continuously determine the homing direction. The agent localizes itself by projecting the landmark vectors at the current location to the reference map. The homing direction can be calculated simply with a vector from the current position to the home location.

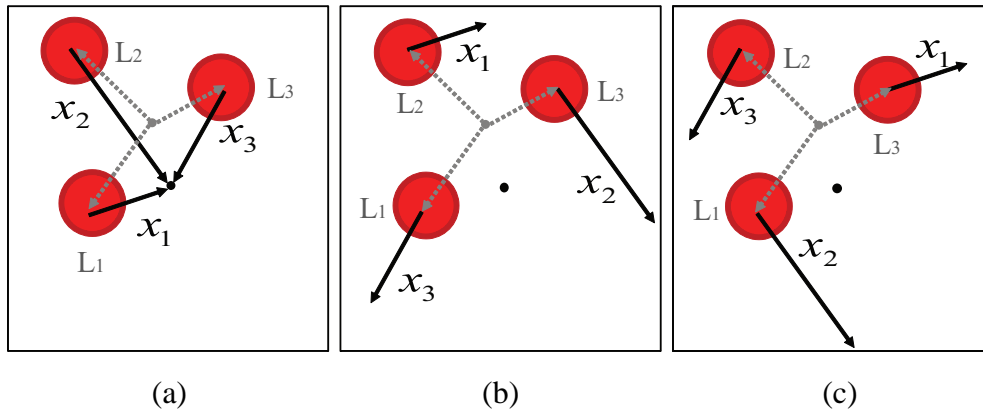


Figure 3.4: Rotational shift of landmark arrangements. Projecting perceived landmark vectors (x_1, x_2, x_3) (black arrows) into the reference map (large circles) depends on the landmark arrangements (x_i indicates the projection of the i -th landmark) (a) correctly matched arrangement, (b) (L_1, L_2, L_3) match (x_3, x_1, x_2), respectively, and (c) (L_1, L_2, L_3) match (x_2, x_3, x_1), respectively (Reprinted from Yu and Kim (2011d))

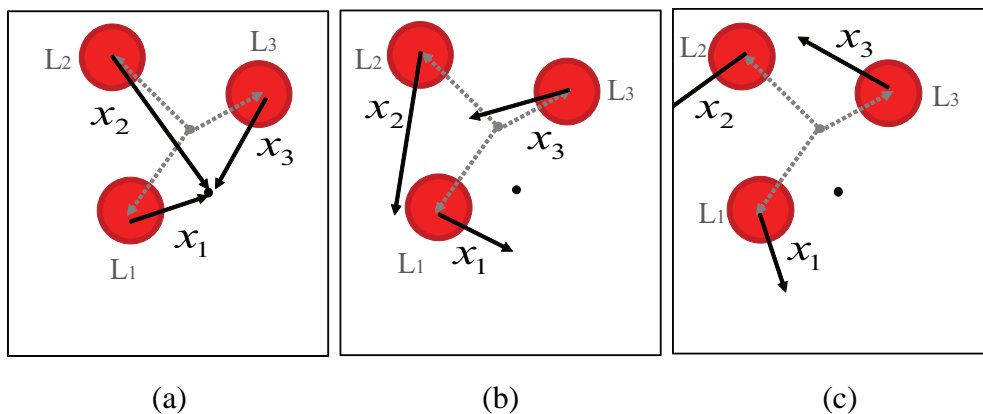


Figure 3.5: Landmark vectors in the reference map with the estimation of head orientations; (x_1, x_2, x_3) are the projected landmark vectors for (a) correct head angle (b) a deviation angle 45° of the head orientation (c) a deviation angle 90° of the head orientation. (Reprinted from Yu and Kim (2011d))

3.2.4 Arrangement matching with landmark vectors

In order to project perceived landmark vectors into the reference map, the DELV method has the correspondence problem between landmarks in the current view and those stored in the reference map. The robot must match the landmarks in the correct order and direction without a reference compass, and it can be accomplished by the rotational arrangement matching.

Figure 3.4 shows the method of the rotational shift of landmark arrangements where the heading direction of the agent is the same as that in the reference map. The figure illustrates a simplified matching process by fixing the head direction at the desired situation which can be an arbitrary direction, in fact. Circles indicate landmarks whose relative positions to the nest are known with egomotion and stored in the reference map. Black arrows (x_1, x_2, x_3) indicate the inversed landmark vectors perceived at the current location of the agent. Because the agent has no information on the heading direction and the identification on landmarks, it is necessary to match the landmarks in the reference map with the perceived landmarks at the current location. Since we have the reference map and perceived landmark vectors, projecting the inversed landmark vectors into the reference map will yield the most converging points, with the estimation of the head direction and the correct landmark arrangement. The Figure 3.4 shows that when the landmark vectors are projected onto the reference map with the right arrangement order, the vectors are likely to point to almost the same point.

In addition, Figure 3.5 illustrates the effect of heading direction in the landmark vector projection, where the landmark arrangements are correctly matched. When the estimation of the head orientation is incorrect, there is no converging point for the current position. Reversely, we can estimate the head orientation as well as the current location of the agent in the reference map coordinate, by employing the convergence property of the projected landmark vectors. Along with the available landmark arrangements, possible head orientations ranging from 0° to 360° within the angular resolution should be tested to achieve the most converging case.

Even when there is no one-to-one relation between landmarks in two views, that is, if the numbers of landmarks in two views are different, the same matching process is applied. If there are additional landmarks left in the reference map, we only consider endpoints of projected vectors to estimate the current location. On the other hand, if the number of landmarks in the current view is larger than that in the reference map, additional landmark vectors are ignored. Since we only consider linear rotational matching of landmark vectors, difference in the number of objects observed may influence the performance in some cases. However, the overall performance in Chapter 5 shows that it does not severely damage the homing rate or the average error in homing vector. In addition, the occlusion problem is likely to be the main cause of different landmark numbers in views. As the occlusion problem and its influence on performance of the method would be investigated in Chapter 5, showing the results with no one-to-one

matching of landmarks.

Theoretically, the end points of projected landmark vectors should converge into one point, when the landmark arrangements and head orientations are correctly matched as in Figure 3.4. Due to various types of errors, the endpoints of projected landmark vectors would not converge to a single point, but rather have some errors. The distance estimation process can be affected by the accuracy of perceived landmark bearings and while the agent moves one step forward to take two snapshots, the moving distance might have odometry errors. These errors can be reduced by eliminating some outliers, which diverge from the rest of the points in serious amount and averaging the endpoints of projected vectors. Our proposed navigation method leads the agent to home by applying the method repeatedly. Moreover, we will show that the navigation method can still operate within some error bound in real robotic experiments.

Once the right head direction of the agent is determined, we can project the landmark vectors into the reference map in the correct order, and localize the agent in the reference frame. While the previous landmark vector models such as ALV and ACV are capable of computing only the homing direction, the DELV method provides the information on the current location, with some errors, and enables the navigation even in the absence of a compass.

3.3 Mathematical description

The proposed DELV method exploits the rotational arrangement matching procedure without a reference compass. Rotational arrangement matching projects the perceived landmark vectors into the reference map by searching head orientation, and estimate the current position of the robot. The algorithm of the DELV method can be summarized in Algorithm 1-3: Algorithm 1 is used for initialization, Algorithm 2 is the main function, and Algorithm 3 determines the homing direction.

In this section, we describe this procedure mathematically and analyze its convergence. We will show the rigorous analysis on the landmark vectors and suggest that the ALV model can be represented as a variation of the DELV method with the level-1 quantized distance information. Following the convergence proof of the ALV method presented by Möller (2000), we also provide the proof of convergence of the movement to the goal point within the proposed landmark vector method.

Algorithm 1 Initialization

- 1: $I_0 \leftarrow takeSnapshot()$ //image taken at the nest
 - 2: $moveForward(d)$
 - 3: $I_1 \leftarrow takeSnapshot()$
 - 4: $LV_{ref} \leftarrow estimateDistance(I_0, I_1)$ //landmark vectors in the reference map
-

Algorithm 2 Homing

- 1: Initialization
 - 2: **loop**
 - 3: $I_0 \leftarrow takeSnapshot()$ //image taken at the nest
 - 4: $moveForward(d)$
 - 5: $I_1 \leftarrow takeSnapshot()$
 - 6: $LV_{new} \leftarrow estimateDistance(I_0, I_1)$ //landmark vectors in the reference map
 - 7: $h \leftarrow matching(LV_{ref}, LV_{new})$ //determine homing direction h
 - 8: turn to the homing direction (h)
 - 9: **end loop**
-

3.3.1 Landmark matching in the arrangement order

Landmark arrangement matching requires two steps: the first step is to create a reference map at the beginning of the exploration, and the second is to project the currently received landmark vectors into the landmarks in the reference map in order to obtain an estimate of the current position. The correct heading direction and the landmark arrangement order is obtained by computing the variance of estimation of the located position. The landmark vector is a vector pointing to the landmark from the current location. Thus, by projecting the reversed landmark vector into the landmarks in the reference map, the current location can be obtained. Theoretically, this procedure should return a single point if landmarks in the snapshot image exactly match those in the reference map. However, due to several noise factors, such as image noise and the error in the distance estimation process, some deviation may be present. Therefore, we compute the mean point and the standard deviation of each located position.

The average point of the projected landmark vectors is defined as $p^k(x)$ as following Equation 3.4. The landmark vectors are projected on the reference map with the k -th arrangement while there are N landmarks available in the environment.

Algorithm 3 Matching

```

1: //for all  $N$  possible arrangement orders
2: for  $k = 1$  to  $N$  do
3:   for  $\alpha = 1^\circ$  to  $360^\circ$  do
4:      $p^k \leftarrow LVProjection(LV_{ref}, LV_{new}, \alpha, k)$ 
5:     if  $convergence(p^k) < convergence(p^{min})$  then
6:       //compare variance of the convergence points
7:        $p^{min} \leftarrow p^k$  //find the location with appropriate arrangement of minimum
          variance
8:        $\alpha_{min} \leftarrow \alpha$  //find the head orientation with minimum variance
9:     end if
10:  end for
11: end for
12: return $[p^{min}, \alpha_{min}]$ 

```

$$p^k(\mathbf{x}) = \frac{1}{N} \sum_{i=1}^N [V_i^R(x_o, \alpha_r) - V_i^k(\mathbf{x}, \alpha)] \quad (3.4)$$

where $\mathbf{x} = (x, y)$ is the current position of a robot, $\mathbf{x}_o = (x_o, y_o)$ is the homing location, the head orientations α and α_r are at the current location and in the reference map, respectively. $V_i^R(x_o, \alpha_r)$ is the landmark vector for the i -th landmark in the reference map, and $V_i^k(\mathbf{x}, \alpha)$ is the i -th landmark vector with the matching order k at an arbitrary location \mathbf{x} while k is one of N possible arrangements based on the rotational matching. As a result, $p^k(\mathbf{x})$ represents the estimated current position relative to x_o .

This matching process will be tested by the rotational shift of landmarks in the reference map, that is, only by changing the arrangement order of landmarks in sequence resulting in N possible arrangements. Since a linear order of landmarks by rotational shift reduces the computation time maintaining performance level, we do not consider all the permutations of landmark ordering.

We find the best matching order and head orientation $[z, \alpha_z]$ based on the convergence criterion with the equation:

$$\arg \min_{k, \alpha} \left[\sum_{i=1}^N [V_i^R(x_o, \alpha_r) - V_i^k(\mathbf{x}, \alpha) - p^k(\mathbf{x})] [V_i^R(x_o, \alpha_r) - V_i^k(\mathbf{x}, \alpha) - p^k(\mathbf{x})]^T \right] \quad (3.5)$$

The inner product of two vectors, $[V_i^R(x_o, \alpha_r) - V_i^k(x, \alpha) - p^k(x)]$ and its transpose leads to the variance of the endpoints of projected landmark vectors. The arrangement is found with minimum variance of the vector sum. This should be run for all possible linear orders of arrangements and possible head angles. In our experiments, an angular resolution of 1° for head orientation angles were tested.

We can project landmark vectors in an appropriate order and determine the mean point $p^z(x)$ as the estimated location of the agent relative to x_o with appropriate z . In the equation, z is the matching arrangement which yields the best convergence of end points of the projected landmark vectors, and α_z is the head orientation angle with the convergence point.

$$p^z(x) = \frac{1}{N} \sum_{i=1}^N [V_i^R(x_o, \alpha_r) - V_i^z(x, \alpha_z)] \quad (3.6)$$

The p^z is the vector pointing from home to the estimation of the current location. Thus, the homing vector $H(x)$ is negative of p^z and can be written as:

$$H(x) = \sum_{i=1}^N [V_i^z(x) - V_i^R(x_o)] = \sum_{i=1}^N V_i^z(x) - \sum_{i=1}^N V_i^R(x_o) \simeq x_o - x \quad (3.7)$$

where the first term is the sum of landmark vectors in a new snapshot image and the second is that in the reference map (we use the sum of vectors for the homing vector instead of the average for convenience). However, we have no prior information of the current position x , and instead $p^z(x)$ can be used for an estimate of homing vector, $\hat{H}(x)$.

$$\hat{H}(x) = \sum_{i=1}^N [V_i^z(p^z(x)) - \sum_{i=1}^N V_i^R(x_o)] \simeq -p^z(x) \quad (3.8)$$

Interestingly, the two terms in Equation 3.7 can be interpreted as the average landmark vector (ALV) suggested by Lambrinos et al. (2000). In the ALV model, two averaged vectors at the current location and at the home location can produce the homing vector while the DELV method uses similar process, but with the distance estimation involved in each landmark vector. In the ALV model, every landmark vector has the same unit length, regardless of the distance from the agent. In our proposed DELV method,

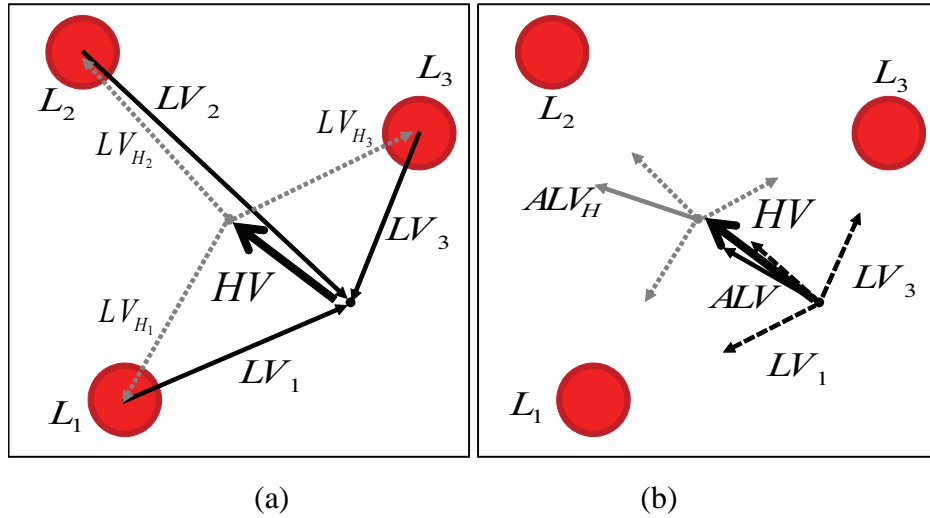


Figure 3.6: Visualization of the (a) DELV and (b) ALV model in same environment. In (b), landmark vectors are represented as dashed arrows, and solid arrows are the average landmark vectors. The large thick solid line arrow is the homing vector (Adapted from Yu and Kim (2011b)).

the distance estimation is applied to the landmark vectors so that distant landmarks have longer landmark vectors. The difference in representation of landmark vectors is illustrated in Figure 3.1. In the ALV model, all trajectories converge to the target location for homing navigation (Möller, 2000) and following a similar procedure, we show the global convergence in our distance estimation model.

3.3.2 The DELV method and the average landmark vector (ALV) model

By introducing landmark vectors with continuous distance to the unit-length landmark vector model, we can see the effect of distance quantization process for a simple representation of the reference map and landmark vectors.

Figure 3.6 (b) illustrates the homing mechanism of the ALV model. A unit vector is aimed at each landmark from the current location while landmark vectors in Figure 3.6 (a) have different lengths. N landmarks are represented by the landmark vectors V_i , where $i = 1, 2, \dots, N$. The sum of the landmark vectors is stored as the ALV. For a current position vector x , the landmark vector V_i with unit length is:

$$V_i(\mathbf{x}) = \frac{L_i - \mathbf{x}}{\|L_i - \mathbf{x}\|} \quad (3.9)$$

and when the distance estimation is included as well, the landmark vector is represented as

$$LV_i(\mathbf{x}) = L_i - \mathbf{x} \quad (3.10)$$

The average landmark vector is

$$ALV(\mathbf{x}) = \sum_{i=1}^N V_i(\mathbf{x}) \quad (3.11)$$

The ALV method estimates the average landmark vector from the snapshot image of a given location of the mobile robot. The homing vector from an unknown location $\mathbf{x} = (x, y)$ directed to the home point $\mathbf{x}_o = (x_o, y_o)$ is obtained by subtracting the average landmark vector at \mathbf{x}_o from that at point \mathbf{x} as follows:

$$H(\mathbf{x}) = ALV(\mathbf{x}) - ALV(\mathbf{x}_o) \quad (3.12)$$

In order to show the convergence of the homing vector in the ALV model, the potential function is derived Möller (2000). The homing vector can be represented by a gradient of the potential as

$$H(\mathbf{x}) = -\nabla U(\mathbf{x}) \quad (3.13)$$

where $U(\mathbf{x}) = \sum_{i=1}^N U_i(\mathbf{x})$ with

$$U_i(\mathbf{x}) = \|L_i - \mathbf{x}\| - \frac{L_i - \mathbf{x}_o}{\|L_i - \mathbf{x}_o\|} \cdot (L_i - \mathbf{x}).$$

where $L_i = (x_i, y_i)$ and $\mathbf{x} = (x, y)$.

To find the minimum of $U(\mathbf{x})$, we use the determinant of the Jacobian matrix:

$$D = U_{xx}U_{yy} - U_{xy}^2$$

where $U_{xx} = \sum_{i=1}^N (y_i - y)^2 / \|L_i - \mathbf{x}\|^3$, $U_{yy} = \sum_{i=1}^N (x_i - x)^2 / \|L_i - \mathbf{x}\|^3$, and $U_{xy} = -\sum_{i=1}^N (x_i - x)(y_i - y) / \|L_i - \mathbf{x}\|^3$. Thus, we obtain

$$\begin{aligned} D &= \sum_{i=1}^N \sum_{j=1}^N \frac{(y_i - y)^2 (x_j - x)^2}{\|x_i - x\|^3 \|x_j - x\|^3} - \sum_{i=1}^N \sum_{j=1}^N \frac{(x_i - x)(y_i - y)(x_j - x)(y_j - y)}{\|x_i - x\|^3 \|x_j - x\|^3} \\ &= \sum_{i=1}^{N-1} \sum_{j=i+1}^N \frac{((x_i - x)(y_j - y) - (x_j - x)(y_i - y))^2}{\|x_i - x\|^3 \|x_j - x\|^3} \end{aligned} \quad (3.14)$$

Based on the equation, it is always $D(x_o) > 0$, $U_{xx}(x_o) > 0$, and $\nabla U(x_o) = 0$ since $H(x_o) = 0$. Finally, $U(x)$ has the minimum value at the point x_o .

Similarly, convergence in the proposed landmark vector method with continuous distance can be shown. Since the landmark vector is not restricted to the unit length, Equation 3.7 can be rewritten to represent the homing vector as

$$\begin{aligned} H(\mathbf{x}) &= \sum_{i=1}^N V_i^z(\mathbf{x}) - \sum_{i=1}^N V_i^R(x_o) \simeq \sum_{i=1}^N [L_i - x_o - p^z(\mathbf{x})] - \sum_{i=1}^N [L_i - x_o] \\ &= \sum_{i=1}^N [-p^z(\mathbf{x})] \end{aligned} \quad (3.15)$$

Assuming that the current location and the head orientation are estimated accurately through the matching process, the homing vector is a gradient of the potential as $H(\mathbf{x}) = -\nabla U(\mathbf{x})$ and

$$U_i(\mathbf{x}) = \frac{1}{2} \|L_i - \mathbf{x}\|^2 - (L_i - x_o) \cdot (L_i - \mathbf{x}) \quad (3.16)$$

We obtain $U_{xx} = \left[\sum_{i=1}^N \left(\frac{1}{2} ((x_i - x)^2 + (y_i - y)^2) \right) \right]_{xx} = -1$, $U_{yy} = -1$ and $U_{xy} = 0$.

Therefore,

$$D = U_{xx}U_{yy} - U_{xy}^2 = (-1)^2 - 0^2 > 0$$

The equations confirm the convergence of the homing vector in the landmark vector model with continuous distance with $D(x_o) > 0$, $U_{xx}(x_o) > 0$, and $\nabla U(x_o) = 0$.

The mathematical convergence presented in this section is a purely theoretical approach to the homing navigation. The error in head direction estimation, landmark segmentation, or occlusion problem would affect the performance.

Now we introduce the quantized distance estimation instead of the continuous distance scheme, that is, the discretization of distance into a coarse resolution. The discretized distance changes the representation of landmark vectors in the mathematical description. Contrary to the case of continuous distance, the landmark vectors in the discretized distance do not represent the actual distance to the landmark any more. For example, with two level discretization, the landmark vector can be represented as:

$$LV_i(\mathbf{x}) = \begin{cases} \frac{a}{2} \frac{L_i - \mathbf{x}}{\|L_i - \mathbf{x}\|} & \text{if } \|L_i - \mathbf{x}\| \leq \frac{a}{2} \\ a \frac{L_i - \mathbf{x}}{\|L_i - \mathbf{x}\|} & \text{if } \|L_i - \mathbf{x}\| > \frac{a}{2} \end{cases} \quad (3.17)$$

Since the distances are discretized relative to the preset value a , the discretized landmark vector is effectively a scaled version of the unit length landmark vector shown in Equation 3.9. Therefore, a series of homing vectors obtained by the discretized landmark vector method also converge to the home point x_o in the same way as the procedure described above.

3.4 Summary of Chapter 3

This chapter suggests a new algorithm, the distance-estimated landmark vector (DELV) for homing navigation. While it takes the concept of landmark vectors used in the previous models, the method is markedly different from its predecessors in taking account of the distance information merged into the vector. The distance to the landmark is estimated by the angular shift from the one step movement of the agent based on the omni-directional snapshot image. Landmark vectors obtained at the target location are stored as a reference map, which is used to localize itself and determine the homing direction. Consequently, the DELV method can match correspondence between the current landmark vectors and those in the reference map even without a reference compass. The arrangement matching of landmark vectors enables the agent to determine an appropriate landmark correspondence as well as its heading direction. The overall procedure is described in a mathematical form along with the investigation of the convergence characteristics. The performance of our proposed method is given in the following chapters.

Chapter 4

Navigation performance

In this chapter, we present the navigation performance of our proposed method. Assuming that landmarks have no distinctive features, we carry out a simple landmark arrangement search to determine the homing direction, which is also effective even when the discretization of distances is applied.

The experiments are conducted in both computer simulations and robotic experiments. In the landmark configuration of robotic experiments, the mobile robot is able to capture snapshot images through the omni-directional camera and determine the homing direction by processing the landmark information from the images. The environment for simulation experiments were set similar to that of a real-world robotic experiment. For the simulation experiment, a various types of landmark configurations are tested and results were analyzed. In this chapter, the performance results of the DELV method are compared to those of a image-based navigation method of the predictive image-matching method suggested earlier by Franz et al. (1998). According to the classification which we introduced in Chapter 2, the predictive image-matching method is a holistic method while our DELV method can be classified as a landmark-based method. However, since the DELV method is able to operate without any reference compass information, we compare the results with the navigation method within the same condition. Since the reference compass is required necessarily for many existing landmark-based homing navigation methods, we also give the comparison of the reference-compass-enabled DELV method in Chapter 5.

First, we discuss the results of our newly suggested DELV method on its own (Yu and Kim, 2011c). Applying the quantized distance scheme, we examine the sensitivity of

the method on the accuracy of the estimated distances (Yu and Kim, 2011d). Since animals as well as humans might perceive the distance in a relative sense rather than in the absolute values, the quantization in several levels is also proper for the bio-inspired navigation model. The results are then compared to those from the predictive image-matching method. Robotic experiments were conducted in two different environments, one with artificial landmarks (Yu and Kim, 2010b) and another in the unstructured environments with natural landmarks (Yu and Kim, 2011d). The analysis of the results from experiments can be expressed in mainly two different forms, a homing vector map and a success rate in homing. The data include a vector map, angular errors, and the success rate of returning home accurately or the catchment area. The detailed criterion is described along with the results.

4.1 Performance evaluation

The performance results of our method are compared to other navigation method in various perspectives. Image-based navigation methods, classified as holistic methods, determine homing direction based on the image differences and usually does not require any reference compass information. The difference or image distance between a pair of images taken at different locations increases when the distance between the locations increases (Zeil et al., 2003), and as a visual homing method, descending in the image distance measure will lead an agent to the goal location (Möller and Vardy, 2006). Similar visual homing approaches calculate the direction of movement based on the intensity of each pixel in the image (Möller, 2009; Stürzl and Zeil, 2007; Zeil et al., 2003).

In this paper, the performance results are compared to the predictive image-matching method suggested by Franz et al. (1998) which is one of the most famous image-based homing navigation methods. As in the chapter introducing backgrounds of vision-based navigation methods, the method by Franz et al. (1998) can be classified as holistic method. The predictive image-matching method of Franz et al. (1998) determines the direction of movement by comparing a snapshot taken at home location with the predicted image at the current location. The mobile robot creates a prediction image by estimating the landmark movement as the robot moves in each direction. Comparing predicted images with the image taken at the target location, the image with the least discrepancy in the size and bearing of landmarks is chosen as the direction to move.

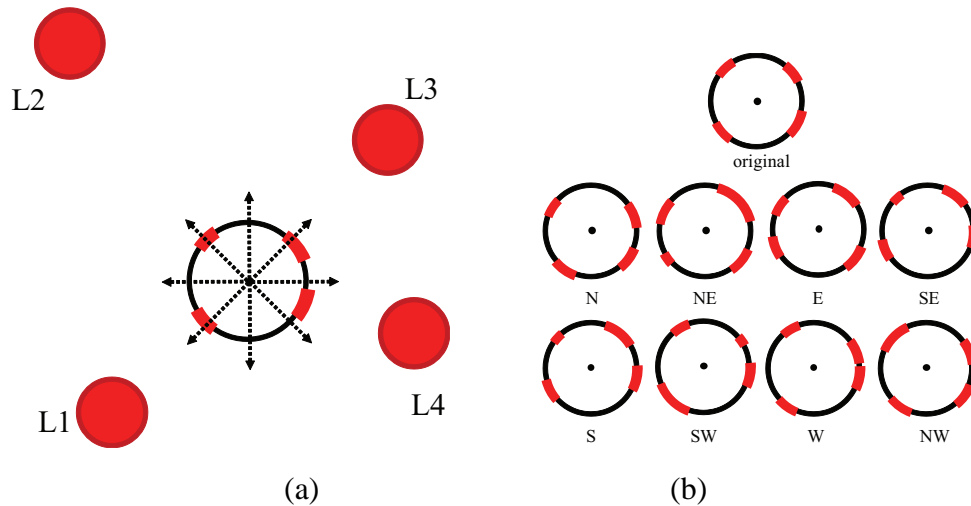


Figure 4.1: Description of the predictive image-matching method (Franz et al., 1998); (a) the possible directions of movement for the agent and (b) the prediction of the captured image for each corresponding direction of movement (Reprinted from Yu and Kim (2011c)).

The predictive image-matching process is described in Figure 4.1. The broken line arrows diverging from the agent in Figure 4.1 (a) indicate possible directions to move, and the number of directions determines the resolution of the prediction step. Figure 4.1 (b) shows predicted images for 8 possible moving directions. The predictive image-matching algorithm assumes equidistance for every landmark, which does not reflect real situations. This is an egocentric model of the vision-based navigation system and the method is in good accordance with the real method that the insects and animals use to recognize the environment. The pixel-based image matching method has advantages in that it does not require a landmark segmentation procedure or a reference compass. The method provides a robust homing performance without a reference compass as it is based only on visual information without any additional information. Since the method does not require reference compass, it is a competitive navigation method with fine performance. However, the predictive image matching method is extremely sensitive to the captured image of the surroundings and the number of landmarks in the environment. With few landmarks in the snapshot image, there is a high probability that the robot could misjudge its direction to home while the robot cannot distinguish and recognize the individual landmarks.

4.2 Simulation experiments

In this section, we provide the simulated robotic experiments results of the DELV method without a reference compass. In DELV, we use the rotation of landmark arrangement to localize the robot in the reference map instead of the reference compass.

For the simulation of robotic navigation, we set the experimental environment as a square ring of landmarks of different sizes and distribution. The center of the area is marked as home of the mobile robot and so served as the start and returning point. It is assumed that the robot can take an omnidirectional view of landmarks around the agent and estimate the landmark distances with its egomotion. The robot determines the direction of movement using a set of landmark vectors. The arrow in the vector map indicates the movement direction at each point. The difference between the angle of the arrow in the vector map and a straight line drawn from each point to the goal was regarded as the angular error. The angular error graphs show errors with respect to the distance from home, one of the criteria for assessing the performance of each navigation method.

Three types of assessments are given. The first is the vector map (see Figure 4.2), which consists of arrows at every location to indicate the homing direction. If the arrow points directly to the goal location, it has zero angular error, while the error increases as the arrow deviates from the desired direction. The error is plotted as an angular error graph. The error graphs are shown as mean values (see Figure 4.4). At each distance, the mean of the errors was calculated. The error bars indicate the mean values and the t -distribution deviations at the 95% percent confidence level. The third performance assessment is the success rate represented as catchment area as shown in Figure 4.5. The mobile robot heads home from an arbitrary location, and the success rate is the number of trials in which the robot returns home within a certain time limit.

Vector maps graphically represent the computed homing vector results for a set of grid points. For a comparison in various environments, three types of landmark environments were constructed. All three environments contain four cylindrical landmarks but with different sizes and angular positions. The first environment is shown in Figure 4.2 (a). Four landmarks are asymmetrically surrounding the home location at (500,500) in environment 1. The environment 2 has a uniform distribution of landmarks (Figure 4.2 (b)). Since there are four landmarks surrounding the goal location, the bearing angle of each landmark, as seen at the goal location, differs by 90° from that of its neighboring

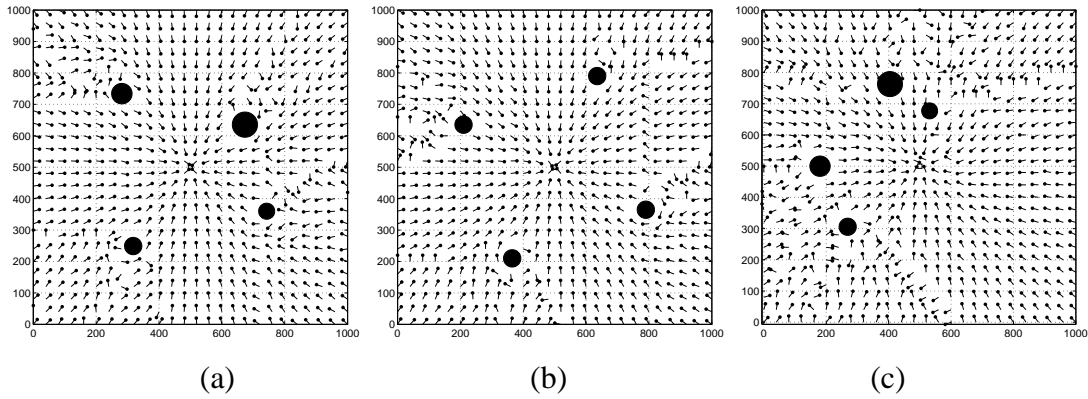


Figure 4.2: Vector map with the DELV method applied in three different environments: (a) environment 1, (b) environment 2, and (c) environment 3.

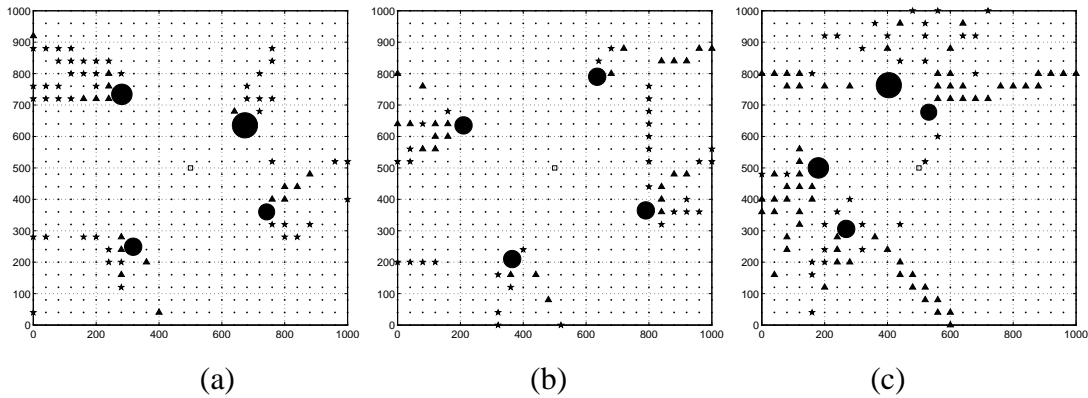


Figure 4.3: Spatial errors in homing vector; Marker of each point indicates the amount of angular error (\cdot : less than 45° , \star : between 45° and 90° , and \triangle : greater than 90°) with corresponding vector maps in Figure 4.2.

landmark. The third environment contains an asymmetric distribution of landmarks. As seen in Figure 4.2 (c), all four landmarks in the third environment are cornered to one side of the home location. These tests in three different environments assess the effect of landmark distribution. From Figure 4.2, we could see that the method performs perfectly when landmarks surround the goal point. Outside of the convex hull of landmarks, some points show errors in decided homing direction, however, not severely affecting the performance level. A quantitative representation of the performance comparison can be obtained from the spatial error graphs in Figure 4.3 and error graphs in Figure 4.4.

The spatial error graphs corresponding to the vector maps in Figure 4.2 are shown in Figure 4.3. We classified the homing vector result at each point into three categories

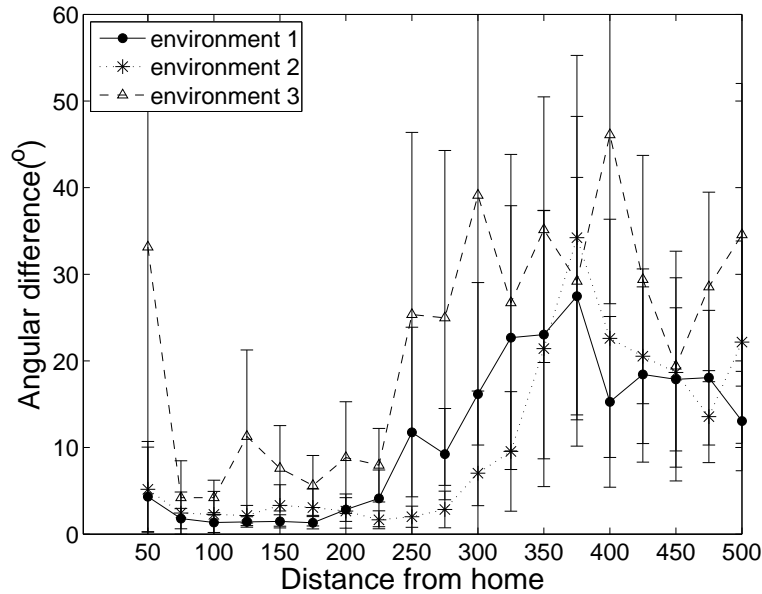


Figure 4.4: Error graphs for the DELV results in three different environments 1, 2, and 3 shown in the vector maps in Figure 4.2.

based on the amount of angular error, which defined as the difference between the decided homing direction and the angle of a desired straight line from the current location to the home location. The points indicated with dots (•) have small errors (less than 45°), while the points represented as stars (★) have errors greater than 45° but less than 90° . Finally, points with angular errors greater than 90° are indicated with a triangle (Δ). The spatial graphs in Figure 4.3 show the angular error pattern in the spatial map. It shows that the DELV method work effectively in all three environments.

Another focus of this study is to investigate the homing paths for the landmark-based homing methods, which is the goal of homing algorithms. The homing ability, to accurately return to home location, is more important than angular error, although the angular error indirectly influences the homing performance. The actual homing ability can be affected by various conditions such as trap points, attractors, and obstacles. The catchment area is defined as a region from which an agent or a robot can ultimately return to the goal point. That is, starting from a point outside of the catchment area, the agent would not be able to reach home. Instead, the agent would be stuck in some single location or would circle around a certain region, known as trap point. Even though the vector map results reveal a sufficiently low number of error points, even a few trap points can keep the agent from moving toward the goal location and thus, degrade the homing performance.

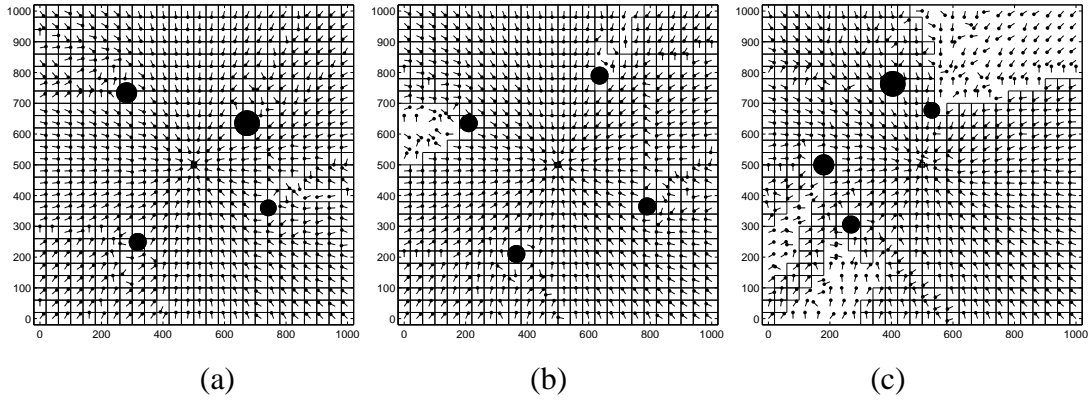


Figure 4.5: Catchment area with vector map for each environment. (a) 98.52%, (b) 95.41%, and (c) 77.66% of the environment. The squared region indicates that the corresponding point is inside the catchment area.

Based on the results of angular errors and catchment area, the DELV shows good performance in various environments. Although it seems to be affected by the distribution of landmarks, they show sufficient level of success rate in homing.

We constructed a landmark map by estimating the distance to every landmark by moving the robot one step forward with moving distance d and observing the image shift. As the distance estimation of a landmark is affected by the accuracy of the image shift (see Equation 3.2), the distance d of one step can be a controlling factor in the method. The landmark arrangement in the current environment is compared with that in the reference map. Then the agent determines the moving direction to the goal point. Figure 4.6 shows vector maps in which arrows represent the moving directions chosen by the mobile robot at each location. Four vector maps show results with varying distances d , but there are no significant difference among the vector map patterns. This indicates that a set of landmarks collectively determine the homing direction, and the resolution of the image shift for a single landmark is not important in our approach.

Figure 4.7 shows the averaged angular errors for vector map results shown in Figure 4.6. The angular errors do not differ by a large amount with varying moving distances d . This shows that the moving distance rarely affects the performance of the method. Through several tests in various environments, $d = 50\text{cm}$ is chosen for good performance in the environment for a robot size about 15 cm in diameter. As the vector map results in Figure 4.6 with respect to the moving distance show very similar patterns in terms of homing performance, the angular errors are not critically affected by the moving distance d in our experiments. Small d s might have a slight improvement in

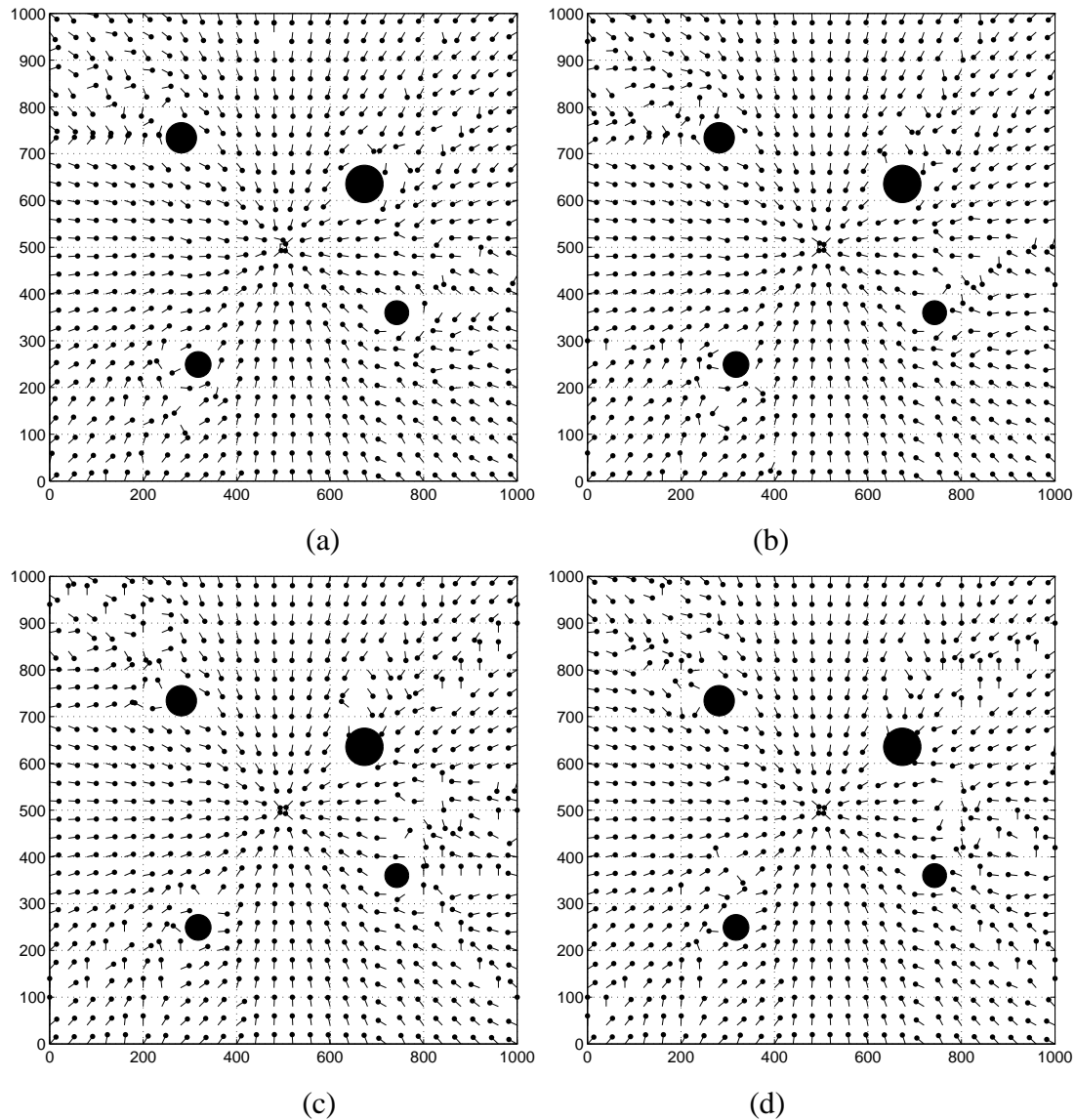


Figure 4.6: Vector map with the landmark arrangement matching method with different moving distance d : (a) $d = 20$, (b) $d = 50$, (c) $d = 100$, and (d) $d = 150$.

the variance of the error or the angular error itself, but the overall performance in the homing direction has similar patterns. To accurately sense the image shift, it is advantageous to increase d , which can lead to a clear difference between snapshots and thus reduce the estimation errors. However, if a very large moving distance is applied, it could be inconvenient in navigation finding the actual home location and also more vulnerable to the odometric errors.

Figure 4.8 displays the vector maps of environments with various landmark configurations and number of landmarks according to the suggested method. As the simulation

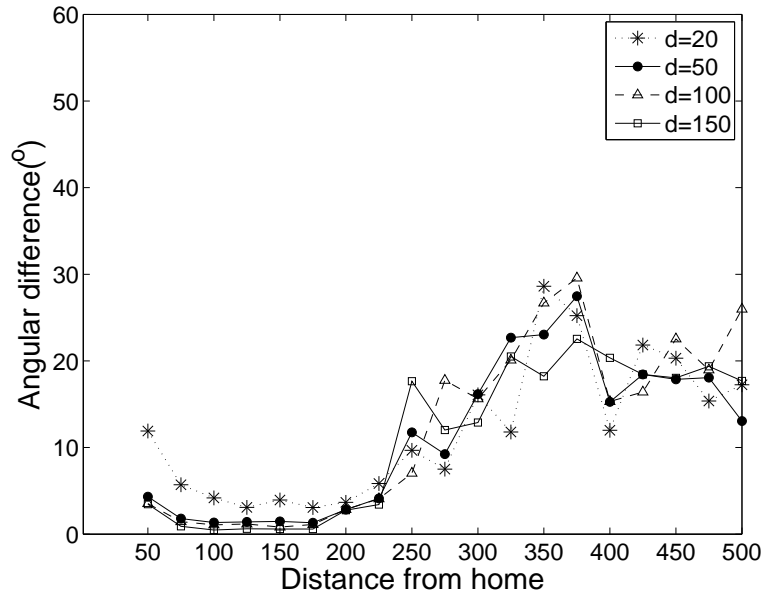


Figure 4.7: Performance of the DELV method with varying moving distances in angular error graphs. Corresponding vector map results are in Figure 4.6.

results show, the method can effectively operate in the environments with asymmetric and unbalanced distribution of landmarks and various landmark numbers as well. The number of landmarks varies from 3 to 5, and they are arbitrarily positioned. Figure 4.8 (f) shows the angular error graphs of three examples shown in Figures 4.8 (b), (c) and (e). At a distance far from the nest, the angular errors are large but still smaller than 90° . We predict that the agent will be able to return home successfully in this situation.

We now compare our method with the predictive image-matching method. In the predictive image-matching method shown in Figure 4.9 the homing direction is computed with a method suggested by Franz et al. (1998) and also investigated in the work of Möller (2009). In the simulation, first the 1-dimensional snapshot of the environment is taken at home location and stored as the reference image. The size of the image is 360 pixels in width which leads to 1° of resolution of the snapshot. Taking snapshot, the landmarks are marked in the omni-directional image as in the DELV method shown in Figure 3.1 (a), however, the difference is that the agent does not set landmark vectors for each landmark but instead treat every pixel in the snapshot individually. At an arbitrary point, the agent takes a snapshot image, and the image is warped with parameters α , ψ , and ρ . The parameters are used as same as it has been mentioned in previous works (Franz et al., 1998; Möller, 2009). The α is the difference between previous heading direction and the moving direction, ψ is the difference in heading directions

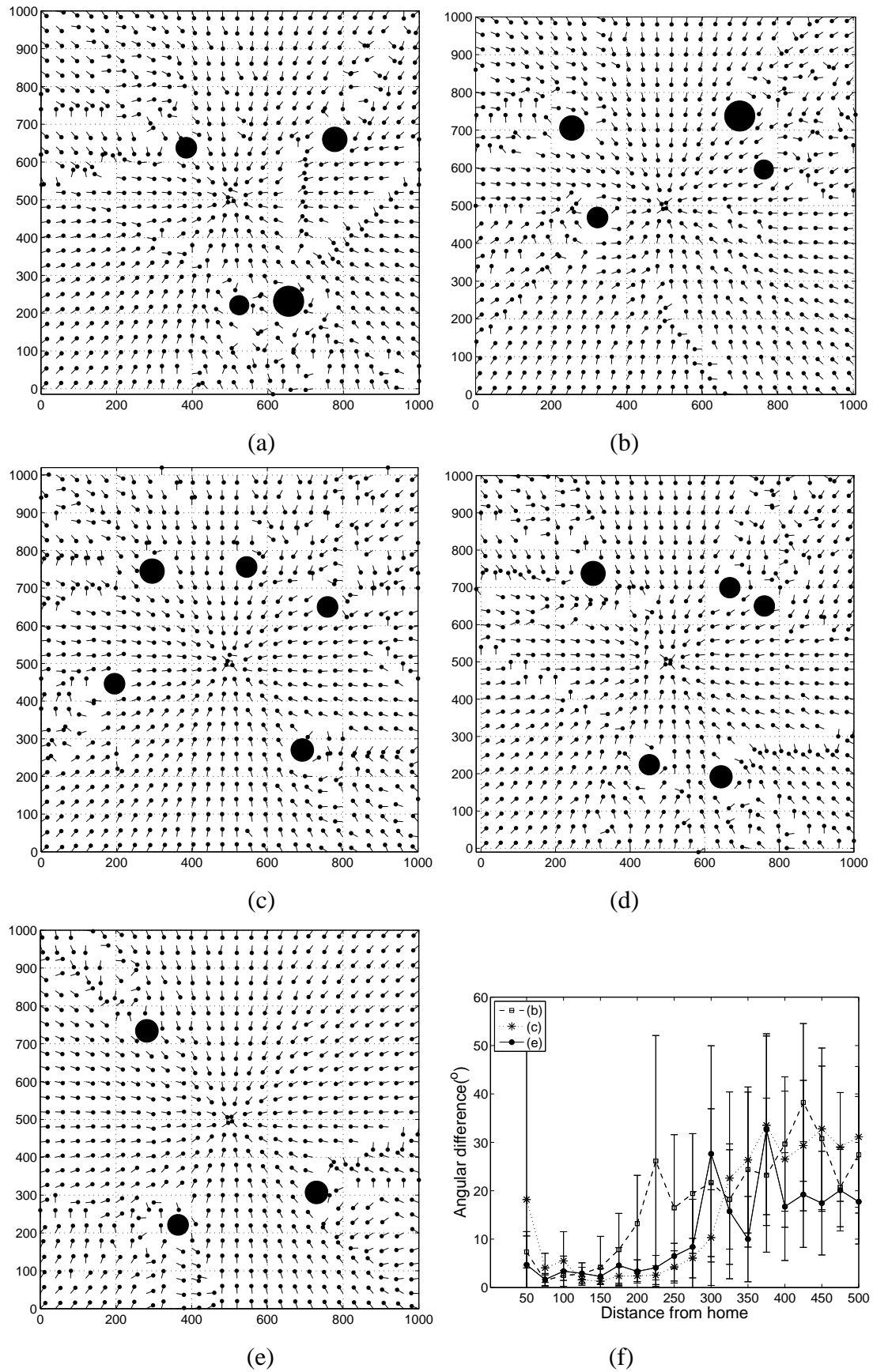


Figure 4.8: Vector maps and angular error performance; (a)-(e) vector maps with the suggested DELV method in environments of various landmark distribution and (f) error graphs for vector maps in (b), (c), and (e).

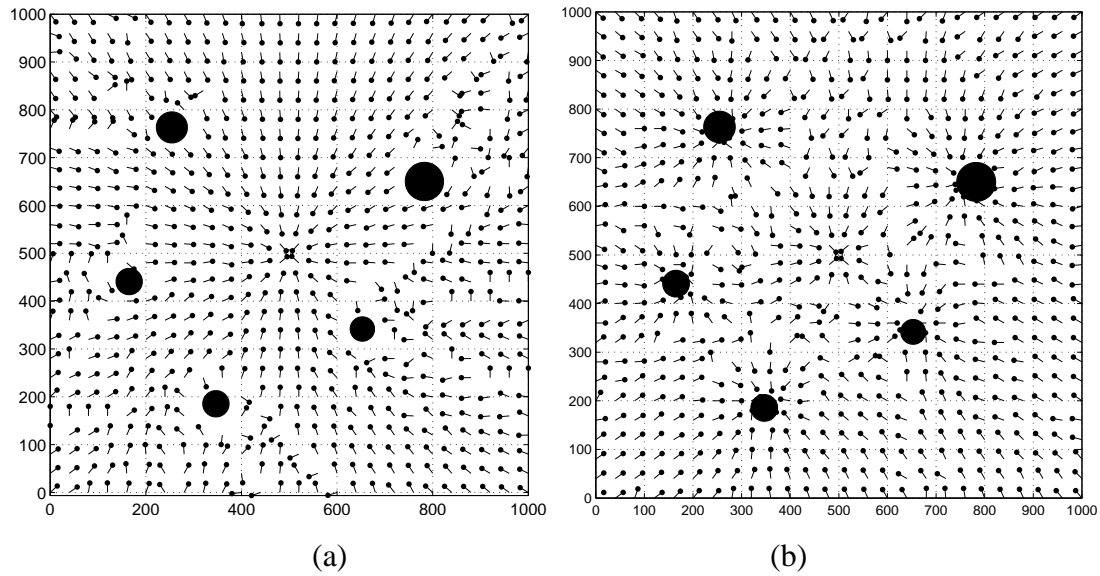


Figure 4.9: Vector maps; (a) the DELV method and (b) the predictive image-matching method (Adapted from Yu and Kim (2011c))

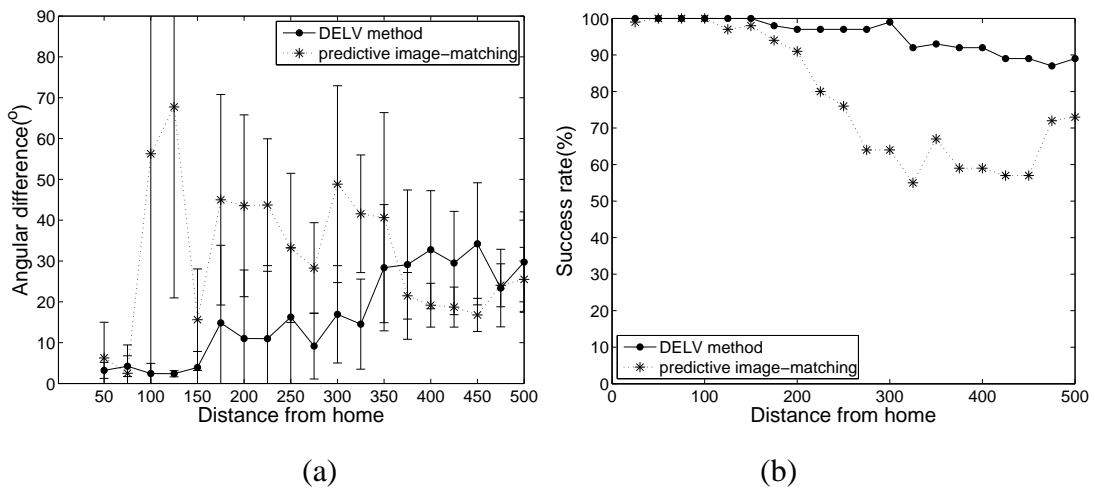


Figure 4.10: Performance comparison of (a) error curves of angular difference for the DELV method and predictive image-matching method and (b) the success rate among 100 trials with respect to the distance from home without a reference compass (Adapted from Yu and Kim (2011c))

of two views and ρ is the relative distance $\rho = d/r$ while assuming all landmarks to be in the same distance r from the current snapshot location. Both α and ψ had 72 steps, which is a 5° resolution in the range of 0° to 360° and 15 steps were used for ρ ranging from 0.1 to 0.8 for every 0.05 step. Using these parameters, a set of distorted image would be produced and by searching the smallest distance with the reference

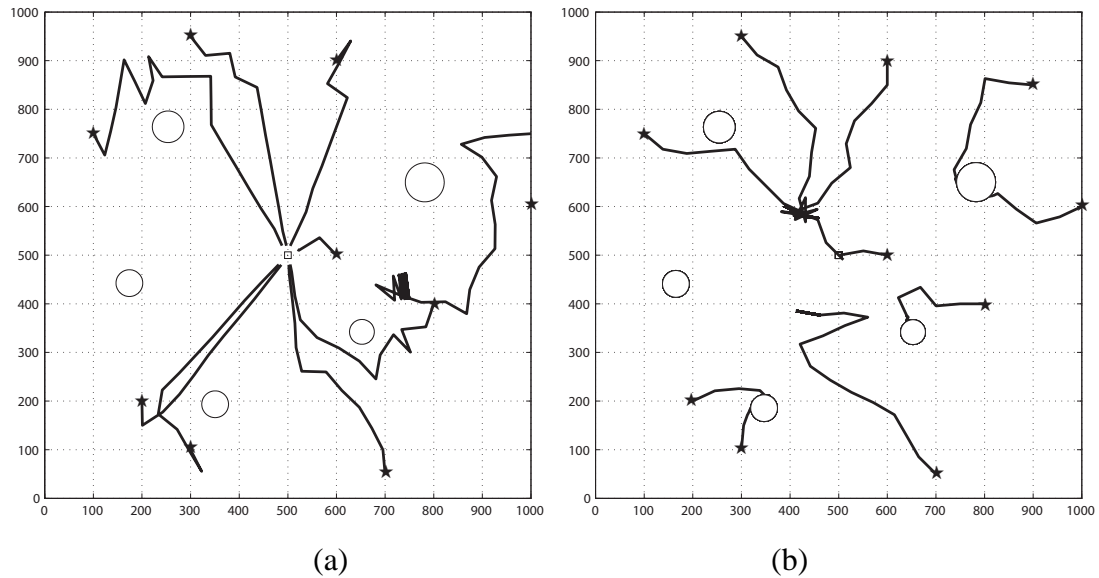


Figure 4.11: Trajectories of a mobile robot at the same starting points for applying each (a) DELV method ($d = 50$) and (b) predictive image-matching method. Black stars indicate starting points. (Adapted from Yu and Kim (2011c))

image, the best matching parameters were selected. Each warped image is compared to the reference image by computing the distance between images. In the experiments, the distance is measured with the absolute of the difference between snapshot intensity values.

The vector maps for DELV and predictive image-matching method in same environment are given in Figure 4.9, and Figure 4.10 (a) shows the angular errors for both methods. The DELV method suggested provides significantly smaller angular errors than the predictive image-matching method do. This result indicates that the suggested method has a higher probability of resulting in a successful return to home. In fact, the DELV approach rarely fails in homing and shows high success rate for almost every case, irrespective of the distance from the release point to the nest. This result is shown in Figure 4.10 (b). Thus, the DELV method is more suitable for homing navigation than is the predictive image-matching method. Figure 4.11 shows the trajectories of robot navigation for our approach and the predictive image-matching method when the mobile robot is released at an arbitrary location with a random heading direction. From the same release points, the robot shows different performances based on the homing method used. The predictive image-matching approach often has difficulty in locating the nest when the robot is in the outer zone of the landmark convex hull. The

main reason for failure in agent movement with the predictive image-matching method is a convergence problem to a landmark. This is due to the process in which the agent tries to maximize the matching score between images. However, if the agent moves extremely close to the landmark, the size of the landmark in view would be large enough to make matching score sufficiently large to move toward. Due to errors in the vector map shown earlier, in Figure 4.9, a ‘trap point’ may be generated, which prevents the agent from moving toward appropriate direction to home.

Our suggested method determines the goal point with a success rate greater than 90% (see Figure 4.10 (b)). For the suggested landmark-matching method, the worsening performance at a far distance from the nest is related to the occlusion of landmarks. If the agent is surrounded by landmarks, that is, inside the convex hull of landmarks, it can easily localize itself in the environment using the landmark arrangement. When the agent leaves the landmark-surrounded area, however, a landmark may be occluded behind another landmark close to the agent or more than one landmark can be overlapped in the view, both of which can influence the landmark arrangement-matching process. This result is also supported by the spatial error graphs in Figure 4.3. The amount of error inside the landmark surrounded-area is almost zero, while the point with errors are main located outside the area, where the agent might not see every landmark in its view.

4.3 Simulation experiments: with quantized distance

The results of DELV with quantized distance is shown in this section as vector maps, angular errors and catchment area. As in the previous chapter, since the ALV model cannot operate without a reference compass, we cannot compare these results with those of the ALV model directly. Instead, we compare them to the pixel-based image matching method suggested by Franz et al. (1998) in this chapter as well. The vector maps shown in Figure 4.12 were obtained using the discretized DELV method without a compass. The arrows indicate the movement direction as determined by the algorithm. The landmark distance quantization levels in Figure 4.12 (a) to (c) are 3 to 5, respectively. The discretization levels slightly influence the homing directions, but still show good performance. As in the case with continuous landmark distance, the landmark arrangement with rotational shift does not guarantee 100% matching between landmarks from different view. There can be error in landmark arrangement matching,

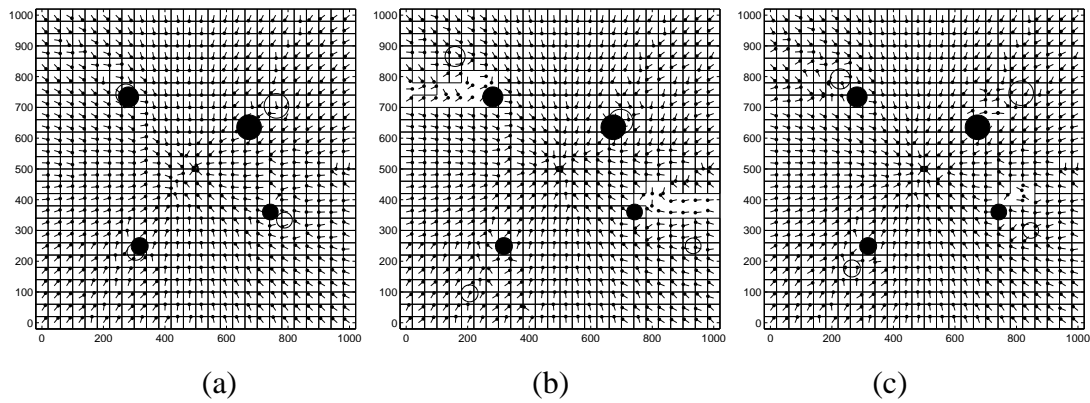


Figure 4.12: Vector map with the DELV method with different quantization levels of the landmark distance: (a) level 3, (b) level 4, and (c) level 5 (● : actual and ○ : perceived location of landmarks).

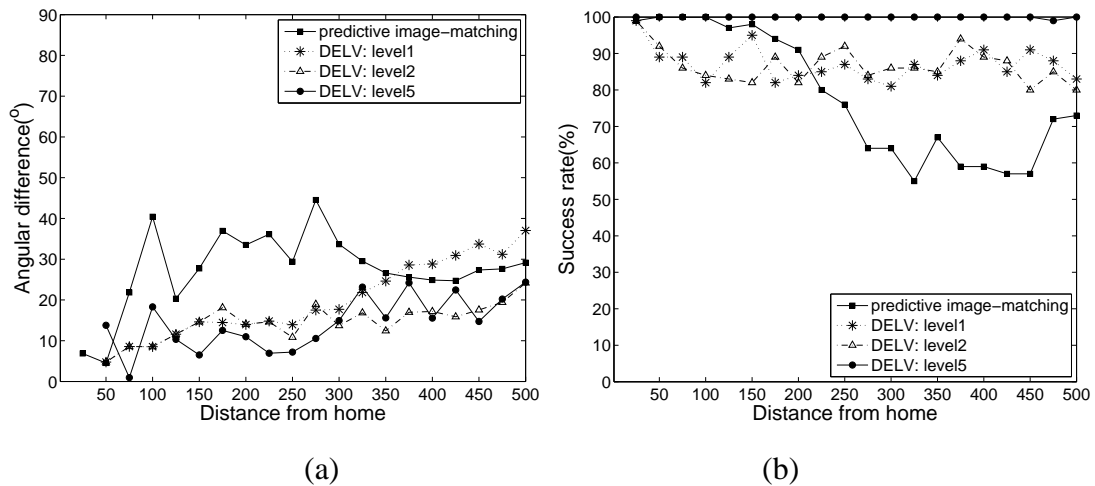


Figure 4.13: Error curves and success rate: (a) error curve results by applying DELV with quantized distances of level 1 to 5 of the corresponding vector map results in Figure 4.12 and (b) success rate for each method

thus in homing vector due to the occlusion of landmarks or the perception of horizon problem.

Figure 4.13 (a) shows the angular errors between the algorithmically determined homing direction and the desired direction. The error graphs are shown for DELV with 1, 2, and 5 levels of quantization compared to the predictive image-matching method. This error may be unavoidable with the lack of a compass, but as can be seen in Figure 4.13 (a), the error mostly remains less than 30 degrees. Interestingly, the angular errors do not change much depending on whether continuous or discretized distances

are applied.

The agent does not know its actual heading direction without a reference compass. Although we show vector maps in Figure 4.12, the trajectory results can vary depending on the heading direction of the robot and its egomotion. Therefore, another criterion is required to compare performances, and the catchment area in Figure 4.12 and the success rate in Figure 4.13 (b) show the percentage of successful return trips. The catchment area shown in Figure 4.12 along with the vector map shows the region of starting points at which the agent can return home successfully. The point with no squared boundary is outside the catchment area. For the success rate graph in Figure 4.13 (b), a trial was regarded as a success if the mobile robot reached home and was counted as failure if it became stuck or continually circled a location that was not the home point. The success rate indicates the number of successful homing out of 100 trials. The agent starting explore from the nest is removed and placed at a random location with a random heading direction. The agent then attempts to return home by applying one of the navigation methods. Here, if a robot returned to its home location from a random position within 50 movements, it was considered successful. We assumed that 50 movement steps were sufficient to return to the home location and 50 iterations of the landmark vector calculation had been applied for each starting position. The main cause of the failure in homing was being stuck in certain location, the ‘trap point’ and continually circling a location due to errors in homing vector decisions.

The suggested algorithm with quantized distance applied has been tested with different numbers and configurations of landmarks. Figure 4.14 shows the vector map results of the environment with three to five landmarks in different distribution. Landmarks in Figure 4.14 (a) surrounded the home location with equally distributed angular position, on the other hand, in Figure 4.14 (b) the home location is slightly outside the convex hull of the landmarks. The homing vector results show low angular errors in various environments, with slightly smaller error if the landmarks surrounded home location perfectly as in (a). Therefore, it is important to select landmark features surrounding the home location in the environment if the mobile agent can select landmarks at the start of the exploration. By choosing the landmark features around the home location, the suggested method could yield better performance.

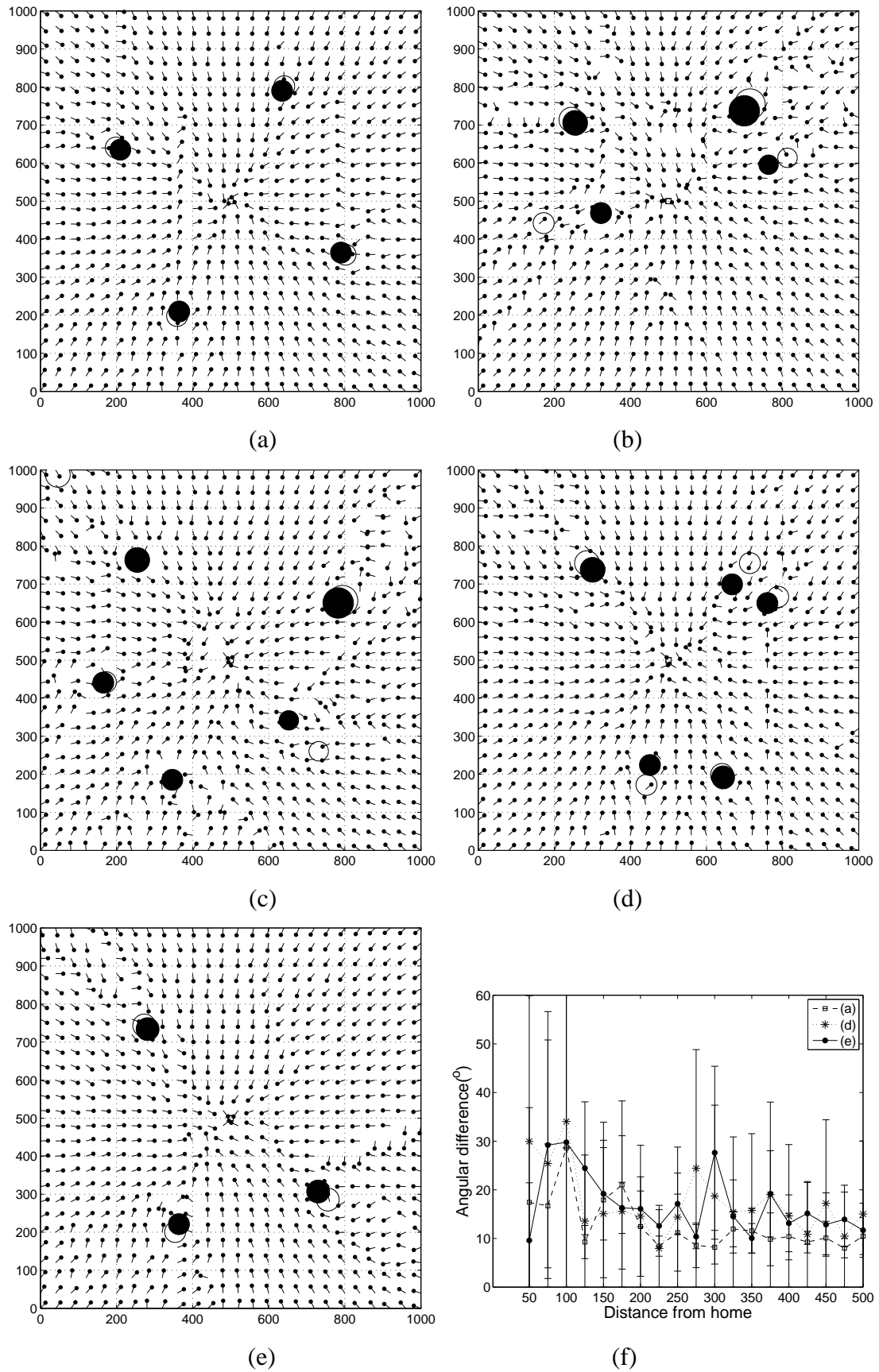


Figure 4.14: Vector maps and angular error performance for quantized DELV: (a)-(e) vector maps with the suggested DELV method with quantization level 3 in environments of various landmark distribution and (f) error graphs for vector maps in (a), (d), and (e).

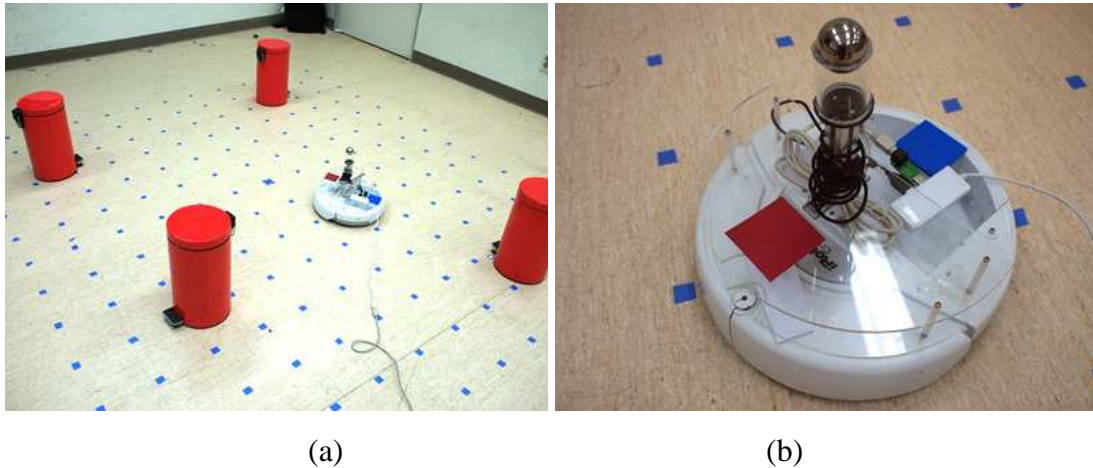


Figure 4.15: Mobile robot and its environment: (a) an experimental environment with four cylindrical landmarks and the (b) ROOMBA robot with an omnidirectional camera on top. (Reprinted from Yu and Kim (2010b))

4.4 Robotic experiments

We showed simulation experiments and the performance evaluation of our tested approach in real robotic experiments. Further, in this section, we show the results of real robotic experiments along with the description on the experimental environment and the mobile robot.

4.4.1 Results with artificial landmarks

In this experiment, ROOMBA, the mobile robot is used to test the homing navigation methods. ROOMBA is a typical mobile robot with two wheels and its movement can be controlled with simple commands. Figure 4.15 (a) and (b) show the robot and the environment with four landmark objects, respectively. An omnidirectional camera is mounted on the ROOMBA robot, and a laptop computer processes the captured images from the camera to determine the moving direction. The diameter of the mobile robot is 32cm, and the omnidirectional camera is placed on top of the robot, which is 25 cm above the floor. The robot can rotate, move forward and backward with simple commands. Four landmarks are red-colored cylindrical objects, and the experimental environment has a total area of 1.8 meters by 1.8 meters.

We tested the homing navigation of a mobile robot in a real environment in which

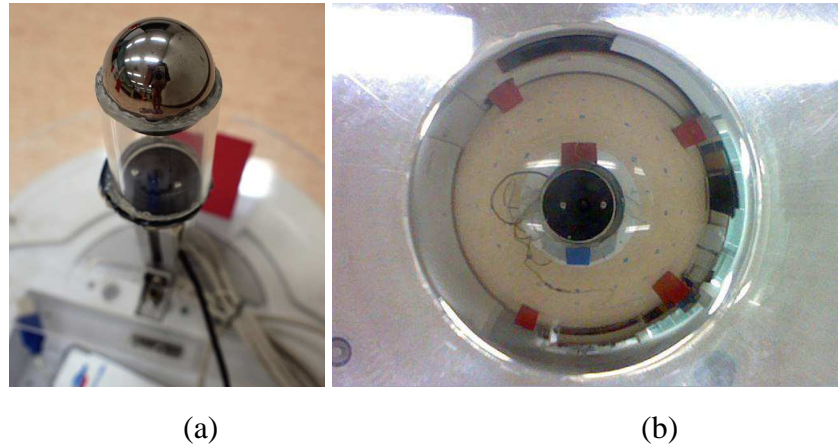


Figure 4.16: Omnidirectional camera and the captured image: (a) camera on the robot and (b) the snapshot taken with the camera at home location (Reprinted from Yu and Kim (2011c))



Figure 4.17: Panoramic snapshot image and landmark detection: (a) panoramic image converted from the omnidirectional snapshot image as Figure 4.16 (b) and (b) the landmark represented as white area (Adapted from Yu and Kim (2010b))

red-colored objects were discriminated from the background image and marked as landmarks in the omnidirectional ring. Figure 4.16 (b) is an omnidirectional snapshot image taken from the camera on the mobile robot, and by converting it, we obtain a panoramic environment snapshot image Figure 4.17 (a). In order to simplify the landmark detection procedure and focus on the performance evaluation of the image-based homing navigation methods, we set red cylindrical objects as landmarks. Based on the predetermined threshold HSV values of each pixel, landmarks could be easily detected. The result in detection of red color region is shown in Figure 4.17 (b). Based on the red-color detected panoramic image, we created one-dimensional ring image by slicing the image of 10 pixels height and averaging vertically. The slicing height is appropriately predetermined considering the height of the omnidirectional camera on ROOMBA.

The one step movement of robot for egomotion is 20 cm. The image shifts resulting

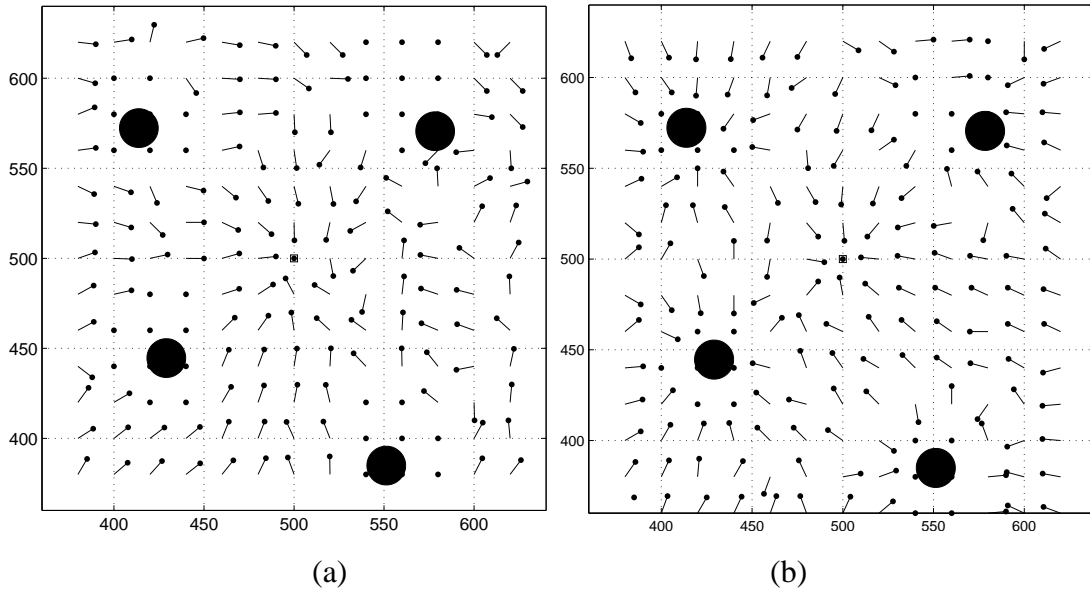


Figure 4.18: Vector map obtained in the mobile robot experiments (a) with the DELV method (adapted from Yu and Kim (2010b)) and the (b) predictive image-matching method. The dots indicate the direction of decided homing vector.

from the egomotion determined the landmark distances, and then landmark arrangements at the current location were projected onto the reference map. The vector map and the angular error results of the robotic experiments are shown in Figure 4.18 and Figure 4.19. Figure 4.18 (a) is the vector map results of DELV in robotic experiments with snapshot images and (b) is that with the predictive image-matching method. The points with no arrows but dots in the vector map are those where the agent could not take the snapshot due to the collision with landmarks. We compared the performance of the results as angular error graphs in Figure 4.19. The angular errors of DELV in real environment were greater than those in the simulation environments, most likely due to the landmark detection error from the snapshot images. However, the method still showed good performance in terms of returning to the target location because the angular errors were relatively small to allow for navigation to the nest.

For quantized distance applied DELV method, we also conducted robotic experiments with artificial landmarks. The experimental environment is as same as those shown in Figure 4.15. Since the navigation method computes the homing direction at each location based on the landmark information in images, we use the set of snapshot images taken from the environment at uniform grid points. The moving distance for the one step movement in DELV method is 20cm, and snapshots were taken for every

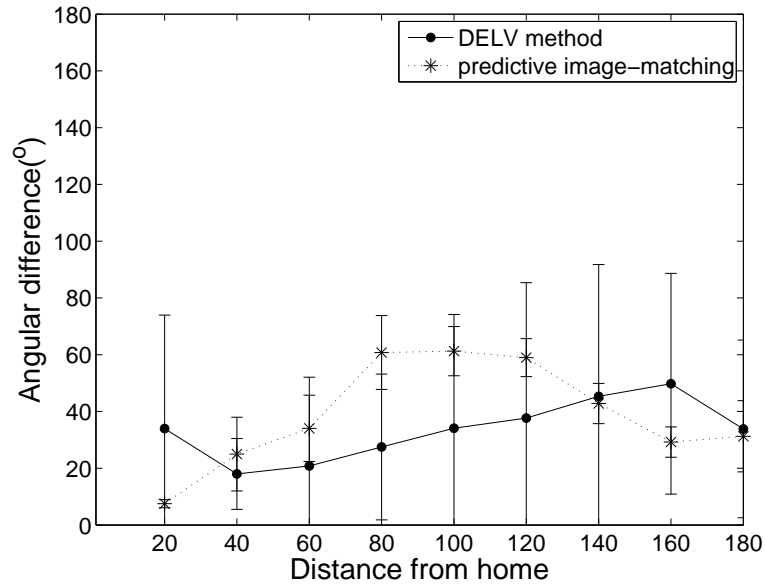


Figure 4.19: Error graphs of the DELV and predictive image-matching methods based on the vector map in Figure 4.18 (Adapted from Yu and Kim (2010b)).

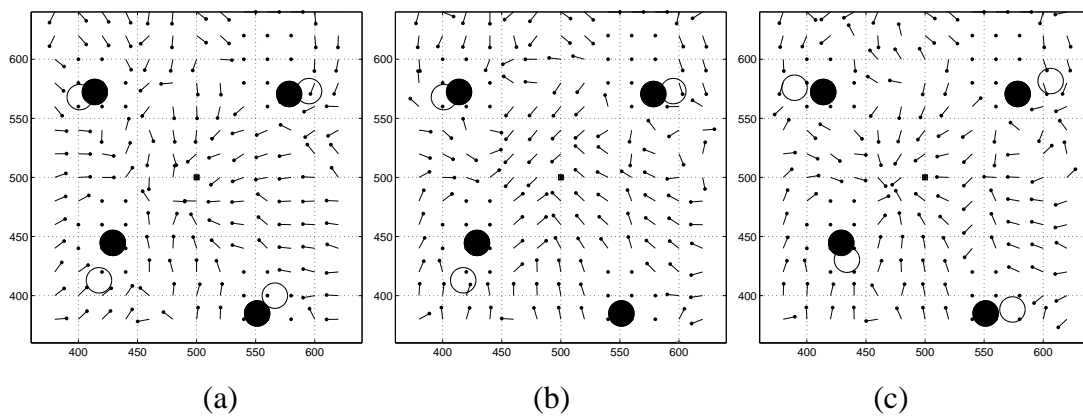


Figure 4.20: Vector map with the DELV method with different quantization levels of landmark distances; (a) level 1, (b) level 4, and (c) level 5.

20cm point in the squared environment of size 1.8m by 1.8m.

Vector maps in Figure 4.20 show homing vector results of DELV method with distance quantization of level 1, 4, and 5, respectively. White circles indicate the perceived landmark position with the quantized landmark distance while black circles are the actual landmark position. For example, in Figure 4.20 (a), landmarks are considered to be in same distance from the agent due to quantization level 1. Distance of landmarks in Figure 4.20 (b) are quantized into four levels, and one at the bottom-right is perceived to have larger distance which does not appear in the arena. Landmarks with quantiza-

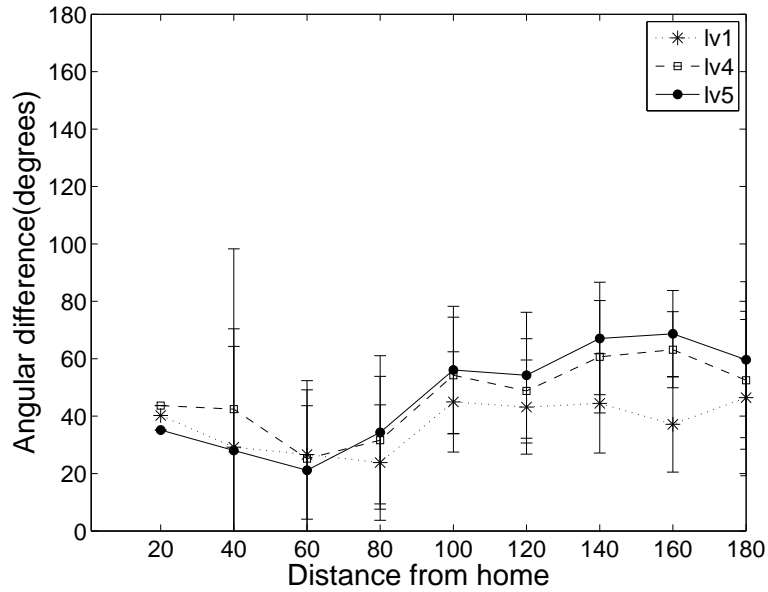


Figure 4.21: Error curves results applying DELV with quantized distance of level 1, 2, and 5 of corresponding vector map results in Figure 4.20

tion level 5 shows close approximation between perceived and actual landmarks as in Figure 4.20 (c).

Since the robotic experiments have additional cause of errors, the vector maps along with the angular error graphs (Figure 4.21 show larger error than those of the simulation experiments. The results of robotic experiments can be affected by errors in landmark position extraction from the image or the odometry error from the robot movement. The error level compared to those in Figure 4.19 did not show significant increase, however, and maintained similar level of errors with respect to the quantization level.

Therefore, through the results of robotic experiments, the DELV method with quantization of landmark distances also showed to be effective when applied to the real-world robotic system, as well.

4.4.2 Results with natural landmarks

For further verification, we performed robotic experiments in different environment. Robotic experiments shown previously were tested in an environment with artificially set landmarks. To simplify the landmark extraction procedure, we set red-colored



Figure 4.22: Unstructured environment for robotic experiments with natural landmarks such as a table, a flower pot and a drawer (Reprinted from Yu and Kim (2011d)).

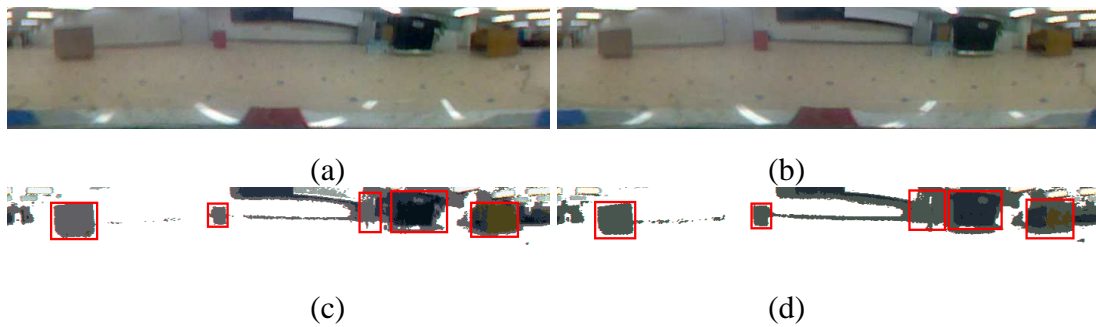


Figure 4.23: Panoramic snapshot images and segmentation of landmarks; (a) and (b) are panoramic snapshots taken and (c) and (d) show the region of interests by eliminating floor, ceiling and wall. The landmarks are marked as squared regions (Reprinted from Yu and Kim (2011d)).

cylindrical objects as landmarks (see Figure 4.15 (a)). They help recognize the environment and focus on the performance of the suggested navigation method. Now we test the method in an environment with natural landmarks. Figure 4.22 shows a new environment for robotic experiment. The environment consists of landmarks including a table, lecture desk, flower pot, and a drawer. ROOMBA, the same mobile robot introduced in Figure 4.15 (b) with omnidirectional camera, were used to test the navigation method in the environment.

Previously in the environment with artificial landmarks, the landmarks were detected based on the HSV level of each pixel, which is based on color information. However,

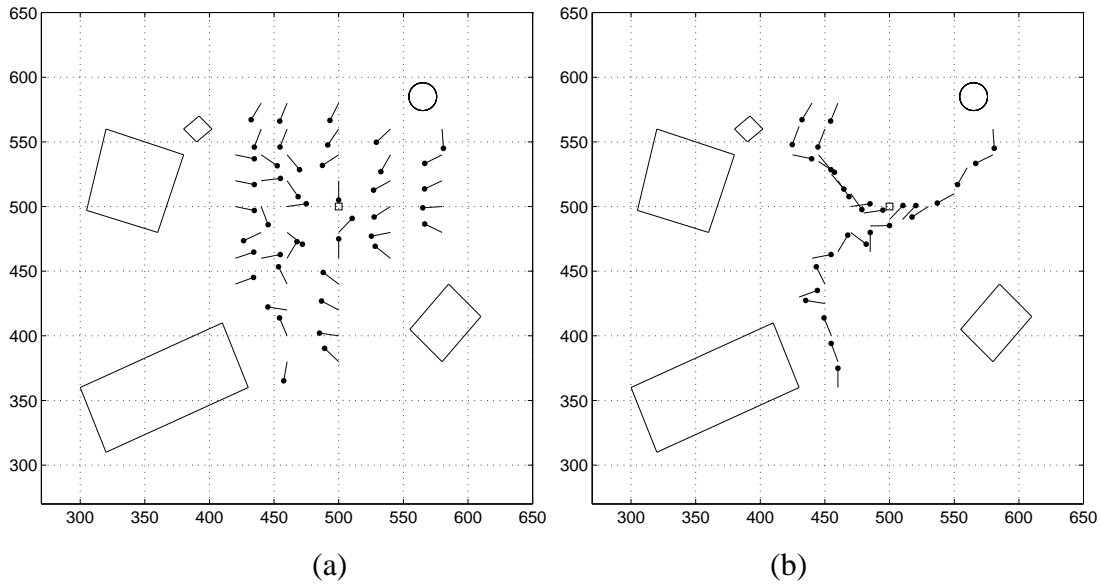


Figure 4.24: Vector map and homing path for several points from the experimental environment shown in Figure 4.22. Landmarks are described as circles and rectangles in the map showing (a) homing path and (b) homing vector (Reprinted from Yu and Kim (2011d)).

in the environment with natural landmarks, landmarks cannot be extracted directly from the snapshot image. In this paper, we applied the mean-shift clustering method (Comaniciu and Meer, 2002a,b) as a pre-processing of the image, then selected landmarks based on color information. This procedure is shown in Figure 4.23. The Figure 4.23 (a) and (b) shows a panoramic snapshot image processed from omnidirectional images obtained. After applying the mean-shift clustering method and eliminating the backgrounds as floor, ceiling and wall, the remains are now the interesting regions with possible landmarks. Then landmarks were segmented from the panoramic image, and relatively small landmarks were removed with a given threshold. Then the agent can select landmarks based on color, size, and considering the total number. The selected landmarks are shown in Figure 4.23 (c) and (d) as squared regions.

The results are shown in Figure 4.24. Circles and rectangles in the map indicate landmarks in the testing environment (see Figure 4.22). Home location is marked as small square at (500,500). The arrows in the vector map indicate the decided direction to move based on the suggested DELV method. The Figure 4.24 (b) shows four homing paths, two starting from the upper region, on front he right and one from the lower point in the map. Due to noise effects and the uncertainty of the type and number of

extracted features, the vector map and homing path show some errors, however, the graph shows that the mobile robot can successfully return home.

In the unstructured environment with natural landmarks, extracted landmarks are not same in every snapshots. The agent may not perceive exactly the same landmarks as those in the reference map in the real-world robotic experiments. These affect the landmark vectors and produce deviation of homing direction. Some points with error in homing vector in Figure 4.24 are caused by matching different landmarks in two snapshots. Solving this problem requires further work along with a more sophisticated landmark extraction technique.

4.5 Summary of Chapter 4

This chapter 4 shows the navigation results of the DELV method along with the comparison with the predictive image-matching method. Initially the distance information in DELV is continuous, then, the quantization of distance is introduced and applied.

Homing performance were shown in both computer simulation and robotic experiments as vector map, catchment area or success rate. For comparison in various environments, several different landmark configurations were tested and the results show low angular error in homing vector and high success rate in homing. As the landmark distance is estimated through one step movement of an agent, the moving distance d can be a controlling factor in the method, and results with different d are compared. The vector map results showed similar patterns and angular error level and had no significant influence on the performance with respect to varying d .

The DELV with both continuous and quantized landmark distances show small angular error in homing vector decision and high success rate in homing. The distance quantization might lead to the degradation in localization performance since the localization in the DELV method significantly depends on the length and angle of the landmark vector. The larger number of failures in homing resulted from smaller number of quantization levels leading to error in localization. However, through the landmark arrangement and the heading direction matching with landmark vector rotation, the method determines the homing direction appropriately. Three-level quantization of each landmark distance is sufficient to guide the robot home in many cases shown. That is, even a rough estimation or a low resolution of landmark distances can lead to

efficient homing performance of the method.

In addition, through simulation experiments in various types of landmark configurations environment, the method shows lower angular error in vector map results with landmarks surrounding the target location. Therefore, if the selected landmarks in environment surrounds home, the method would perform better.

Comparison to the predictive image-matching method indicated that the suggested method has a higher probability of resulting in a successful return to home. The landmark extraction step is required in DELV method while it does not in the predictive image-matching method, however, the results of accurate homing vector decision and the higher success rate compensate the additional process.

The method is tested in the robotic experiments in addition to the analysis on simulation results. The simple mobile robot ROOMBA with an omnidirectional camera is used for the experiment and the landmark environment is composed in two type, one with artificial landmarks and another with natural landmarks. In robotic experiments, the method showed good performance in angular error and homing path results, as well.

Chapter 5

DELV with reference compass

In the previous chapters, we have proposed the DELV method, a new landmark-based homing navigation method operating without a reference compass, and investigated its performance in the perspectives of spatial angular error and catchment area along with the comparison with an image-based navigation method of the predictive image-matching method.

In this Chapter, we present some experiments of the DELV method with a given reference compass. In our proposed navigation method, DELV does not necessarily require the reference compass information. Indeed the method can find the heading direction through the landmark rotational matching. To demonstrate its capability, we show both DELV experimental results with and without the reference compass. The results verify that the method shows a good performance even without a reference compass.

Along with the performance evaluation of the method in angular error graphs and catchment area, the results will be compared with other landmark-based navigation method too. In the previous chapter we compared the results of DELV without a reference compass to those of the predictive image-matching method. In this chapter, we will make a comparison with the ALV and another method suggested by Hong et al. (1992) and Weber et al. (1999), which was introduced in Chapter 2. This method computes a correction vector of each landmark pair. By summing all correction vectors, the agent can find the homing vector to move along. In addition to the concept of the correction vector initially suggested by Hong et al. (1992), in the work of Weber et al. (1999), the correspondence matching of landmarks has been simplified and results were improved as well. The method is similar to the ALV model in a way that

it involves the creation of a unit landmark vector but different that it uses correction vectors to compute the homing vector. In this paper, we call this method the average correction vector (ACV) method, since the method computes the homing vector based on the correction vector of each landmark. The ACV method using the correction vector, as well as the ALV model, still requires a reference compass information. Thus its the precision plays an important role in the performance of the model. The ACV method was introduced in previous chapter as a method sharing a similar concept of the landmark vectors. However, due to the different computational method of homing vector, it requires a reference compass to operate the ACV method. Therefore, it is legitimate to compare our DELV results including a reference compass with those of the ACV model in several perspectives. The bulk of this chapter is reported in Yu and Kim (2011b,a).

5.1 Performance evaluation

In this chapter, we compare DELV with another landmark-based navigation method, the ACV approach for performance evaluation. The homing algorithm suggested by Weber et al. (1999) introduces a concept of correction vector. Instead of directly exploiting the landmark vectors to obtain the homing vector, the correction vector for each landmark is computed first. The correction vector for each landmark indicates a direction to move to match the currently obtained landmark vector to that of the home point. The correction vectors are then averaged to obtain the final homing vector. Unlike the DELV method, the landmark vectors are considered as unit vector, that is, landmark vectors only contain angular information. The correction vector is defined based on the difference between corresponding landmark vectors from two snapshot images, and the length of the correction vector is defined as the difference in paired angles. The angle of the correction vector is perpendicular to the corresponding landmark vector, and the direction decided by comparing the angles. If the difference between the angles of paired landmark vectors is large, the agent obtains correction vector with longer distance, influencing the homing vector to compensate the difference more. Following Equation 5.1 and 5.2 describe the concept of landmark vector and homing vector computation for DELV and ACV, respectively and therefore show the similarity and difference between methods.

In DELV, as described in Equation 5.1, the agent first stores landmark vectors store

landmark vectors LV_i^R at home location which operate as a reference map for the subsequent homing task. At an arbitrary location, perceived landmark LV_i is projected on the reference map, LV_i^R and the result yields the projected vector PV_i for each landmark. Finally, a homing vector HV is determined by averaging the projected vectors. Detailed computation is shown previously in Equation 3.4 through Equation 3.8 in Chapter 3. In this chapter, we only show the simplified version of mathematical description of the method in order to compare the concept with the ACV model, and the detailed procedure was given in Chapter 3.

$$LV_i^R = (R_i, \theta_i) \text{ and } LV_i = (d_i, \alpha_i)$$

$$PV_i = LV_j - LV_i^R \quad (5.1)$$

$$HV = \frac{1}{N} \sum_{i=1}^N PV_i$$

In ACV method, the correction vector CV is introduced. Since the landmark vectors only consist of angular positions of landmarks, difference between paired angles θ_i and α_i defines the correction vector CV_i . The first equation in Equation 5.2 shows the representation of landmark vector of ACV in polar coordinate and the second equation shows the correction vector computation. Finally, the average in correction vectors define the homing vector HV .

$$LV_i^R = (1, \theta_i) \text{ and } LV_i = (1, \alpha_i)$$

$$|CV_i| = |\theta_i - \alpha_j|, \angle CV_i = \begin{cases} \alpha_i + 90^\circ & \text{if } \theta_i < \alpha_i \\ \alpha_i - 90^\circ & \text{if } \theta_i \geq \alpha_i \end{cases} \quad (5.2)$$

$$HV = \sum_{i=1}^N CV_i$$

The graphical representations in three-landmark environment are given in Figure 5.1. The dotted arrows indicate the landmark vector perceived at the home location LV_i^R , while the solid arrows indicate new landmark vectors LV_i at the current location to be compared to the stored LV_i^R . While two methods have significantly different types of landmark vector and procedures to compute homing vector, the resulting homing vectors in both methods are similar and directed toward home.

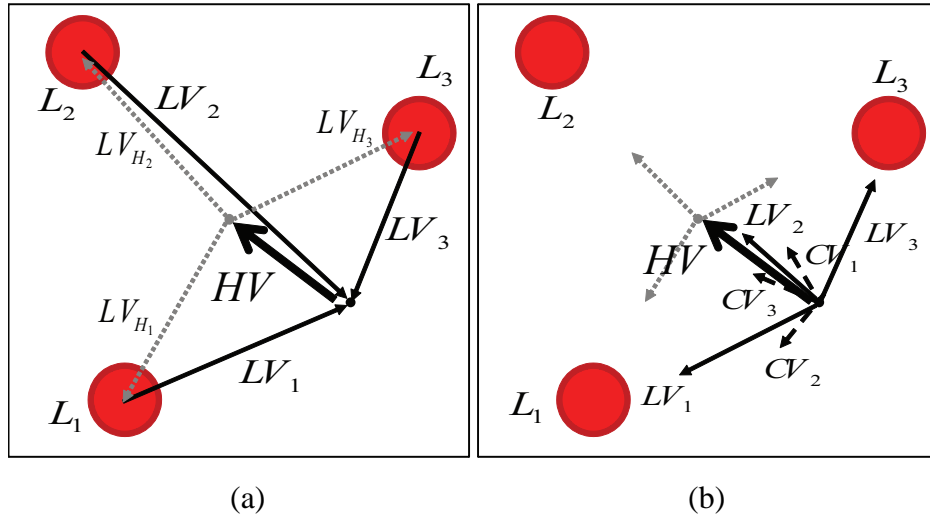


Figure 5.1: Summary of the homing vector (HV) computation in both (a) DELV and (b) ACV method. Dotted arrows: landmark vectors at home location, solid arrows: landmark vectors at current location (Reprinted from Yu and Kim (2011b))

Both methods exploit landmark information extracted from a snapshot image, and both attempt to derive a homing vector in a step-wise fashion via appropriate landmark arrangement matching between a pair of snapshots. The difference between two methods exist in the procedure for computing the homing vector and the criterion used for the arrangement decision. The DELV and ACV model have different computation methods in computing homing vector from the landmark information obtained from the snapshot, however, since the methods share similar concepts in setting landmark vector set, we compare the performance of both methods in same experimental conditions. Both DELV and ACV method requires landmark matching. While in the work of Weber et al. (1999) suggested various types of landmark matching, only rotational landmark vector matching is considered in this paper for an appropriate comparison. The ACV method requires a reference compass for orientation, therefore we compare the DELV method with reference compass information even though the DELV method is capable of estimating the current heading direction through landmark vector rotation.

Applying these experimental conditions, we compare the performance of navigation methods and compare the characteristics in following sections.

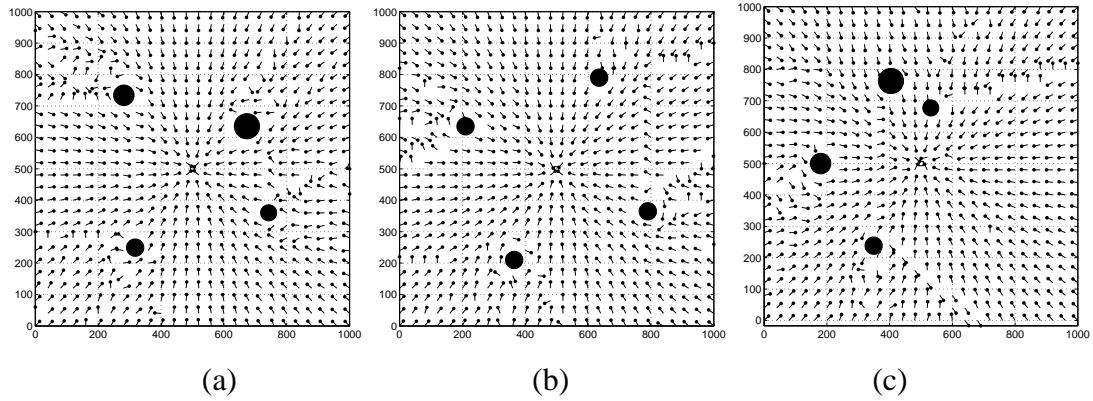


Figure 5.2: Vector map with DELV method applied in three different environments with reference compass (Reprinted from Yu and Kim (2011b)).

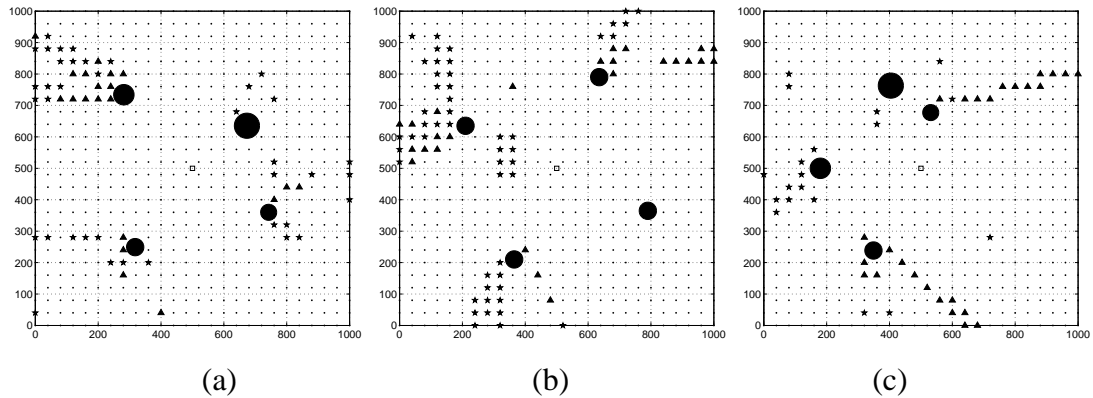


Figure 5.3: Spatial errors in homing vector. Marker of each point indicates the amount of angular error (•: less than 45° , ☆: between 45° and 90° , and \triangle : grater than 90°) with corresponding vector maps in Figure 5.2. (Reprinted from Yu and Kim (2011b)).

5.2 Simulation experiments

The vector maps of DELV method with reference compass is shown in Figure 5.2. Three different types of environment with different landmark configurations were applied as in Figure 4.2 for DELV without the reference compass. The spatial error graphs corresponding to the vector maps in Figure 5.2 are shown in Figure 5.3. We divided the homing vector result based on three level of angular errors and depicted the result graphically with dots, stars and triangles in the map.

In Chapter 4, we have shown the results of DELV method without the reference compass in same three environments. Therefore, we compare the results of both DELV methods with and without the reference compass in angular error graphs. Figure 5.4

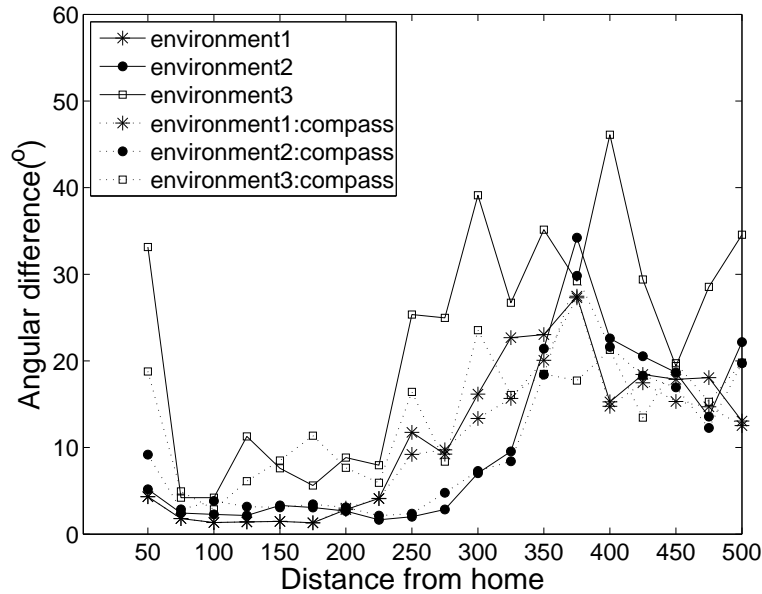


Figure 5.4: Error graphs for DELV results in three different environments 1, 2, and 3 shown in vector maps in Figure 4.2.

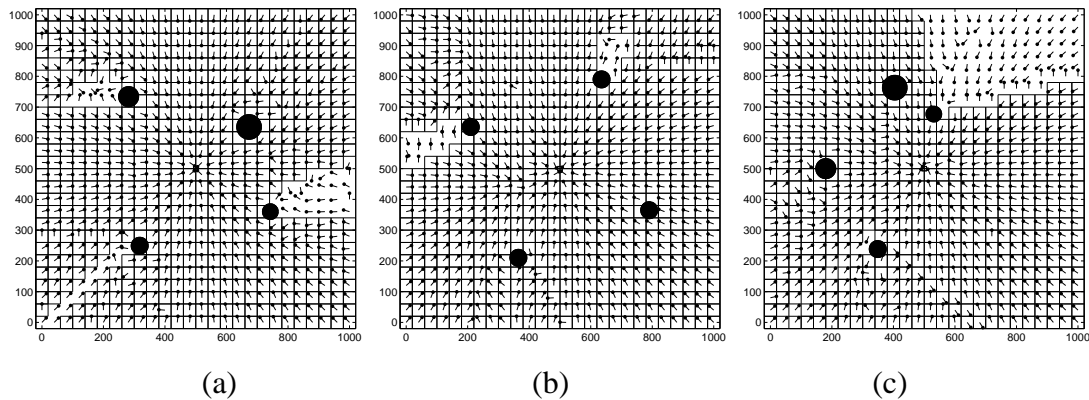


Figure 5.5: Catchment area with vector map for each environment: (a) 92.01%, (b) 97.04%, and (c) 84.91% of the environment. The squared region indicates that the corresponding point is inside the catchment area (Reprinted from Yu and Kim (2011b)).

depicts the angular error graphs of results shown in Figure 4.2 and Figure 5.2. The first three graphs with solid lines show angular graphs in three environments for DELV without reference compass and the last three with dotted lines are the results of those with the reference compass. Based on the error graphs, the method with the reference compass shows slightly smaller errors in average, which results from the error in the heading direction estimation. However, the difference between methods are not as significant while other methods show severely degraded performance or are even not able

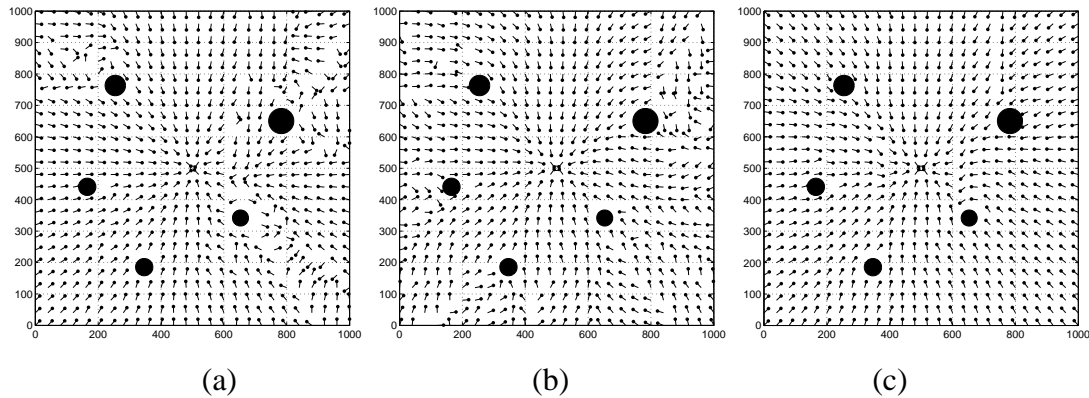


Figure 5.6: Vector maps: (a) DELV method (b) ACV method, and (c) ALV model with a reference compass

to operate when deprived of the reference compass.

The performance of the DELV method can be also shown by catchment area. In Figure 5.5 shows the catchment area with vector map for each environment. The percentage of the catchment area for each environment is 92.01%, 97.04%, and 84.91% while those of the results with DELV without reference compass were 98.52%, 95.41%, and 77.66%. In environment 1, shown in Figure 5.5 (a), the DELV method showed even better performance than without the reference compass using its own rotational matching for heading direction estimation. The level of the catchment area in environment 2 were similar in both cases, but lower in DELV without reference compass for environment 3. The results imply that for the environment with severe asymmetric landmark configurations, the heading direction estimation show might lead to more errors than in other cases. However, The overall level of the methods in both conditions show good performance.

5.3 Robustness analysis

As we previously compared the DELV method with the predictive image-matching method suggested by Franz et al. (1998) which also operates without the reference compass, in this chapter, ACV method is compared for the performance evaluation of the DELV method with reference compass.

The vector maps for DELV, ACV and ALV methods in same environment are given in Figure 5.6, and Figure 5.7 (a) shows the angular errors for both methods. In the

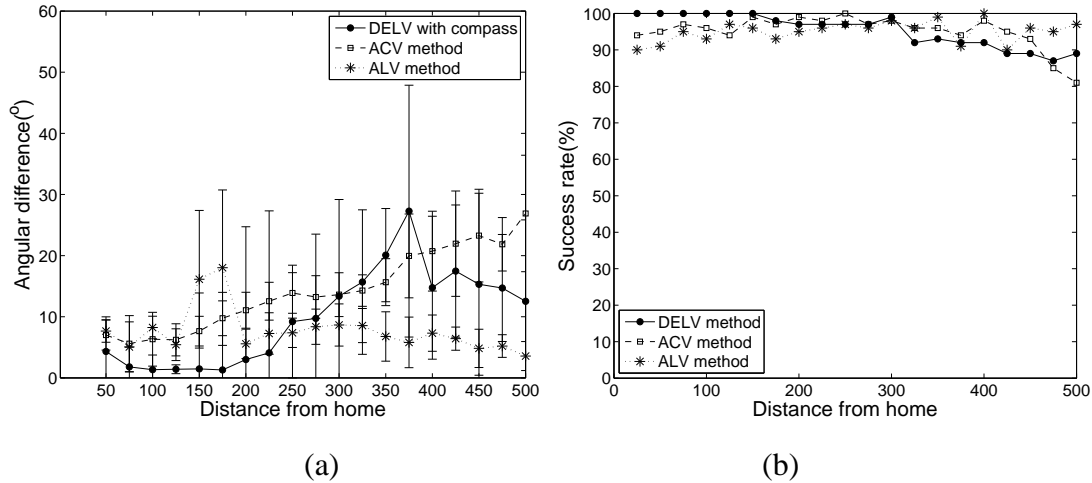


Figure 5.7: Performance comparison of (a) error curves of angular difference for DELV, ACV, and ALV method all with reference compass and (b) success rate among 100 trials with respect to the distance from home with a reference compass

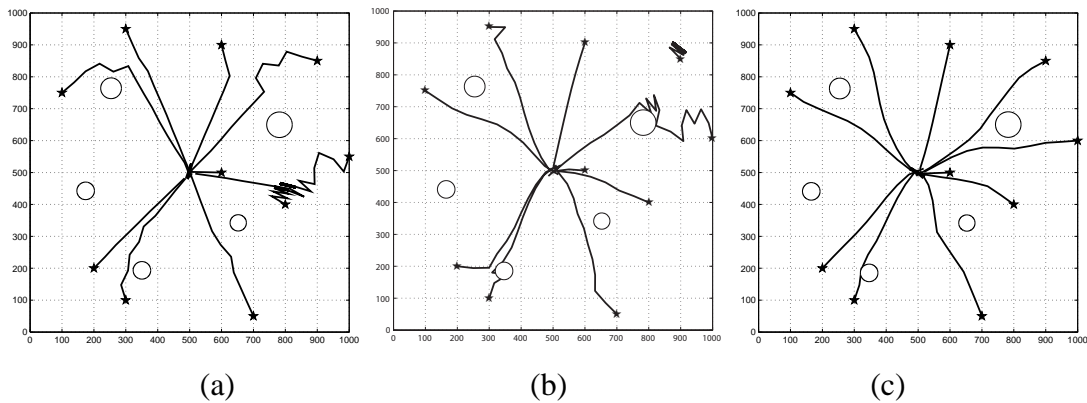


Figure 5.8: Trajectories of a mobile robot at the same starting points for (a) DELV method ($d = 50$), (b) ACV method, and (c) ALV model with starting point indicated as black stars

vector map results from DELV method, points with error in homing vector, that is, the deviated homing vector are randomly distributed. In ACV method, the vector map shows some flow in direction of decided homing vector (see Figure 5.6 (b)). Therefore, the overall homing vector can possess some errors, but the sudden deviation in points are fewer than that of the results of DELV method. The difference between methods is also shown in error graphs. As in Figure 5.7, the error level of DELV with reference compass is smaller than the ACV method in most of the region, but slightly higher in some. Similarly, comparing the performance with ALV, DELV show smaller angular error in some regions, but higher in others.

Success rate in Figure 5.7 (b) indicate the similar level of performance in both methods as well. The DELV method with reference compass showed little higher success rate in closer starting points while it decreased for the further starting point cases. Overall, the navigation method shows similar performance level based on the spatial angular errors and the success rate in homing task. In addition, to further investigate the characteristics of the homing algorithms, we observe the results of the performance with respect to the occlusion problem in the following section.

5.3.1 Occlusion problem

Previously in this paper, the homing vector computation were obtained based on the assumption that the agent can perceive every landmark without any occlusion or the horizon of perception problem. However, when one or more of landmarks disappear compared to the view the agent initially perceived at home location, the occlusion problem occurs since the agent cannot match landmarks in current view with those in the reference map. When the agent moves sufficiently far from home it may encounter occlusions or the disappearance of landmarks. Some landmarks may be hidden by other landmarks or background objects, or they could disappear from the view due to the distance. In addition, relatively small-sized landmarks may be invisible in a noisy environment. In real-world robotic experiments, occlusions can also exist due to many other factors, such as passing humans, the lighting condition, or faults in the feature or landmark extraction procedure. Here, we assume that all of these cases classified as occlusions.

In following simulation experiments, some landmarks may be intentionally removed to monitor the effect of occluded landmarks. All three methods were explained under the assumption that the robot would perceive the same landmarks observed at the home location and the occlusion problem would affect the performance of navigation.

With the presence of several landmarks in the environment, there will be some occlusion regions, and more landmarks tend to produce more occlusions. Independent to the occlusions that would occur naturally by the other landmark, we simulated occlusions by artificially removing one of the landmarks when a robot attempted to perform homing navigation. As a result, the agent may not be able to see the occluded landmark. Using this situation, we actually create discrepancy between two snapshots and thus can analyze the performance of each method in the presence of an occlusion.

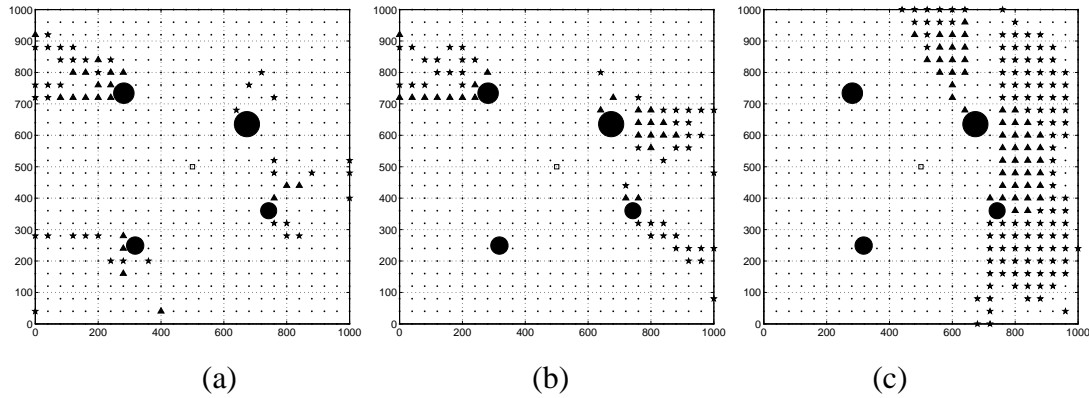


Figure 5.9: Graphs showing error points as the number of occluded landmarks increases from (a) zero, (b) one to (c) two (Reprinted from Yu and Kim (2011b)).

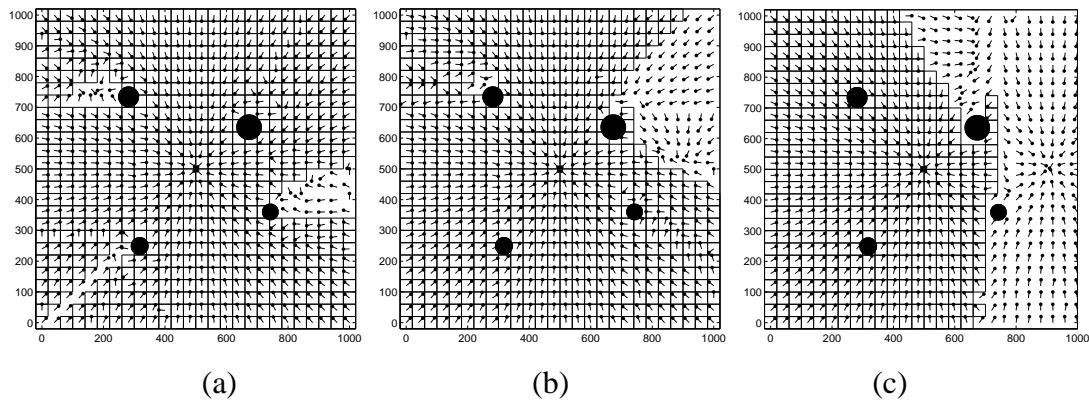


Figure 5.10: Catchment area with vector map for each environment: (a) 92.01%, (b) 82.04%, and (c) 59.11% of the environment. The number of landmarks is zero for (a) and one, two for (b) and (c), respectively (Reprinted from Yu and Kim (2011b)).

The landmark occlusion simulation results in environment 1 are shown in Figure 5.9 and Figure 5.10. The results are displayed with error points plotted according to the same criterion described in previous sections. The results with none of the landmarks being intentionally occluded is Figure 5.9 (a), while (b) and (c) have one and two occluded landmarks, respectively. The occluded number of landmarks are one, two and three in Figure 5.10 (a), (b), and (c) as well.

Figure 5.9 shows that as the number of occluded landmarks increase, the region of homing vector with errors also increases. More detailed numerical results and comparison with the ACV method is in Tables 5.1 and Tables 5.2. For each method DELV, ACV, and ALV, the error point percentage is shown along with the different numbers of occluded landmarks in environment 1, 2, and 3 are shown in Table 5.1. The first

Occluded #		none		1		2	
Error amount		e > 45°	e > 90°	e > 45°	e > 90°	e > 45°	e > 90°
Environment 1	DELV	8.75	3.02	13.99	3.62	20.48	6.49
	ACV	9.80	0.15	42.50	10.07	80.63	33.54
	ALV	0.00	0.00	8.64	1.92	12.07	3.34
Environment 2	DELV	7.99	4.07	13.61	4.00	20.15	6.33
	ACV	7.99	0.15	39.37	8.71	74.33	36.32
	ALV	0.00	0.00	10.24	2.60	14.91	4.95
Environment 3	DELV	6.79	3.92	8.33	3.24	14.78	4.68
	ACV	33.33	2.71	53.47	12.18	73.88	27.63
	ALV	0.00	0.00	4.87	1.40	8.74	2.19

Table 5.1: Error point rate(%) for each environments with different landmark distribution (Adapted from Yu and Kim (2011b))

row in the table, results of DELV in environment 1 corresponds to the error graphs in Figure 5.9. DELV method results of the first column with no occlusions corresponds to the vector map results and the angular error graphs in Figure 5.2 and Figure 5.3.

Comparing the DELV and ACV methods, the DELV method exhibits a smaller error rate and better performance. Even though an increase in the error rate is observed for both methods as the number of occluded landmarks is increased, the ACV method exhibits much more rapid increase in the error rate compared to that of the DELV model (see Table 5.1. It implied that the ACV method is more sensitive to snapshot discrepancies when determining the one-point homing vector.

In some normal environments, the ALV model shows perfect homing vector results with no involved perception problem as listed in Table 5.1. However, in some cases, ALV shows a larger error rate. As we have examined in the previous chapter, the DELV performs better when selected landmarks surround the target location. The environments tested in Table. 5.2 include equally distributed landmarks configuration with different landmark numbers, in which the DELV method could show the best performance.

The vector maps and catchment area results along with the landmark occlusion in the environment are shown in Figure 5.10 and numerical results in Table 5.3 and Table 5.4. Comparing the results, the ACV method is found to yield a larger catchment area

Occ #		none		1		2		3	
		e > 45°	e > 90°						
L=3	DELV	5.23	2.69	6.43	0.75	36.62	9.12	-	-
	ACV	23.77	2.09	42.75	12.11	84.3	28.25	-	-
	ALV	0.00	0.00	13.62	5.94	27.00	7.29	-	-
L=4	DELV	8.75	3.02	13.99	3.62	20.48	6.49	-	-
	ACV	9.80	0.15	42.50	10.07	80.63	33.54	-	-
	ALV	0.00	0.00	10.24	2.60	14.91	4.95	-	-
L=5	DELV	13.29	7.10	12.39	4.08	27.19	9.21	27.19	9.21
	ACV	13.14	3.47	37.46	5.29	86.10	39.27	86.10	39.27
	ALV	0.00	0.00	5.80	1.75	12.08	3.71	17.07	6.65
L=6	DELV	19.94	9.97	16.31	8.16	18.43	6.04	27.95	7.10
	ACV	21.87	8.60	35.60	12.22	51.43	18.25	27.90	7.09
	ALV	0.00	0.00	3.84	1.14	7.73	2.09	13.61	5.10

Table 5.2: Error point rate(%) for each environments with different landmark number (Adapted from Yu and Kim (2011a))

with almost 100% than does the DELV method (92.01%). This is also true in the environment with one occluded landmark; the catchment area percentages are 49.11% for DELV and 52.88% for ACV method. However, the percentage of catchment area in both methods severely decreases as the number of occluded landmarks increases which may be the natural consequences. An analysis of the obtained results reveals that landmark occlusions affect the performances of the navigation algorithms and increase the angular error of the overall region. The occlusions also shrink the catchment area, as shown in Table 5.3. The noticeable trend shown in the table is that the catchment area generated with the ACV method shrinks more rapidly than that of the DELV method. As a result, the catchment area of the DELV method exceeds the result of the ACV method when two out of four landmarks are occluded in the environment. This indicates that the ACV method, despite its large catchment area in the environment with no occlusions, is one again vulnerable to the occlusion problem compared to the DELV method. An examination of the vector map results reveals that the difference between the vector maps from each method can be based on the existence of the vector flow. There are flows in resulting vector map when obtained homing vectors for points nearby have similar directions. This flow was one of the reasons for an increase in the angular error but the flow may possibly result in successful homing.

Occluded #		none	1	2
Environment 1	DELV	92.01	49.11	40.3
	ACV	100.0	52.88	24.14
	ALV	100.0	7.84	20.44
Environment 2	DELV	97.04	53.96	51.86
	ACV	100.0	54.99	25.47
	ALV	100.0	17.09	23.10
Environment 3	DELV	84.91	69.08	62.34
	ACV	98.67	45.34	18.46
	ALV	100.0	23.15	20.59

Table 5.3: Catchment area rate(%) for each environments with different landmark distribution (Adapted from Yu and Kim (2011b))

Similar patterns are shown in the results compared with ALV method. The ALV method, as well as in the error point rates results, shows perfect homing ability with catchment area rate of 100% when all landmarks are perceived. When one or more landmarks are occluded, the rate of the catchment area obtained with ALV method rapidly decreases. As in Table 5.3 and Table 5.4, the catchment area of the ALV method is much smaller than those of the DELV method when landmarks were occluded.

In this section, the characteristics and advantages of the landmark-based methods in certain environments and situations were investigated, with primary focus on the homing vector and the rate of successful homing. When comparing the DELV with ACV and ALV methods, the DELV method shows similar error rate in the vector map results. With small occlusions, the ACV and ALV approach exhibits better homing ability, however, the DELV method tolerates the occlusion problem with better performance, even if the method shows increased error rates as the number of occlusions increases.

5.3.2 Navigation method with visual reference compass

Many robotic navigation methods, such as ACV and ALV models, require reference compass information. However, in indoor environments, difficulties in the use of a magnetic compass or other reference compasses may be encountered. Thus, a navigation method that is independent of the reference compass is advantageous. Several

Occluded #		none	1	2	3
L=3	DELV	94.82	100	17.46	-
	ACV	99.56	8.28	5.62	-
	ALV	100.0	9.82	10.36	-
L=4	DELV	92.01	49.11	40.3	-
	ACV	100.0	52.88	24.14	-
	ALV	100.0	17.09	23.10	-
L=5	DELV	87.43	87.13	83.58	2.96
	ACV	91.12	85.06	54.14	1.78
	ALV	100.0	12.46	18.73	8.98
L=6	DELV	85.65	84.32	70.71	2.96
	ACV	87.28	77.96	66.57	3.4
	ALV	100.0	13.74	34.05	11.74

Table 5.4: Catchment area rate(%) for each environments with different landmark number (Adapted from Yu and Kim (2011a)).

visual homing methods determine the homing direction without compass information through the use of a snapshot image, and the DELV method suggested in this paper also estimates the heading direction by landmark arrangement matching.

In addition, the method named as “visual compass” (Zeil et al., 2003; Labrosse, 2006) was suggested which determines the heading direction via computing the rotational matching of two snapshots. The visual compass method has been suggested by Labrosse (2006) to estimate a heading direction based on snapshot images. The method computes the discrepancy between a pair of omnidirectional images by rotating the image. It then determines the current heading direction based on a reference image. Setting the heading direction of the snapshot at the goal location as the reference, the visual compass method offers the current head direction based on the comparison of another snapshot, the reference. The method has its basis concept of estimating the physical distance between the locations with the image distance by pixel differences between two snapshot images (Zeil et al., 2003). When the method is applied in real-world robotic experiments, the images obtained by the omnidirectional camera are compared. However, in this work, we applied the method in a simulation environment. Therefore, organizing the environmental conditions could affect the performance of the method. In order to effectively apply the visual compass method, appropriate background set-

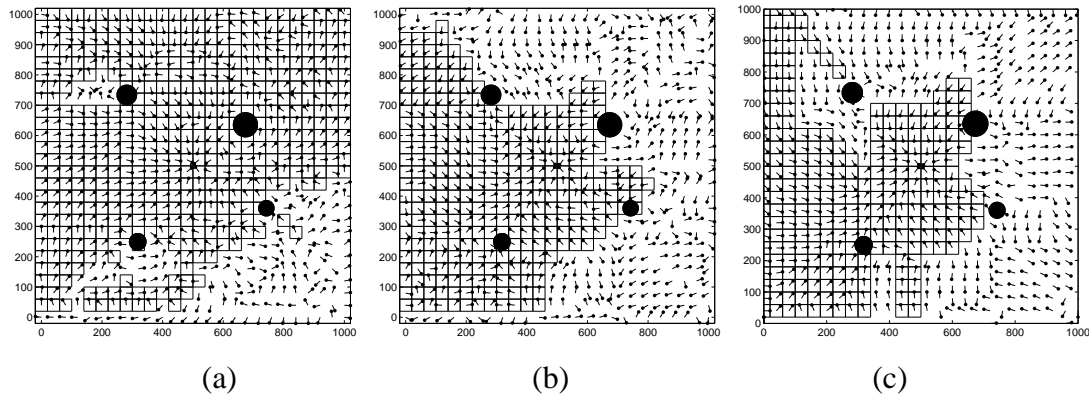


Figure 5.11: Vector maps and catchment area obtained with (a) DELV, (b) ACV and (c) ALV algorithms along with the heading direction estimation obtained with the visual compass method. Catchment areas for each case are 74.85%, 47.04%, and 40.68%, respectively (Reprinted from Yu and Kim (2011b)).

tings of the simulation environment are required.

In this section, we compare the navigation results of DELV, ACV, and ALV applying visual compass method instead of the given reference compass information. Substituting the reference compass with the visual compass obtained from the image enables the navigation method to become independent of the external information but to focus on the exploiting the snapshot image information. In addition, applying the visual compass method, which may not be perfect in estimating the heading direction, the results show the dependency on the accuracy of the reference compass of the method.

Figure 5.11 show the result of applying three navigation method with visual compass method as the compass information. Since the heading estimation according to the visual compass method does not guarantee 100% of accuracy, the results show larger error in the direction of the homing vector compared to the results obtained when a reference compass is given (see Figure 5.2 and Figure 5.6). Homing path analysis is important since increasing the homing accuracy is the ultimate goal of the navigation algorithms. The catchment area includes points that could successfully lead to the home location using the decided homing vector. The size of the catchment areas in the maps for DELV, ACV, and ALV methods are 74.85%, 47.04%, 40.68%, respectively. The reason for the low catchment areas with the ACV and ALV methods seems to be related to an increase in the trap points in the environment.

The error graphs are shown in Figure 5.12. The DELV method has smaller errors than

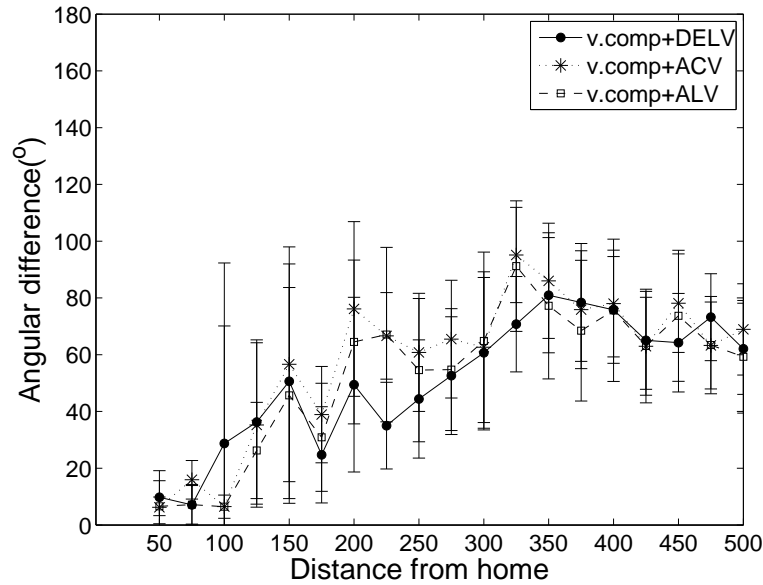


Figure 5.12: Error graphs obtained from the DELV, ACV, and ALV methods with the visual compass method. The corresponding vector maps are shown in Figure 5.11 (Reprinted from Yu and Kim (2011b)).

other models. In the results obtained with the reference compass information, the error rate of the ALV model is found to be extremely low, while those of the DELV and ACV methods are quite similar in some environments. However, upon application of the visual compass method, the error of the DELV method is smaller than that of the ALV model, whose error rate is the most increased. The results indicates that the ALV and ACV models are dependent on the compass information, and thus, the performance of the navigation is vulnerable to the accuracy of the reference compass. Therefore, we can assume that the DELV method is more robust when there is no reference compass information.

The results show that the DELV method exhibits robust navigation performance not only with respect to the spatial error rate, but also with regard to the homing path analysis.

5.4 Summary of Chapter 5

This chapter investigated several perspectives of the DELV method with reference compass. While the previous performance evaluation was shown in comparison with

the predictive image-matching method, the holistic method, the DELV method with reference compass is compared to the landmark-based navigation method with similar concept of landmark vector requiring the compass information.

First, the performance of the DELV with and without the reference compass is compared. Experimental results in the same environments showed that the DELV method shows similar level of performance even without the reference compass while many navigation methods are significantly dependent to the existence and the accuracy of the compass information. The results are also shown by applying visual compass method to substitute the reference compass. The visual compass was applied for the heading direction estimation to each DELV, ACV and ALV method. The results showed that DELV method is less affected by the accuracy of the heading direction estimation than other two methods.

Then, the comparison with results of ACV and ALV method is given in vector maps, angular error graphs, success rate and trajectory. The results from both methods do not show significant difference in these perspectives, however, the advantage in the DELV lies in that the method does not necessarily require the reference compass while the ACV model does. Additionally, the robustness of methods were examined through the investigation on the occlusion problem. In the series of tests, the DELV method showed higher robustness compared to the other methods.

Chapter 6

Conclusion

In this thesis, we investigate a new landmark-based homing navigation algorithm without any reference compass information. Our distance-estimated landmark vector (DELV) model extracts landmark information from the snapshot image and incorporates it into vectors to be used for the determination of the homing vector. The model utilizes the quantized distance information, which is demonstrated to give a good performance level in homing navigation. Chapters 3 and 5 describe the detailed methods of the proposed homing navigation. Chapters 4 and 5 provide the corresponding results of experiments. The experiments were conducted in both computer simulations and in robotic experiments. Although the proposed DELV method does not require a reference compass, the reference-compass-enabled method is also introduced in Chapter 5 for comparison.

The basic concept of the DELV model is to create a set of landmark vectors with the estimated distances to landmarks and the angular positions as obtained from the omnidirectional snapshot image. The landmark distance is estimated from the angular shift of the landmark after one step movement. Using the geometric relations, the distance to the landmark can be determined from the previous angular position, the current angular position of the landmark, the rotated angle in the procedure, and the moving distance of the mobile robot. The reference map is defined as a set of landmark vectors with their bearings and distances at the target location. The same information of landmark vectors at another location is now projected into the reference map so as to obtain a homing direction. Landmark projection requires the landmark correspondence matching in advance. In our navigation method, the correspondence problem

along with the heading-direction estimation is resolved by the landmark arrangement matching with rotated vectors. The endpoints of the projected landmark vectors on the reference map converge best when applied with an appropriate landmark order and the heading direction. Therefore, by searching the two-dimensional configuration space of possible landmark orderings and monitoring the variance of the endpoints, the agent can determine the landmark matching between a pair of snapshot images.

The landmark vector projection can be regarded as a kind of image comparison in the snapshot model. A search for the minimum variance of the endpoints of projected landmark vectors corresponds to the minimization of the discrepancy between snapshot images in the image-based navigation method. Therefore, although our homing navigation method is classified as one of the landmark-based methods, the basic concept and methodology of our method share some aspect of the image-based holistic method.

In experiments, we set up the experimental environments with cylindrical landmarks. The mobile agent can perceive an omni-directional view of surroundings. The agent is assumed to have started the exploration from the target location, and replaced at an arbitrary location. At each location, the agent determines the homing direction according to the methods provided, and the results are illustrated as vector maps. Based on the vector maps, we obtain the angular error graphs. The difference between the obtained angle in the vector map and the ideal direction, which is a direction of a straight line from the current location to the target point, is considered as an error in the homing vector. The errors for the points in certain distances from home are averaged and plotted in terms of angular error graphs. The success rate of homing and the catchment area capture slightly different perspectives on the performance of the method. While the vector map and the angular error graphs show the performance in a static point of view, the success rate is rather a continuous and sequential result of performance.

6.1 Estimation and quantization of the landmark distance

The distance estimation is one of the essential parts of the proposed method. The localization and correspondence matching are made by the projection of appropriate

landmark vectors to the accurate reference map. The distance to landmark is estimated by the angular shift of the landmark in an omni-directional snapshot between the movement. If the agent observes a moving object, motion parallax would give information on their distance. Conversely, if the agent moves in a static environment, it will be able to estimate the position of each landmark in the environment. Although the distance-estimation procedure used in this method can be affected by the odometry error and the accuracy of the landmark extraction results, the results in the previous chapters demonstrate that, the homing performance of our method is quite good.

The distance-quantization is one way to reduce the effect of noise in the estimation of landmark distance. Since the quantization of landmark distance employs discrete levels to assign each landmark at the pre-determined distance, the accuracy of the estimated distance becomes less important. Indeed, distance quantization may affect the accuracy of the localization results. In order to estimate the current location accurately, one should obtain the distance to each landmark along with appropriate projecting order and heading direction. However, our method is proved to be effective even with the quantized distance. Even though the distance in the landmark vector does not reflect the actual distance to the landmark, we can obtain the direction of the homing vector by deploying appropriate landmark order and heading direction. In addition, the quantization of the landmark distance has an advantage of reducing the amount of memory required to store the landmark vectors.

6.2 Comparison with other methods

The performance results of our DELV method are mainly compared to two different types of navigation methods. In the comparison, the DELV method without the reference compass is matched against the predictive image-matching method, while the results of DELV method with the compass information enabled are compared with the ACV model. In the overall analysis, our DELV method demonstrates a successful performance on the homing navigation.

While it requires an additional process of the landmark extraction compared to the predictive image-matching method, the DELV method poses a significantly smaller error in the homing vector results and in the homing success rate as well. There is no big difference in the angular error or catchment area results between the DELV and ACV

method. Furthermore, the DELV method shows more robust performance when the perceived result of environment is damaged. For example, when the perceived environment is damaged deliberately by hiding certain landmarks, the DELV performed better than other navigation methods. In addition, to examine the effect on the accuracy of the reference compass, we have applied the visual compass method to the navigation methods. Both results indicated that the DELV method is insensitive to the accuracy of the environmental perception and the compass sensor information.

6.3 Future work

6.3.1 Landmark extraction

One of the important issues in the landmark-based navigation method is an effective extraction of landmark information from the image background. In this study, we employed color information to detect landmarks. In simulation experiments, we used red-colored cylindrical objects as artificial landmarks because they could be easily detected by the threshold of pixel values. In a natural environment, we can select landmarks based on the mean-shift clustering results, which are also based on color information. Even though the comparison of the DELV method with the image-based navigation method in Chapter 4 shows a better navigation performance of our method, the additional process required to extract the landmarks can be disadvantageous to our method. Many researchers prefer to use the descent in the image distance or image warping methods including the predictive image-matching method, which do not require an extraction of landmark features. These visual navigation methods may be simpler as demonstrated in this thesis, but the landmark-based navigation yields better homing performance in the environment where landmarks can be distinguished. Therefore, once an efficient and robust feature-extraction scheme is implemented, the landmark-based navigation methods can be more effective.

6.3.2 Localization

In the DELV method proposed in this thesis, when landmark distances are continuous, the agent can localize itself with landmark vector projection. Though the performance of localization has not been shown in this thesis, in additional experiments, we observe

that the agent could localize itself accurately inside the area surrounded by landmarks. On the other hand, however, when the agent is located outside the area surrounded by landmarks, the localization results have errors in many cases. The errors arise from the wrong landmark order matching or heading direction estimation. The localization problem is not crucial in homing task as we have shown through the experiments in the previous chapters. In most cases, the agent could return home successfully without the errors in localization. Moreover, in the DELV method, the accuracy in the estimation of the current position becomes higher as the agent moves toward home. Therefore, no additional work was needed for the localization.

In the homing navigation, we only focused on the performance of homing vector and homing path, but in the mapping or exploration of the unknown environment, the localization is an important task. To improve the localization performance, we can apply the continuous and probabilistic update in localization. Since most of the error in the location estimation is caused in the process of searching for landmark arrangement or heading direction with landmark vector rotation, additional information on the right order may improve the result. The information on the previous location provides additional information to determine the appropriate order in the rotational projection of landmark vectors. The previous location information can be updated in time or also operate in a probabilistic manner leading to a gradual increase in probability of the estimated location.

In this way, the performance of localization can be improved and the method can also be applied in mapping or exploration tasks.

6.3.3 Occlusion problem

Another issue in the image-based homing navigation is in the robustness problem. The robustness of the navigation methods are analyzed in two perspectives: the occlusion problem and the accuracy on a reference compass. The occlusion problem is a crucial issue in the real-world robot navigation as well as in the simulation experiments. As it has been shown from the results, the points outside the area surrounded by landmarks pose larger errors than those in the insider. The main cause of this result is attributed to the occlusion problem. In the real-world robotic experiments, the landmark detection and even the shape of objects can affect the image process. A moving person can affect the view of the agent, and the false detection of landmarks can also lead to error

in landmark matching. In the image-based navigation method, the occlusion problem has not been investigated much yet due to the complexity of the problem. A solution on the occlusion problem might significantly improve the performance of the image-based navigation methods.

Using the distance-estimated landmark vector method alone, it is difficult to overcome the occlusion problem. One solution is to combine it with other methods, especially the image-based navigation methods. While the performance of the landmark-based methods shows a difference between inside and outside of the area surrounded by landmarks, the image-based matching methods such as warping maintain a similar level of performance, in spite of the larger errors in homing on average. Therefore, the agent may apply image-based navigation method when it can not determine an appropriate homing direction including the landmark occlusions, but use the landmark vector method otherwise. Combining two methods in a complementary manner, the performance can be improved. The remaining problem, however, is to determine when and how to incorporate the image-based method. There may be several strategies for merging different methods. The agent can use one of them as the main method, and be assisted by another method. When the agent detects when the main method does not operate well at a certain point, another method can be picked up, depending on the current environment, and override the main method. In order to choose the method appropriately, the characteristics of the methods, the advantages and weakness should be investigated in advance. Based on their characteristics, the agent could apply the selected results at each location. Investigation on these points could lead to navigation method with better performance.

6.3.4 Interaction with odometry information

In the point of view of combinations, the most commonly known method is to combine vision-based navigation with path integration. The path integration is a long-range navigation method which is affected by the accumulated error throughout the exploration. Using the path integration, the agent can return to the vicinity of a target location, but pinpointing the target location accurately is difficult due to the accumulated errors. Therefore, we may consider the method to combine the odometry information with the vision-based navigation method as suggested in this thesis. The agent can return to the area near home with the long-range navigation and then switch to the vision-based

navigation method to accurately find the target location. Since the odometry information includes errors from the long distance of exploration and the visual information is more effective when the agent is near home area, the combinational approach can compensate for the weakness of each method.

The interaction between the odometry information and visual information has been also observed in experiments on animals' behaviors (Etienne and Jeffery, 2004; Collett and Collett, 2000; Vladusich et al., 2005).

There are several different ways to combine information from odometry and visual input. The simplest way is to use path integration for a long distance exploration and to switch to a vision-based navigation method when it has no more odometry information. More sophisticated method is to use an interaction between two types of information case-by-case. For example, in the experiments on honeybees (Vladusich et al., 2005), bees showed behaviors indicating that they use interactions of visual odometry and landmark guidance during food search. As other insects, honeybees use odometry information to find the target location while its fidelity is influenced by the landmark information. In addition, when two cues conflict, honeybees relied on the familiar landmark cues than the odometry information. Based on their behavior, one method does not always override the other, and they interact with each other to decide the direction and distance to move.

Inspired by the behavior of insects and other animals shown in previous works, we can develop a navigation system with effective interaction between two different navigation cues. This type of combination method may show good performance in robotic experiments.

6.3.5 Combination with place cell

Another method to be investigated is to introduce a place cell concept. Mammals including rodents and gerbils exploit the place cells of hippocampus for navigation. Each place cell is associated with certain location in the environment, and when the animal explores in a specific region, the place cell is activated. Several robotic systems applying the concept of place cell have been suggested (Goedemé et al., 2005). If the agent obtains the snapshot image at visited points, the mobile robot could return home or navigate in the environment with localizing itself by comparing the current

snapshot image to the stored images. The images can be compared by computing distance measure or matching several features in the images. However, in order to apply the method in mobile robot navigation with good performance, a large number of images should be stored. Since the distance-estimated landmark vector method has been shown to be efficient in large area, it can assist the place cell navigation method. A snapshot image may form a place cell and it can cover similar landmark features. Therefore, combining the place cell concept with the vision-based navigation method, the agent may move in the environment more efficiently.

6.3.6 Biological modeling

One of the purpose of the bio-inspired researches are to suggest an effective, robust yet simple method with good performance inspired by the behavior and mechanisms of insects and other animals. Insects and other animals use simple sensory-motor system. Therefore, another future work would be to suggest a navigation method that can be modelled biologically as well. In order to model the method biologically, the method should include simple sensory input as well as computation with low complexity.

Along with the analysis on the characteristics and the performance level of our homing navigation method, a simpler and more robust navigation method can be introduced. The future work may focus on enhancing the performance of the algorithm in real-world experiments with a simple and robust method.

Bibliography

- Basten, K. and Mallot, H. (2010). Simulated visual homing in desert ant natural environments: efficiency of skyline cues. *Biological Cybernetics*, 102(5):413–425.
- Butz, M., Shirinov, E., and Reif, K. (2010). Self-organizing sensorimotor maps plus internal motivations yield animal-like behavior. *Adaptive Behavior*, 18(3-4):315–338.
- Cartwright, B. and Collett, T. (1983). Landmark learning in bees. *Journal of Comparative Physiology A*, 151(4):521–543.
- Cartwright, B. and Collett, T. (1987). Landmark maps for honeybees. *Biological Cybernetics*, 57(1):85–93.
- Collett, M. and Collett, T. (2000). How do insects use path integration for their navigation? *Biological Cybernetics*, 83(3):245–259.
- Collett, T. (1996). Insect navigation en route to the goal: multiple strategies for the use of landmarks. *Journal of Experimental Biology*, 199(1):227–235.
- Comaniciu, D. and Meer, P. (2002a). Mean shift: A robust approach toward feature space analysis. *Pattern Analysis and Machine Intelligence, IEEE Transactions on*, 24(5):603–619.
- Comaniciu, D. and Meer, P. (2002b). Robust analysis of feature spaces: Color image segmentation. In *Computer Vision and Pattern Recognition, 1997. Proceedings., 1997 IEEE Computer Society Conference on*, pages 750–755. IEEE.
- Davison, A. (2003). Real-time simultaneous localisation and mapping with a single camera. In *Ninth IEEE International Conference on Computer Vision, 2003. Proceedings*, pages 1403–1410.

- Etienne, A. and Jeffery, K. (2004). Path integration in mammals. *Hippocampus*, 14(2):180–192.
- Etienne, A., Maurer, R., and Séguiot, V. (1996). Path integration in mammals and its interaction with visual landmarks. *Journal of Experimental Biology*, 199:201–209.
- Franz, M. and Mallot, H. (2000). Biomimetic robot navigation. *Robotics and Autonomous Systems*, 30(1-2):133–154.
- Franz, M., Schölkopf, B., Mallot, H., and Bühlhoff, H. (1998). Where did I take that snapshot? Scene-based homing by image matching. *Biological Cybernetics*, 79(3):191–202.
- Gallistel, C. (1990). *The organization of learning*. MIT press Cambridge, MA.
- Goedemé, T., Tuytelaars, T., Van Gool, L., Vanacker, G., and Nuttin, M. (2005). Feature based omnidirectional sparse visual path following. In *2005 IEEE/RSJ International Conference on Intelligent Robots and Systems, 2005.(IROS 2005)*, pages 1806–1811.
- Goldhoorn, A., Ramisa, A., de Mantaras, R., and Toledo, R. (2007). Using the average landmark vector method for robot homing. *Frontiers in artificial intelligence and applications*, 163:331–338.
- Gourichon, S., Meyer, J., and Pirim, P. (2002). Using coloured snapshots for short-range guidance in mobile robots. *International Journal of Robotics and Automation*, 17(4):154–162.
- Graham, P. and Collett, T. (2002). View-based navigation in insects: how wood ants (*Formica rufa* L.) look at and are guided by extended landmarks. *Journal of Experimental Biology*, 205(16):2499–2509.
- Grasso, F. (2001). Invertebrate-inspired sensory-motor systems and autonomous, olfactory-guided exploration. *The Biological Bulletin*, 200(2):160–168.
- Haferlach, T., Wessnitzer, J., Mangan, M., and Webb, B. (2007). Evolving a neural model of insect path integration. *Adaptive Behavior*, 15(3):273–287.
- Hafner, V. (2001). Adaptive Homing–Robotic Exploration Tours. *Adaptive Behavior*, 9(3-4):131–141.

- Hafner, V. and Möller, R. (2001). Learning of visual navigation strategies. In *European Workshop on Learning Robots (EWLR), Prague*. Citeseer.
- Hemmi, J. and Zeil, J. (2003). Burrow surveillance in fiddler crabs. II. The sensory cues. *The Journal of Experimental Biology*, 206(22):3951–3961.
- Hong, J., Tan, X., Pinette, B., Weiss, R., and Riseman, E. (1991). Image-based homing. In *1991 IEEE International Conference on Robotics and Automation, 1991. Proceedings.*, pages 620–625.
- Hong, J., Tan, X., Pinette, B., Weiss, R., and Riseman, E. (1992). Image-based homing. *Control Systems Magazine, IEEE*, 12(1):38–45.
- Huang, F. and Klette, R. (2009). Stereo panorama acquisition and automatic image disparity adjustment for stereoscopic visualization. *Multimedia Tools and Applications*, pages 1–25.
- Huber, S. and Bülthoff, H. (1998). Simulation and robot implementation of visual orientation behaviors of flies. In *From animals to animats 5: proceedings of the Fifth International Conference on Simulation of Adaptive Behavior*, pages 77–85. The MIT Press.
- Kim, S., Spenko, M., Trujillo, S., Heyneman, B., Santos, D., and Cutkosky, M. (2008). Smooth vertical surface climbing with directional adhesion. *Robotics, IEEE Transactions on*, 24(1):65–74.
- Labrosse, F. (2006). The visual compass: performance and limitations of an appearance-based method. *Journal of Field Robotics*, 23(10):913–941.
- Lambrinos, D., Kobayashi, H., Pfeifer, R., Maris, M., Labhart, T., and Wehner, R. (1997). An autonomous agent navigating with a polarized light compass. *Adaptive Behavior*, 6(1):131–161.
- Lambrinos, D., Moller, R., Labhart, T., Pfeifer, R., and Wehner, R. (2000). A mobile robot employing insect strategies for navigation. *Robotics and Autonomous Systems*, 30(1-2):39–64.
- Lowe, D. (2004). Distinctive image features from scale-invariant keypoints. *International Journal of Computer Vision*, 60(2):91–110.
- Luschi, P., Papi, F., Liew, H., Chan, E., and Bonadonna, F. (1996). Long-distance

- migration and homing after displacement in the green turtle (*Chelonia mydas*): a satellite tracking study. *Journal of Comparative Physiology A*, 178(4):447–452.
- Matsumoto, Y., Inaba, M., and Inoue, H. (2002). View-based approach to robot navigation. *Journal-Robotics Society of Japan*, 20(5):44–52.
- Mittelstaedt, M. and Mittelstaedt, H. (1980). Homing by path integration in a mammal. *Naturwissenschaften*, 67(11):566–567.
- Möller, R. (2000). Insect visual homing strategies in a robot with analog processing. *Biological Cybernetics*, 83(3):231–243.
- Möller, R. (2001). Do insects use templates or parameters for landmark navigation? *Journal of Theoretical Biology*, 210(1):33–45.
- Möller, R. (2009). Local visual homing by warping of two-dimensional images. *Robotics and Autonomous Systems*, 57(1):87–101.
- Möller, R., Krzykawski, M., and Gerstmayr, L. (2010). Three 2D-warping schemes for visual robot navigation. *Autonomous Robots*, pages 1–39.
- Möller, R. and Vardy, A. (2006). Local visual homing by matched-filter descent in image distances. *Biological Cybernetics*, 95(5):413–430.
- Möller, R., Vardy, A., Kreft, S., and Ruwisch, S. (2007). Visual homing in environments with anisotropic landmark distribution. *Autonomous Robots*, 23(3):231–245.
- Moravec, H. (1977). Towards automatic visual obstacle avoidance. In *Proceedings of the 5th International Joint Conference on Artificial Intelligence*, volume 99, page 584. Cambridge, Massachusetts, USA.
- Müller, M. and Wehner, R. (1988). Path integration in desert ants, *Cataglyphis fortis*. *Proceedings of the National Academy of Sciences of the United States of America*, 85(14):5287–5290.
- Müller, M. and Wehner, R. (1994). The hidden spiral: systematic search and path integration in desert ants, *Cataglyphis fortis*. *Journal of Comparative Physiology A: Neuroethology, Sensory, Neural, and Behavioral Physiology*, 175(5):525–530.
- Muller, R. (1996). A quarter of a century of place cells. *Neuron*, 17(5):813–822.
- O’Keefe, J. and Burgess, N. (1996). Geometric determinants of the place fields of hippocampal neurons. *Nature*, 381(6581):425–428.

- Papi, F. (1990). Olfactory navigation in birds. *Cellular and Molecular Life Sciences*, 46(4):352–363.
- Rossier, J., Haeberli, C., and Schenk, F. (2000). Auditory cues support place navigation in rats when associated with a visual cue. *Behavioural Brain Research*, 117(1-2):209–214.
- Se, S., Lowe, D., and Little, J. (2002). Mobile robot localization and mapping with uncertainty using scale-invariant visual landmarks. *The International Journal of Robotics Research*, 21(8):735–759.
- Seguinot, V., Maurer, R., and Etienne, A. (1993). Dead reckoning in a small mammal: the evaluation of distance. *Journal of Comparative Physiology A*, 173(1):103–113.
- Smith, L., Philippides, A., Graham, P., Baddeley, B., and Husbands, P. (2007). Linked local navigation for visual route guidance. *Adaptive Behavior*, 15(3):257–271.
- Stürzl, W. and Mallot, H. (2002). Vision-based homing with a panoramic stereo sensor. In *Biologically Motivated Computer Vision*, pages 3–14. Springer.
- Stürzl, W. and Zeil, J. (2007). Depth, contrast and view-based homing in outdoor scenes. *Biological Cybernetics*, 96(5):519–531.
- Sun, Y., Cao, Q., and Chen, W. (2004). An object tracking and global localization method using omnidirectional vision system. In *Proceedings of the 5th World Congress on Intelligent Control and Automation WCICA*, volume 6, pages 4730–4735.
- Szenher, M. (2008). Visual Homing in Dynamic Indoor Environments. The University of Edinburgh.
- Touretzky, D. and Redish, A. (1996). Theory of rodent navigation based on interacting representations of space. *Hippocampus*, 6(3):247–270.
- Trullier, O. and Meyer, J. (2000). Animat navigation using a cognitive graph. *Biological Cybernetics*, 83(3):271–285.
- Trullier, O., Wiener, S., Berthoz, A., and Meyer, J. (1997). Biologically based artificial navigation systems: Review and prospects. *Progress in Neurobiology*, 51(5):483–544.

- Vardy, A. and Möller, R. (2005). Biologically plausible visual homing methods based on optical flow techniques. *Connection Science*, 17(1):47–89.
- Vardy, A. and Oppacher, F. (2003). Low-level visual homing. *Advances in Artificial Life*, pages 875–884.
- Vladusich, T., Hemmi, J., Srinivasan, M., and Zeil, J. (2005). Interactions of visual odometry and landmark guidance during food search in honeybees. *Journal of Experimental Biology*, 208(21):4123–4135.
- Webb, B. (1995). Using robots to model animals: a cricket test. *Robotics and Autonomous Systems*, 16(2-4):117–134.
- Weber, K., Venkatesh, S., and Srinivasan, M. (1999). Insect-inspired robotic homing. *Adaptive Behavior*, 7(1):65–97.
- Wehner, R., Michel, B., and Antonsen, P. (1996a). Visual navigation in insects: coupling of egocentric and geocentric information. *Journal of Experimental Biology*, 199(1):129–140.
- Wehner, R., Michel, B., and Antonsen, P. (1996b). Visual navigation in insects: coupling of egocentric and geocentric information. *Journal of Experimental Biology*, 199:129–140.
- Wehner, R. and Räber, F. (1979). Visual spatial memory in desert ants, *Cataglyphis bicolor* (Hymenoptera: Formicidae). *Cellular and Molecular Life Sciences*, 35(12):1569–1571.
- Wehner, R. and Srinivasan, M. (1981). Searching behaviour of desert ants, genus-*Cataglyphis* (Formicidae, Hymenoptera). *Journal of Comparative Physiology A*, 142(3):315–338.
- Wei, R., Austin, D., and Mahony, R. (2005). Biomimetic application of desert ant visual navigation for mobile robot docking with weighted landmarks. *International Journal of Intelligent Systems Technologies and Applications*, 1(1):174–190.
- Yamauchi, B., Schultz, A., and Adams, W. (1999). Integrating exploration and localization for mobile robots. *Adaptive Behavior*, 7(2):217–248.
- Yu, S.-E. and Kim, D. (2010a). Discretized landmark distance estimation method for mobile robot navigation. *Korea Robotics Society Annual Conference 2010*, pages 136–137.

- Yu, S.-E. and Kim, D. (2010b). Distance estimation method with snapshot landmark images in the robotic homing navigation. In *Intelligent Robots and Systems (IROS), 2010 IEEE/RSJ International Conference on*, pages 275–280. IEEE.
- Yu, S.-E. and Kim, D. (2011a). Analysis on occlusion problem of landmark-based homing navigation methods. *Journal of Control, Robotics and Systems*, 17(6):596–601.
- Yu, S.-E. and Kim, D. (2011b). Analyzing the effect of landmark vectors in homing navigation (in preparation).
- Yu, S.-E. and Kim, D. (2011c). Image-based homing navigation with landmark arrangement matching. *Information sciences*, 181(16):3427–3442.
- Yu, S.-E. and Kim, D. (2011d). Landmark vectors with quantized distance information for homing navigation. *Adaptive Behavior*, 19(2):121–141.
- Zeil, J. and Hemmi, J. (2006). The visual ecology of fiddler crabs. *Journal of Comparative Physiology A*, 192(1):1–25.
- Zeil, J., Hofmann, M., and Chahl, J. (2003). Catchment areas of panoramic snapshots in outdoor scenes. *Journal of the Optical society of America A*, 20(3):450–469.